Chemotherapy-induced intestinal mucositis: The role of apoptosis regulators

Literature Review

1.0 Introduction

This thesis investigates mucosal barrier injury following chemotherapy. Cytotoxic agents used during chemotherapy are effective at killing cancerous cells however they also indiscriminately target certain healthy tissue. The mucosal surfaces of the body are especially sensitive to these drugs and so the term 'mucositis' is used to describe the damage arising from treatment (Keefe, 1998; Keefe et al., 2000). While all mucosal membranes of the body experience toxicity associated with cancer treatment, for the purpose of this thesis mucositis will refer to the gastrointestinal (GI) damage and exclude other areas. Mucositis is common, occurring in approximately 40% of patients after standard doses of chemotherapy, and in 100% of patients undergoing high dose chemotherapy and stem cell or bone marrow transplantation (Keefe et al., 1997; Pico et al., 1998). The World Health Organisation has a grading system for GI mucositis, with symptoms scaled from mild to potentially life threatening. Considerable morbidity is associated, with symptoms affecting the entire GI tract and including pain, ulceration, vomiting and diarrhoea. Occasionally mucositis can be fatal, especially in the case of irinotecan use, but more commonly it requires that treatment be ceased or doses reduced to alleviate symptoms. The net result is increased length of hospital stay, use of opioids for pain management and importantly increased costs (Keefe et al., 2004; Pico et al., 1998). Intestinal mucositis is a major oncological problem that is now one of the most significant dose-limiting toxicities and at the time of writing is without any listed preventative treatments. This review examines the current literature concerning the mechanisms known to cause mucositis in the intestine, concentrating especially on the molecular pathways involved.

1.1 The intestinal epithelium

1.1.1 Structure and function

The simple columnar epithelium of the intestine is made up of highly specialised cells whose primary function is to aid in absorption of nutrients across the epithelial lining whilst maintaining a physical barrier to the external environment (Junqueira et al., 1986). Efficient absorption is facilitated within the small intestine through finger-like projections called villi, which greatly enhance the surface area and therefore contact with luminal

contents. The large intestine does not contain villi. A barrier is maintained by the epithelial cells, which are joined by tight junctions on their lateral boarders, thus limiting the passage of luminal contents across the cell (Sherwood, 1997). Throughout the intestine, flask-like structures called crypts contain proliferative units and are responsible for maintaining epithelial integrity through constant production of new cells (Trier, 1962).

1.1.2 Cell proliferation and loss

The intestinal epithelium is one of the fastest proliferating tissues in the body (Potten, 1990). Epithelial cells are constantly being produced within the crypts of the small and large intestine and differentiating into specialised absorptive cells as they migrate towards the lumen. Cell proliferation is especially quick in the small intestine, with a cell division occurring every 5 minutes in the mouse (Potten, 1992). In fact, the entire lining of the small intestine is replaced every 2 to 3 days in the rodent and every 5 to 6 days in humans (Westcarr et al., 1999). The turnover rate is 2 to 4 times slower in the large intestine (Potten, 1992). Obviously, an equal rate of cell loss is required to maintain homeostasis within the tissue, and while it is accepted that there is extensive and constant cell loss from the epithelium, there remains some controversy as to the exact nature of cell loss from the villous tip and luminal boarder of colonic crypts. It is generally accepted that once epithelial cells complete their migration along the crypt-villous axis they are sloughed off into the lumen. Once detached they undergo a programmed form of cell death due to loss of adhesion to the basement membrane which is called ‘anoikis’ and are subsequently removed by local macrophages (Grossmann et al., 2001; Potten et al., 1997b; Watson, 1995). This notion of cell loss by exfoliation has been refuted by Hall and colleagues, who have attempted to prove that cells instead undergo programmed cell death whilst still attached to the basement membrane, and are phagocytosed by surrounding enterocytes. They found that spontaneous cell death is responsible for, and closely approximates to the total cell loss required to balance cell production in the murine small intestine (Hall et al., 1994). They did however concede that loss of cells from the villi is partially due to shedding, as some cellular mass was found to accumulate in the lumen. Further to this, cuffs of cells present at the villous tip undergoing programmed cell death have been shown in the rat small intestine (Westcarr et al., 1999). Thus, it is likely a combination of both cell sloughing and death is responsible for normal epithelial cell loss. A diagram of both the small and large intestinal crypt is shown in Figure 1.1.

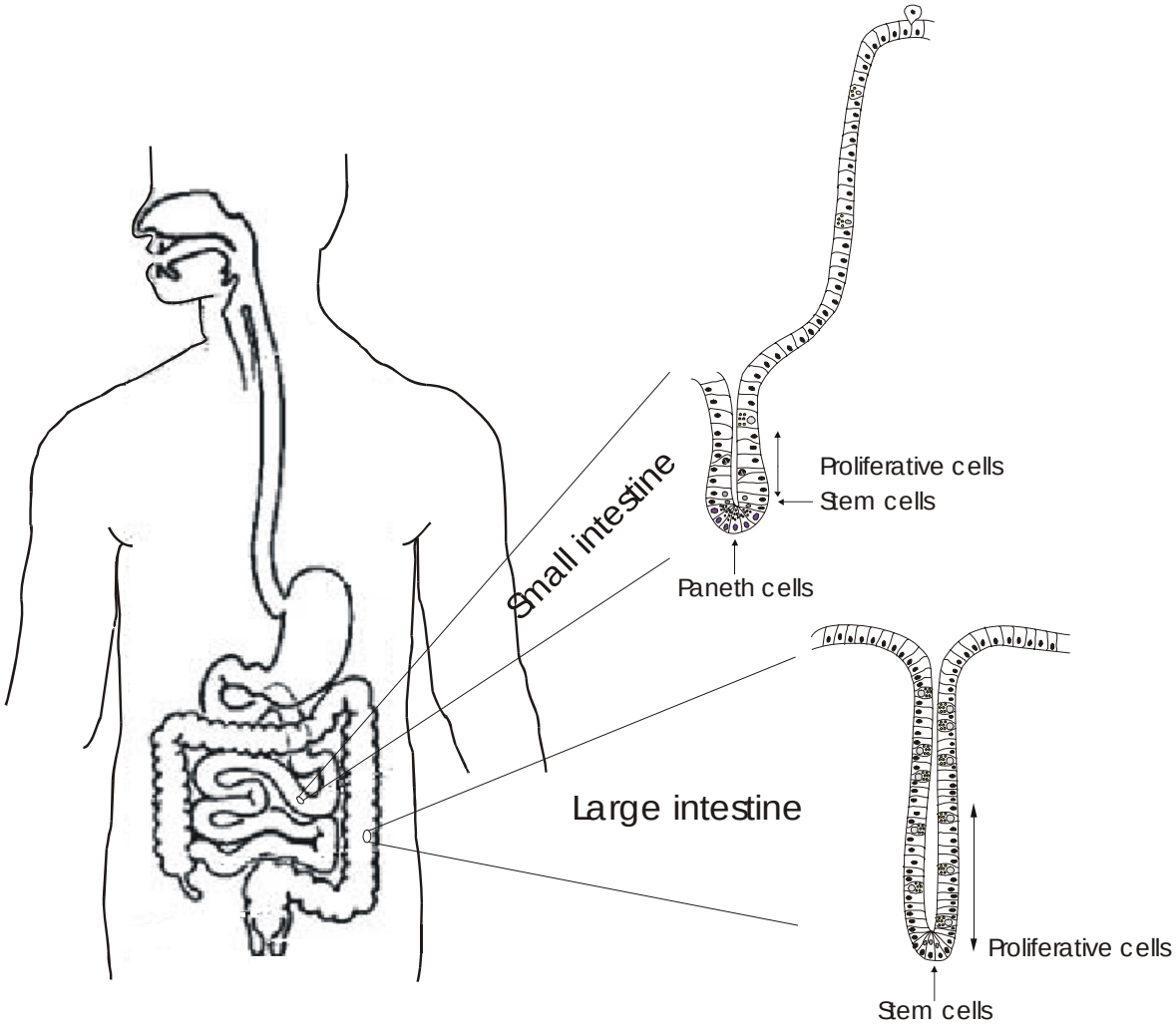

Figure 1.1. Diagram of small and large intestinal epithelium showing crypts and villi. Stem cells located in the basal region of the crypt and daughter cells located directly above produce progenitor cells that migrate up the crypt axis and feed onto multiple villi in the small bowel or move towards the table region in the colon. Ageing cells differentiate as they move towards the lumen for extrusion.

1.1.3 Stem cells

The stem cells of the small intestine are located within the lower part of the epithelial crypts and they possess an element of pluripotency. They are capable of producing all four differentiated cell lineages within the crypt, hat is the enteroendocrine cells, absorptive enterocytes, paneth cells and the goblet cells (Potten and Loeffler, 1990). Each cell divides without maturation approximately every 20 hours in the murine small intestine, with daughter cells undergoing further divisions as they migrate up towards the villi, with the exception of the paneth cells which move to the crypt base (Potten et al., 1995).

A clonogenic assay was devised by Withers and Elkind in 1969 to estimate the number of cells with a clonogenic capacity and hence the potential number of stem cells per crypt (Potten and Loeffler, 1990). This assay has since been used extensively and it has been determined that approximately 4-16 and 1-4 stem cells are located in the small and large intestines, respectively. The stem cells are located within the crypts at position 4-6 in the small intestine and 1-2 in the large intestine in the crypt cell hierarchy (Potten and Grant, 1998). However, some stem cells in the small intestine may intermix in the paneth cell region at the crypt base. There are thought to be a further population of cells capable of clonogenic division, however these are recruited to act as stem cells only following extensive crypt damage and loss of true stem cells (Potten, 1998).

1.2 Apoptosis

John Kerr was the first to discover a novel form of cell death observed during his studies of acute liver injury in rats in the late 1960s. The unique morphological changes seen in this type of cell death were described and were initially called shrinkage necrosis, but later re-named apoptosis (Kerr, 1971; Kerr et al., 1972). The classic morphological characteristics of a cell undertaking apoptosis include shrinking of the cellular cytoplasm, detachment from neighbouring cells and condensation of chromatin around the nuclear membrane. This is followed by blebbing of the cellular membrane and fragmentation of the nucleus and cytoplasm into membrane-bound vesicles. These are called apoptotic bodies and are quickly phagocytosed and degraded by surrounding cells (Gavrieli et al., 1992; Kerr et al., 1994). In contrast to necrosis, apoptosis affects individual cells and there is no cellular leakage at any stage of the process. This avoids the inflammatory response and major tissue disturbance that is associated with necrosis (Reed, 2000).

1.2.1 The role of apoptosis

Apoptosis is an important homeostatic mechanism with wide ranging applications throughout the body, including foetal development, demolition of redundant tissue and maintenance of tissue structure. A classic example of apoptosis is removal of autoreactive T-cells in the thymus. It is also important for removing senescent cells or those that have sustained genomic damage, which left unchecked could lead to neoplasia. Apoptosis is an active and genetically regulated process in which an individual cell responds to an internal or external stimulus resulting in its death. Deregulation of apoptosis can lead to pathological states such as neurodegenerative disease (excess cell loss) or cancer and autoimmune disease (excess cell accumulation) (Konopleva et al., 1999; Renehan et al., 1995; Strasser et al., 2000a). The intestinal epithelium has constant cell production and so well-defined mechanisms are needed to regulate cell removal. In this instance apoptosis is seen to be as important as or even more important than control of cell proliferation in maintaining correct tissue structure (Renehan et al., 2001; Tarnawski and Szabo, 2001). Spontaneous apoptosis occurs in intestinal crypts, albeit not at a high frequency, removing what appear as normal healthy cells (Potten, 1997). This is thought to remove excess stem cells which helps maintain a balance of proliferation (Potten et al., 1997a).

1.3 Chemotherapy, apoptosis and mucositis

1.3.1 The treatment of cancer

Cancer has to date been treated by surgery if appropriate or by use of cytotoxic chemotherapy and radiation therapy. These techniques have been successful in many haematological malignancies and a few solid tumours, but the majority of malignancies have proved resistant to these interventions (Hickman et al., 1994). In all cases though, the effectiveness of cytotoxic treatments have been limited by the side effects of these agents on normal tissues and cells. Various forms of supportive measures have been developed to reduce these toxicities, such as bone marrow rescue, antibiotics and growth factor support, but overall the dose of treatment must still be limited (Hannun, 1997). The underlying problem is that chemotherapy drugs target some populations of normal cells including enterocytes, causing apoptosis without being selective only to tumour cells (Decker-Baumann et al., 1999).

1.3.2 Chemotherapy treatment and mucositis

Cytotoxic agents induce gastrointestinal toxicity to differing degrees, causing the severity of mucositis to vary between patients depending on their cancer and treatment regimen (Ijiri and Potten, 1983; Ijiri and Potten, 1987). This may be a factor of different classes of cytotoxic agents acting at particular cell positions within the crypt hierarchy. For example, drugs such as doxorubicin and bleomycin are known to act a cell positions 4-6, while actinomycin-D and cyclophosphamide act at positions 6-8 and methotrexate and 5-fluorouracil act slightly higher at positions 8-11 (Ijiri and Potten, 1983; Ijiri and Potten, 1987).

Classically, intestinal mucositis has been attributed to the high proliferation rate in the intestine that is interrupted and reduced by chemotherapy drugs, and also to direct killing of crypt cells (Keefe, 1998). While this is still true, a new paradigm for mucositis has arisen. The term alimentary mucositis (AM) has been coined to describe the damage that occurs to the whole alimentary tract, rather than looking at oral mucositis and GI mucositis as separate pathologies, as has been done in the past. This is based on the realisation that the alimentary tract is all one structure embryonically, from mouth to anus, coupled with the body only having limited ways in which to respond to damage. Therefore, it is likely that the mechanisms behind the pathobiology of mucositis are also similar regardless of region (Keefe, 2004). If this holds true, then the five phase model described for oral mucositis also must be applied to the intestine (Sonis, 2004b). The five phases are: initiation, upregulation and message generation, signalling and amplification, ulceration and inflammation and finally healing. Briefly, initiating events of chemo and radiotherapy is the generation of oxidative stress and reactive oxygen species (ROS) which directly damage cells, tissues and blood vessels. Secondly, the transcription factor NFκB is activated and this leads to the upregulation of many genes, including those responsible for the production of the pro-inflammatory cytokines, as well as adhesion molecules and cyclooxygenase-2. The result being further tissue injury and apoptosis. During the third phase, a feedback loop occurs whereby TNF-α acts on a number of pathways to reinforce NFκB activation as well as the ceramide pathway. Following this we see the ulcerative phase, with bacterial colonisation, subsequent increased pro-inflammatory cytokine production and hence inflammation. Finally, healing occurs with renewal of epithelial proliferation and differentiation and re-establishment of the normal local microbial flora. These events are occurring in virtually all cells and tissues of the mucosa, and also with

considerable crossover of phases (Sonis, 2004a; Sonis, 2004b; Sonis et al., 2004). Thus, mucositis is not a linearly occurring, epithelial-only mediated event. This remains an hypothetical pathway in the intestine and this review will continue to concentrate on the epithelial injury portion of mucositis research.

Both radiotherapy and chemotherapy damage the intestinal lining, causing apoptosis rather than necrosis of epithelial crypt cells, and crypt hypoplasia (Anilkumar et al., 1992). There is also increased permeability through loosening of tight junctions and an increased susceptibility to infection. Structural changes in the small intestine following treatment are also thought to be responsible for malabsorption and patient symptoms peak on days 3-5 (Keefe, 1998). Once established, there is no effective treatment for mucositis except limiting the dose of chemotherapy drugs administered per session, which may reduce the chance of remission. Mucositis has become a limiting factor in the effectiveness of cancer treatment since bone marrow toxicity can be managed by supportive care, blood transfusion and colony-stimulating factors (Keefe et al., 2000).

1.3.3 Methotrexate and the intestine

Methotrexate (MTX) is a commonly used chemotherapy drug in the treatment of leukaemia and a variety of tumours. It is an anti-metabolite that attacks the cell in its S phase and disrupts DNA synthesis. Its mode of action is to inhibit dihydrofolate reductase (DHFR), a key enzyme in cell replication, leading to its sub-category as a folate antagonist (Huennekens, 1994; Tenenbaun, 1994). Methotrexate induces diarrhoea and anorexia, accompanied by malabsorption, malnutrition and dehydration in patients. It also inhibits epithelial proliferation and enterocyte function and increases the risk of gut associated sepsis due to disruption of the mucosal barrier. Gastrointestinal toxicity is now the major dose-limiting factor for methotrexate administration (Papaconstantinou et al., 2001; Verburg et al., 2000). The toxicity of MTX to the gastrointestinal epithelium is dependent on duration of cytotoxic exposure rather than peak levels achieved by the drug. Clearance of MTX from plasma following intravenous injection is triphasic and the terminal half-life, which begins around 24-36 hours following treatment initiation, contributes the most to gastrointestinal toxicity(Mitchell and Schein, 1984).

In the GI tract, the small intestine is the predominant site of damage after treatment with MTX. The most severe effect can be seen in the proximal small bowel with pronounced crypt and villus ablation. Treatment with MTX causes an increase in apoptosis that reaches its peak approximately 6 hours after administration in the rat. The majority of

apoptosis occurs in the crypt, removing the proliferative cells and leading to crypt hypoplasia. The crypt is unable to sufficiently supply the villus with new cells and atrophy occurs, reaching a nadir by 48 hours. Once this initial injury to the mucosa is over, the epithelium enters a highly proliferative state to repair and regenerate the intestinal lining (Horie et al., 1999; Howarth et al., 1996; Taminiau et al., 1980).

1.3.4 Irinotecan and the intestine

Irinotecan hydrochloride (or CPT-11) is a reasonably new chemotherapeutic drug, used primarily to treat colorectal carcinoma, as well as other solid tumours. Its action on cells is to inhibit the DNA enzyme topoisomerase I. The main side effect of it use is severe and frequent gastrointestinal toxicities, most notably, diarrhoea (Cao et al., 1998a; Ikuno et al., 1995; Takasuna et al., 1996). Irinotecan damages both the small and large intestine (Gibson et al., 2003). Through laboratory investigations using a number of animal models, the response of the gastrointestinal tract to irinotecan has been somewhat elucidated, however the exact mechanism of diarrhoea induction remains unknown (Araki et al., 1993; Cao et al., 1998a; Ikuno et al., 1995; Takasuna et al., 1996). Changes seen in the gut following irinotecan administration include; vacuolation of the epithelium, blood vessel dilatation and infiltration of polymorphic cells, and goblet cell metaplasia. It is suggested that these changes lead to malabsorption of water and electrolytes and mucin hypersecretion, resulting in diarrhoea (Ikuno et al., 1995). An opposing theory is that the diarrhoea is due to haemorrhagic enterocolitis. The active metabolite of irinotecan, SN-38, is retained within the intestine, and so high levels persist to cause damage (Araki et al., 1993). Further to this, the microflora of the intestine contain β-glucuronidase activity which can convert SN-38 glucuronide (a detoxified form of SN-38) back to SN-38. Since it is SN-38 that causes intestinal cytotoxicity, inhibition of β-glucuronidase should improve irinotecan-induced diarrhoea. This has been shown, where administration of antibiotics reduced colonic β-glucuronidase activity and markedly ameliorated diarrhoea (Takasuna et al., 1996).

A better understanding of the mechanisms behind irinotecan-induced toxicity is important because of its wide-spread use. The antimetabolite fluorouracil has been the drug of choice in the treatment of metastatic colorectal cancer for several decades, however patients who progress from this treatment are then given irinotecan. Currently irinotecan is one of only two drugs approved in the USA for second-line treatment of colorectal cancer (Govindarajan et al., 2000). However its continued use will be questionable if the dose-

limiting and often life-threatening diarrhoea associated with treatment can not be prevented (Govindarajan, 2002).

1.4 Molecular control of cell death

The nematode, C. elegans, contains the best defined genetic pathway of cell death, which consists of two autosomal recessive death effector genes, CED-3 and CED-4, and one autosomal dominant death repressor gene CED-9. CED-3 and CED-4 are essential for programmed cell death during the worm's development, and CED-9 can prevent their action. It has since been found that CED-3 belongs to a family of cysteine proteases called caspases, the effectors of apoptosis. CED-4 has Apaf-1, a mammalian adaptor protein as its mammalian homologue. CED-9 and mammalian Bcl-2 have also been proved to be structural and functional homologues, both having a survival function within the cell (Hengartner, 1999; Hengartner and Horvitz, 1994; Liu and Hengartner, 1999).

1.5 The Bcl-2 family

Bcl-2 is the mammalian homologue of CED-9. It is a proto-oncogene that was first discovered due to the characteristic t(14;18) translocation found in the majority of follicular lymphomas. In this translocation, Bcl-2 at chromosome segment 18q21 is juxtaposed with the immunoglobulin heavy chain locus at 14q32, resulting in deregulated and subsequent overexpression of the gene's protein product. It is the first example found of an oncogene that aids tumourogenesis via lack of cell death rather than by increasing proliferation (Adams and Cory, 1998; Yang and Korsmeyer, 1996). Bcl-2 holds cells in G_0/G_1 phase of the cell cycle, and this accounts for the usual early appearance of low grade disease comprising small resting B-cells in follicular lymphomas which overexpress Bcl-2 (Park and Hockenbery, 1996). It has been shown in T-cells that Bcl-2 maintains G_0 phase by delaying the loss of the cyclin-dependent kinase inhibitor, p27, by inhibiting IL-2 production by the transcription factor NFAT (Linette et al., 1996). Activation of NFAT requires calcineurin, a calcium-dependent phosphatase, which Bcl-2 is able to bind effectively (Fadeel et al., 1999). Bcl-xL has also been shown to delay cell cycle entry by elevating p27 levels in fibroblasts (Greider et al., 2002). More pertinent to this review though is that Bcl-2 has been shown to have the ability to rescue cells from apoptosis in response to a wide range of stimuli, including radiation, heat, chemotherapy agents and granzyme B. The exact way in which Bcl-2 inhibits apoptosis has been difficult to elucidate due to its lack of conformational similarity to other proteins which have a known

function (Miyashita and Reed, 1993; Yin et al., 1995), but possible mechanisms will be discussed below.

Bcl-2 is an integral membrane protein and is the founding member of a family that now has at least 20 members identified in mammalian species (Herr and Debatin, 2001). The Bcl-2 family consists of both pro-apoptotic and anti-apoptotic members, and their main action appears to be regulation of cellular protease activation. Anti-apoptotic family members include Bcl-2, Bcl-xL, Bcl-w, Mcl-1 and A1. Pro-apoptotic family members belong to one of two groups, the Bcl-2-like proteins including Bax and Bak, and the single domain proteins including Bcl-xS, Bad, Bim, Bid, Noxa and Puma (Chao and Korsmeyer, 1998; McDonnell et al., 1996; Nakano and Vousden, 2001; Oda et al., 2000). The protein structure of the Bcl-2 family members consists of conserved regions of amino acids called Bcl-2 homology (BH) domains. The BH domains allow interaction between the family members, which form homodimers and heterodimers with each other. Thus far there are four domains identified, BH-1 to BH-4, and family members can contain from only one up to all four of the domains. The BH-1 and BH-2 domains are thought to be critical for the anti-apoptotic action of Bcl-2 and Bcl-xL, whilst the BH-3 domain is primarily associated with inducing death in the pro-apoptotic family members (Chao and Korsmeyer, 1998; Kelekar and Thompson, 1998; Yin et al., 1995). In the pro-survival members, the central BH-1, -2 and -3 domains form a hydrophobic cleft which is stabilised by the N-terminal BH-4 domain. While the BH-3 motif of pro-apoptotic family members consists of an amphipathic helix. This allows the α-helix of antagonising pro-apoptotic Bcl-2 family members to dock within the hydrophobic groove of the anti-apoptotic protein, in a similar fashion to a receptor ligand interaction, and regulate its action within the cell (Borner, 2003; Cory et al., 2003; Fleischer et al., 2003). Figure 1.2.

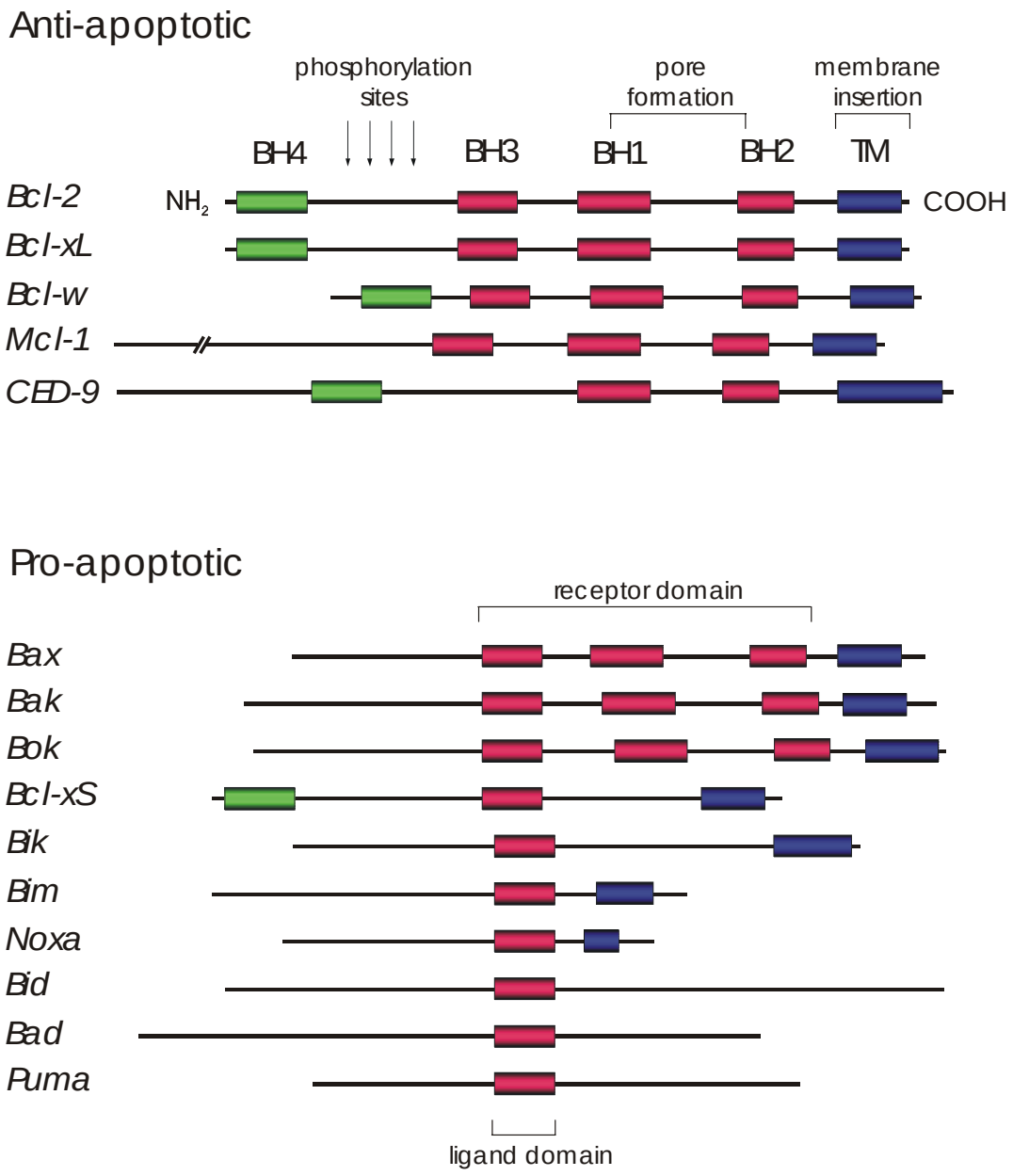

Figure 1.2. Domain arrangements of various Bcl-2 family proteins, showing the 1 to 4 Bcl-2 homology (BH) domains and transmembrane domain at the carboxy terminus. Also indicated is the proposed function of each of the areas or domains.

The ratio of pro-apoptotic to anti-apoptotic family members within each cell is extremely important for determining protein-protein interactions and ultimately the cell's sensitivity to an apoptotic stimulus (Oltvai et al., 1993; Raisova et al., 2001; Sedlak et al., 1995). There have been two main models proposed for how this ratio determines a cell's propensity for apoptosis. The first is that Bcl-2 and Bcl-xL are passive receptors of the apoptosis-inducing BH-3 domain of pro-apoptotic members, so that when they are abundant in the cell, heterodimerisation with Bax prevents the formation of toxic Bax homodimers simply by sequestration, resulting in cell survival. The second theory is that Bcl-2 and Bcl-xL are active repressors of cell death, and heterodimerisation with Bax blocks their ability to prevent apoptosis (Kelekar and Thompson, 1998; Konopleva et al., 1999). Studies using mutant forms of Bcl-2 expressed in mammalian tissue found that mutated Bcl-2 that failed to bind Bax lost it's death-sparing function. This suggests that anti-apoptotic members of the Bcl-2 family require heterodimerisation to protect the cell from apoptosis (Hanada et al., 1995). It has also been shown that certain pro-apoptotic family members require heterodimerisation with the anti-apoptotic members of the family to exert their death promoting activity. Bad is a BH-3 only domain protein that requires its ability to dimerise with Bcl-xL to induce cell death. Kelekar stated that Bad induces cell death by dimerising with and deactivating Bcl-xL (Kelekar et al., 1997), whereas Yang reported that Bad's mode of action is simply to sequester Bcl-xL from Bax, leaving Bax to form toxic homodimers and induce cell death (Yang et al., 1995). It has also been shown that Bax and Bak are critical for BH-3-only protein-induced cell death. In experiments using $Bax^{-/-}Bak^{-/-}$ cells, Bim, Bid and Bad failed to induce apoptosis despite heterodimerisation with anti-apoptotic Bcl-2 family members (Wei, 2001; Zong et al., 2001). Thus there remains some controversy as to whether the pro-apoptotic or anti-apoptotic proteins play the dominant role in regulating cell death. Further to this, new hypothetical models of the way Bcl-2 family members interact in the cell to control apoptosis have been proposed. These include the suggestion that an intermediary protein, Bid, is responsible for Bax activation once all cellular Bcl-2 is saturated with BH-3-only proteins. It has also been postulated that heterodimerisation does not play a role at all and instead Bcl-2 prevents Bax activation through an indirect mechanism such as a sequestering an as yet unknown protein or the small molecules released during early apoptosis that drive Bax activation. Or, it seems possible that in accordance with the C. elegans model, Bcl-2 acts to sequester a CED-4 like molecule, to prevent it from causing downstream activation of Bax via caspases (explained in later section of this review).

There are a considerable number of ways that the Bcl-2 family can be regulated to affect cellular survival or apoptosis, including transcription, translation, posttranslational control, alternative splicing and intracellular redistribution (Akgul et al., 2004). In viable cells, the majority of Bax is monomeric and found either in cytoplasm or loosely attached to intracellular membranes. After an apoptotic stimulus, Bax translocates to the mitochondria where it becomes an integral membrane protein and cross-linkable as a homodimer. Therefore, activation of Bax appears to involve subcellular translocation and dimerisation. It has been suggested that this translocation is effected through exposure of its amino terminal domain, which is concealed under normal conditions to keep the molecule in a closed configuration. The pro-apoptotic family member Bid has been proposed to be involved in exerting the conformational change to Bax after an apoptotic stimulus (Eskes et al., 2000; Gross et al., 1999). Bcl-2 activity can be regulated by phosphorylation, which occurs at serine residues 70 and 87. Phosphorylation has been associated with loss of Bcl-2's anti-apoptotic action and can be induced by microtubule-damaging chemotherapy agents such as Taxol. Bcl-2 phosphorylation has been shown to inhibit heterodimerisation with Bax (Haldar et al., 1995; Pratesi et al., 2001; Solary et al., 2000; Srivastava et al., 1998).

Pro-apoptotic family members Bad, Bid and Bim are also controlled by distinct post-translation modifications. In the presence of IL-3, Bad is hyperphosphorylated and sequestered by the cytosolic phosphoserine-binding protein 14-3-3. Thus, it is unable to dimerise with anti-apoptotic Bcl-xL and is essentially inactive. Following IL-3 deprivation, Bad is dephosphorylated allowing it to associate with Bcl-xL. The ability of Bad to induce cell death is dependent on it being able to dimerise with anti-apoptotic members of the Bcl-2 family, but requires dephosphorylation after an apoptotic stimulus for this to occur (Kelekar et al., 1997). Bid is activated through caspase-mediated proteolysis. This activation allows Bid to induce the conformation change in Bax and Bak required for mitochondrial membrane insertion (Eskes et al., 2000; Strasser et al., 2000a). Finally, Bim is regulated by binding to the dynein motor complex. In healthy cells, Bim is bound to LC8 cytoplasmic dynein light chain and therefore sequestered to the microtubule-associated dynein motor complex. Apoptotic stimuli disrupt the interaction between LC8 and the dynein motor complex, thus freeing Bim. This allows Bim to translocate to the mitochondrial membrane where it interacts with Bcl-2, neutralising its anti-apoptotic activity (Puthalakath et al., 1999; Puthalakath and Strasser, 2002; Strasser et al., 2000b).

Little is known about the transcriptional regulation of Bcl-2 family proteins in normal cells, although a number of transcription factors are slowly becoming evident. Firstly, it is known that p53 has both positive and negative regulatory effects on Bax and Bcl-2 respectively. In most settings, an apoptotic stimulus causes a p53-dependent increase in Bax transcription and a decrease in Bcl-2 transcription to alter the Bax/Bcl-2 ratio and induce cell death (Miyashita et al., 1994; Miyashita and Reed, 1995; Weller, 1998). Control is through a p53-responsive binding site in the promoter of the Bax gene and Bcl-2 containing a p53-dependent negative response element in its 5'untranslated region (Benchimol, 2001; Miyashita et al., 1994). Other Bcl-2 family members known to be p53-responsive include Bak, Bid, Bcl-xL, Noxa and Puma (Kannan et al., 2001; Nakano and Vousden, 2001; Sax et al., 2002; Shibue et al., 2003). Nuclear factor kappa B has also been investigated for its role in modulating transcription of anti-apoptotic Bcl-2 family members, in particular A1 (Wang et al., 2001). In resting cells, NF-κB is sequestered in the cytoplasm in an inactive form which is bound to its inhibitor protein IκB. Upon stimulation (such as during chemotherapy treatment) IκB is phosphorylated, dissociates from NF-κB and is degraded by proteases. This allows NF-κB to become activated whereby it translocates to the nucleus and binds to and upregulates target genes, including Bcl-2, Bcl-x and A1 (Catz and Johnson, 2001; Chen et al., 2000). The retinoblastoma protein (pRB) has also been shown to transcriptionally activate the Bcl-2 gene in epithelial cells in conjunction with the transcription factor AP-2, which both bind to the same promoter sequence (Decary et al., 2002). Further to this, the E2F1 transcription factor, which is a downstream target of pRB has been shown to upregulate the expression of pro-apoptotic Bcl-2 family members Puma, Noxa and Bim by binding to their respective promoters (Hershko and Ginsberg, 2004). Finally, there is evidence that growth factors, such as GM-CSF and IGF-1, regulate activity of Bcl-2 proteins post-transcriptionally by altering the rate of protein synthesis (Hu et al., 1996; Linseman et al., 2002; Tamatani et al., 1998).

1.6 Caspases

Caspase-dependent cell death is the best defined pathway in apoptosis and can be regulated by the Bcl-2 family (Thornberry, 1998). Caspases are a group of cysteine proteases so called due to their specific cleavage of proteins after aspartic residues. Caspases share similarities in amino acid sequence, structure and substrate specificity, and are synthesised within the cell as minimally active precursors to avoid premature activation. Under non-

apoptotic conditions, each caspase is expressed as a 30 kDa to 50 kDa inactive pro-enzyme (zymogen), which contains three domains; the NH2-terminal domain, a large subunit approximately 20 kDa in size and a small subunit approximately 10 kDa in size (Cohen, 1997; Slee et al., 1999; Thornberry and Lazebnik, 1998). Activation of caspases results from proteolytic processing between its domains, followed by association of the small and large subunits to form a heterodimer. To initiate this activation, the caspases must have proteolytic cleavage at aspartic residues by either themselves or by other caspases. In this way, proteins that promote caspase aggregation play an important role in proximal caspase activation events and can lead on to a cascade of sequential caspase activation (Cohen, 1997; Slee et al., 1999; Thornberry and Lazebnik, 1998).

The role of caspases is to inactivate proteins that protect the cell from apoptosis. A clear example is the cleavage of I/CAD, an inhibitor of the nuclease responsible for DNA fragmentation. Other negative regulators of apoptosis cleaved by caspases are the anti-apoptotic members of the Bcl-2 family. Cleavage of these appears to not only inactivate the proteins, but also promote apoptosis in a positive feedback fashion. Direct disassembly of cell structures is another caspase function, as illustrated by the destruction of nuclear lamina, which contributes to chromatin condensation. Caspases also cleave several proteins involved in cytoskeleton regulation and inactivate proteins involved in DNA repair, replication and mRNA splicing (Nicholson and Thornberry, 1997; Thornberry and Lazebnik, 1998).

There have been 12 caspases identified to date in mammals and these are expressed in virtually all cells (Launay et al., 2005). Individual caspases are numbered and can be grouped according to their function within the cell, specifically; apoptotic initiators 8, 9 and 10; executioners 2, 3, 6 and 7 or inflammatory mediators 1, 4, 5, 11 and 12 (Creagh et al., 2003; Martinon and Tschopp, 2004). Caspase-3 in particular has been labelled the quintessential executioner caspase, with its expression classed as a positive marker for apoptosis (Marshman et al., 2001; Sabbatini et al., 2004). Initiator caspases are those that are activated first in the apoptotic sequelae, such as in response to death receptor activation and mitochondrial factor release (described in detail later in this review) Figure 1.3. While caspase-1 is essential for the production of pro-inflammatory cytokines including mature interleukin-1β, interleukin-1α and interleukin-18 (Creagh et al., 2003).

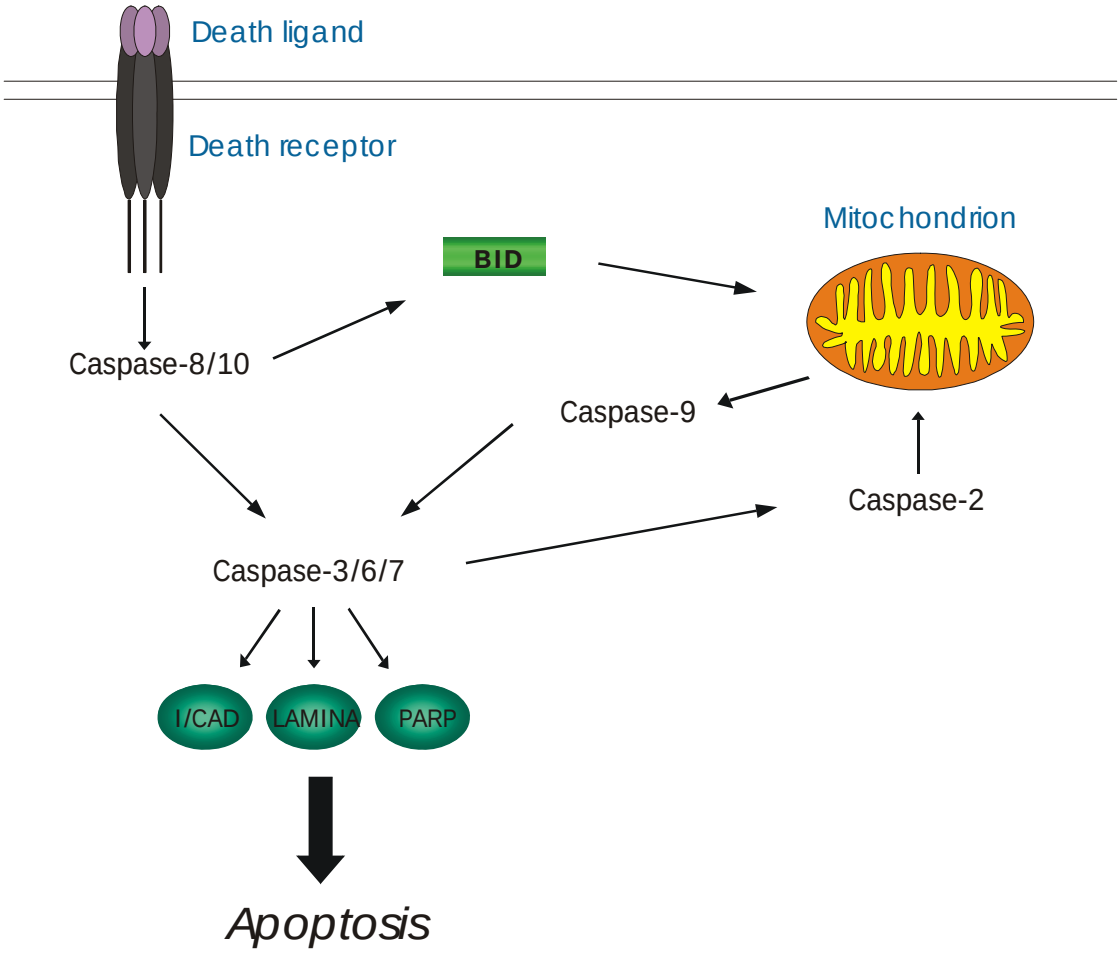

Figure 1.3. Diagram of caspase cascade leading to apoptosis in mammalian cells. Initiator caspases are activated by cell death stimuli originating from membrane receptors and mitochondrion. This leads to sequential activation of executioner caspases, which are responsible for cleavage of cellular substrates and positive reinforcement of cascade.

Caspase-independent cell death can also be controlled by Bcl-2, with studies showing an inhibition of apoptosis in response to nitric oxide, hydrogen peroxide and menadione. This work has led authors to suggest that Bcl-2 may also work in an anti-oxidant pathway to regulate free radical generation at intracellular membranes, therefore inhibiting cell death (Hockenbery et al., 1993; Okuno et al., 1998).

1.7 p53

Wild type p53 is a nuclear phosphoprotein. It was first described in 1979 when it was discovered as part of studies investigating SV40 (simian virus) transformed cells. It was found to complex with the SV40 DNA tumour virus large T antigen and so was classified as a transformation-related protein (DeLeo et al., 1979; Lane and Crawford, 1979; Linzer and Levine, 1979). Interestingly, p53 was first thought to be a proto-oncogene as initial studies showed that it was overexpressed in mouse and human tumour cells (Dippold et al., 1981). It was also able to immortalise cells in culture, however it became apparent some time later that these experiments were actually using mutant forms of the protein which was acting in a dominant negative fashion to inhibit the function of the normal protein (Finlay et al., 1989; Hinds et al., 1989). Subsequent research confirmed that wild type p53 is a tumour suppressor gene, due to its ability to suppress transformation by oncogenes and inhibit growth of transformed cells (Baker et al., 1990). Further to this, p53 gene knockout mice have an increased risk for development of malignancy, as do families with the Li-Fraumeni syndrome who have germline mutations of p53 (Ko and Prives, 1996).

Tumour protein p53 belongs to a family of proteins that contains three members; p53, p63 and p73. The human p53 gene encodes a single protein containing 393 amino acid residues and is 53,000 kDa in size. It consists of four main functional domains: a transactivation domain (residues 1-42); a polyproline-rich region (residues 61-94); a central core domain, required for sequence-specific DNA binding (residues 102-292); and the oligomerisation domain (residues 324-355). There is also the C-terminus which contains a nuclear localisation sequence and possesses both RNA and non-specific DNA-binding activities (residues 356-393) (Slee et al., 2004). The half-life of the p53 protein is relatively short (only 20 minutes) and so normally the cellular concentration remains very low. It may also exist in a latent form and require activation to carry out functions within the cell. The functions of p53 are diverse and complex however the main cellular responses following activation of the protein include cell cycle regulation, DNA repair and apoptosis (Smith et al., 2003).

Levels of p53 protein are increased after various stress stimuli including hypoxia, ultraviolet radiation, hypoxia, heat shock, growth factor withdrawal, oncogene activation and cytotoxic drugs (Vousden and Lu, 2002). This occurs mainly due to increases in p53 stability, through phosphorylation of the protein and a decrease in association with the Mdm2 protein that normally targets it for degradation via the ubiquitin-mediated proteasome pathway. It is then able to act as a transcriptional activator of target genes to induce G_1 cell cycle arrest and/or apoptosis. Apoptosis is the dominant mechanism by which p53 inhibits tumour development and is highly conserved through evolution. The homologues for p53 in Drosophila and C. elegans are Dmp53 and Cep-1 respectively (Slee et al., 2004; Vogelstein et al., 2000). The amino acid sequence of human and rat p53 is shown in Figure 1.4.

A)

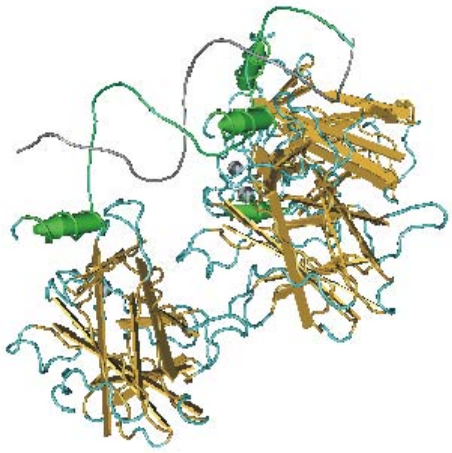

B)

Transactivation domain

```
p53_Huamn MEEPQSDPSVEPPLSQETFSDLWKLLPENNVLSPLPS---QAMDDLMLSP 47
p53_Rat   MEDSQSDMSIELPLSQETFSCLWKLLPPDDILPTTATGSPNSMEDLFL-P 49
          **:.*** *:* ******** ****** :::*.. .:   ::*:**:* *

          DDIEQWFTEDPGPDEAPRMPEAAPPVAPAPAAPTPAAPAPAPSWPLSSSV 97
          QDVAELLE---GPEEALQVSAPAAQ-EPGTEAPAPVAPASATPWPLSSSV 95
          :*: : :    **:** ::. .*.   *.. **:*.***.*..******* 
```

DNA binding domain

```
          PSQKTYQGSYGFRLGFLHSGTAKSVTCTYSPALNKMFCQLAKTCPVQLWV 147
          PSQKTYQGNYGFHLGFLQSGTAKSVMCTYSISLNKLFCQLAKTCPVQLWV 145
          ********.***:****:******* **** :***.**************

          DSTPPPGTRVRAMAIYKQSQHMTEVVRRCPHHERCSDSDGLAPPQHLIRV 197
          TSTPPPGTRVRAMAIYKKSQHMTEVVRRCPHHERCSDGDGLAPPQHLIRV 195
           *****************:********************.************

          EGNLRVEYLDDRNTFRHSVVVPYEPPEVGSDCTTIHYNYMCNSSCMGGMN 247
          EGNPYAEYLDDRQTFRHSVVVPYEPPEVGSDYTTIHYKYMCNSSCMGGMN 245
          ***   .******:****************** *****:************

          RRPILTIITLEDSSGNLLGRNSFEVRVCACPGRDRRTEEENLRKKGEPHH 297
          RRPILTIITLEDSSGNLLGRDSFEVRVCACPGRDRRTEEENFRKKEEHCP 295
          ********************:*********************:*** *
```

Oligomerisation domain

```
          ELPPGSTKRALPNNTSSSPQPKKKPLDGEYFTLQIRGRERFEMFRELNEA 347
          ELPPGSAKRALPTSTSSSPQQKKKPLDGEYFTLKIRGRERFEMFRELNEA 345
          ******:*****..****** ************:****************
```

C terminus

```
          LELKDAQAGKEPGGSRAHSSHLKSKKGQSTSRHKKLMFKTEGPDSD 393
          LELKDARAAEESGDSRAHSSYPKTKKGQSTSRHKKPMIKKVGPDSD 391
          ******:*.:*.*.******: *:*********** *:*. *****
```

Figure 1.4. A) 3 Dimensional structure of tumour suppressor p53 protein complexed with DNA and B) Amino acid sequences of human and rat p53, compared and aligned using ClustralW (ClustalW WWW Service at the European Bioinformatics Institute). Position of functional domains indicated by overlayed boxes.

1.8 Bcl-2 family and the apoptotic pathway

1.8.1 Mitochondria and the Bcl-2 family in apoptosis

The mitochondria play a crucial role in the activation of apoptosis. In fact there is growing evidence that all Bcl-2 family members described so far act exclusively on the cytoplasmic face of the mitochondria (and/or the endoplasmic reticulum) (Schinzel et al., 2004). Apoptotic stimuli have been shown to initiate a change in mitochondrial membrane potential prior to caspase-dependent cell death. Loss of membrane potential may be due to opening of a non-selective ion channel called the permeability transition (PT) pore or mitochondrial megachannel. Opening of this pore allows release of proteins usually restricted to the matrix of the mitochondria that have apoptogenic potential. These proteins include apoptosis inducing factor (AIF), which has been found to break down chromatin into large molecular weight fragments, and cytochrome-c, which once released facilitates activation of caspases through its association with the adaptor molecule Apaf-1 (Green and Reed, 1998; Susin et al., 1998). Also released is second mitochondria-derived activator of caspases (Smac) which is a mammalian IAP inhibitor that binds to and neutralises their anti-apoptotic activity (Herr and Debatin, 2001). Further to this, the mitochondrial intermembrane space also contains certain pro-caspases, which upon release become enzymatically active (van Loo et al., 2002).

The mitochondrial PT pore is thought to occur at the site of contact between the inner and outer mitochondrial membranes. Constituents of the pore include the voltage dependent anion channel (VDAC), adenine nucleotide translocator (ANT) and cyclophilin D. Inhibitors of the membrane permeability transition are able to block apoptosis, thus suggesting that the PT pore is central to the apoptotic process(Bradham et al., 1998; Marzo et al., 1998). Also, it has been found that hypoxia-induced increases in free cytosolic calcium is able to open the PT pore (Crompton, 1999). Bcl-2 family proteins interact with the PT-pore by modulating VDAC activity (Shimizu et al., 2000). Bcl-2 is anchored to the outer mitochondrial membrane and its primary role is suggested to be regulation of cytochrome-c release (Kluck et al., 1997; Rosse, 1998). Bcl-xL has fractions in both the cytosol and the mitochondrial membrane, whilst Bax is a cytosolic protein under normal conditions. After an apoptotic stimulus Bax and Bcl-xL translocate to the mitochondrial membrane, thus membrane association has been implicated in these proteins regulatory functions (Gross et al., 1999; Hsu et al., 1997). It is thought that the BH-4 domain of Bcl-2 and Bcl-xL is responsible for directly inhibiting VDAC activity, whilst Bax and Bak

stimulate VDAC activity through their BH-3 domains, allowing passage of cytochrome-c (Narita et al., 1998; Shimizu et al., 2000).

Alternatively, Bcl-2 family members may act as ion channels themselves at the mitochondrial membrane (Henry-Mowatt et al., 2004). Bax has been shown to form pH and voltage dependent ion channels in lipid bilayers which can be inhibited by Bcl-2. Thus rather than acting on the VDAC directly, Bax may elicit its pro-apoptotic effects through an intrinsic pore forming action (Antonsson et al., 1997). Based on predicted three-dimensional structures, possibly similar to the pore-forming domain of bacterial toxins, various other proteins in the Bcl-2 family may also act at the mitochondria by forming ion-conducting channels (Reed, 2000).

Distribution of Bcl-2 family proteins after an apoptotic stimulus in relation to the mitochondria appears to influence greatly the effect on the cell. Khaled and colleagues found that after withdrawal of IL-7 and IL-3 from a dependent cell line, a transient rise in intracellular pH occurred. This alkalisation resulted in exposure of the hydrophobic transmembrane domain of Bax and translocation to the mitochondria (Khaled et al., 1999). Hsu and colleagues looked at normal mouse thymocytes treated with dexamethasone to induce apoptosis. This treatment did not cause an overall increase in the level of Bcl-2, Bcl-xL or Bax protein but did induce the translocation of Bcl-xL and Bax to the outer mitochondrial membrane. Inhibition of apoptosis by the drug cycloheximide blocked the shift of these proteins to the membranes. Also, removing the c-terminus from the proteins halted membrane insertion but did not alter their death promoting or inhibiting action (Hsu et al., 1997). Although little data is published, proteins that may be involved in binding the Bcl-2 family to the mitochondria or putative membrane receptors include the TOM-proteins (TOM-20 and 22) and mitochondrial FK506-binding protein 38 (Schinzel et al., 2004).

1.8.2 ER and the Bcl-2 family in apoptosis

Bcl-2 family proteins are also localised to the endoplasmic reticulum membrane although little is known about their action there. Several ER membrane proteins though have been shown to interact with the Bcl-2 proteins to enhance their anti-apoptotic ability, for example Bax inhibitor-1 and Bcl-2/Bcl-xL-associated Bap-31. Similarly, Cnx1 interacts with Bak to increase its pro-apoptotic potential. In contrast, members of the ER-anchored reticulon family NSP-C and RTN-Xs bind to Bcl-xL and Bcl-2 and contribute to apoptosis (Herr and Debatin, 2001). It is known that the ER plays an active role in apoptosis by

activating stress response pathways, JNK, NF-κB and caspase-12, and now growing evidence suggests that there is considerable cross talk between the ER and mitochondria. It is also thought that Bcl-2 may exert its protective effect in the compartments by controlling calcium homeostasis (Ghribi et al., 2001). It is thought that expression of Bcl-2 decreases the free Ca^{++} concentration within the ER lumen by increasing the Ca^{++} permeability of the ER membrane and hence works in an ion channel function possibly similar to the mitochondria (Foyouzi-Youssefi et al., 2000).

1.8.3 Death receptors and the Bcl-2 family

The Bcl-2 family can also regulate apoptosis at the cell surface level through the death receptor pathway. The death receptor Fas (which belongs to the tumour necrosis factor superfamily) and its ligand have been shown to activate caspases rapidly after an apoptotic stimulus. Fas utilises an adaptor protein Fadd to recruit caspase-8 to initiate a cascade of sequential caspase activation that leads to cell death (Ashkenazi and Dixit, 1998; Nagata, 1994). There is also significant cross talk with the mitochondrial pathway of cell death, particularly through the Bcl-2 family member Bid. Bid is activated by caspase-8, which in turn initiates the conformational transformation of Bax and its subsequent insertion into the mitochondrial membrane (Luo et al., 1998). The Bax/Bcl-2 ratio within a cell has also been recognised as a predictor of the susceptibility of cells to Fas-mediated apoptosis (Raisova et al., 2001), and in many cells overexpression of Bcl-xL or Bcl-2 can inhibit the Fas signalling pathway (Scaffidi et al., 1998). High levels of Fas and FasL have been found in the intestine (Pinkoski et al., 2000).

1.9 Bcl-2 and apoptosis in the intestine

1.9.1 Protein expression of Bcl-2 members in the intestine

Krajewski and colleagues have published a number of papers examining the expression of different Bcl-2 family members throughout normal and neoplastic tissue (Krajewska et al., 2002; Krajewski et al., 1995; Krajewski et al., 1996; Krajewski et al., 1994a; Krajewski et al., 1994b). Using immunohistochemistry, they have observed differences in expression profiles between the small and large intestines and also within the tissue's regions for the Bcl-2 family members. Most importantly, Bcl-2 is strongly expressed within the crypts of the colon whereas there is very little to no expression within the crypts of the small intestine. Conversely, there is intense staining of Bax within the crypts of the small intestine and weak expression within the colonic crypts. This pattern of expression for pro and anti-apoptotic family members may be a contributing factor in the increased sensitivity

of small intestinal stem cells to apoptosis compared to those of the large intestine (Merritt et al., 1995; Pritchard et al., 1999).

The Bcl-x gene can produce two protein products, anti-apoptotic Bcl-xL and pro-apoptotic Bcl-xS. It is believed that Bcl-xS is not expressed within the intestine but the long isoform Bcl-xL has widespread expression within the small and large intestine. This anti-apoptotic family member has shown expression within the crypts and villi of the small intestine and predominant staining in the apical region of the colonic crypts (Krajewski et al., 1994b). The pro-apoptotic family member Bak is also found to be strongly expressed within the intestine and is functionally similar to Bax (Chernavsky et al., 2002). Indeed, tissues which express little to no Bax, such as the absorptive epithelial cells of the jejunum and ileum, often contain prominent Bak immunostaining. It has also been suggested that Bak may be the principal promoter of apoptosis in the intestinal epithelium. This is due to its increased expression in regions of apoptosis and the lack of consistent changes in expression after an insult in the other family members (Moss et al., 1996).

Bim is a BH-3 domain only member of the Bcl-2 family that is also expressed throughout the intestine. Its pattern of expression is somewhat reciprocal to that of Bax, with staining seen in the base of the colonic crypts and also throughout the villi (O'Reilly et al., 2000). Another BH3-only protein, Bad, has significantly more restricted expression than other pro-apoptotic Bcl-2 family proteins with very weak or absent expression in the intestine (Kitada et al., 1998). By Western Blot analysis, the anti-apoptotic Bcl-2 family protein, Bcl-w, was found to be expressed strongly in the colon and moderately in the small intestine (O'Reilly et al., 2001). Lastly, Mcl-1 an anti-apoptotic family member which is closely related to Bcl-2 has been examined. In the small intestine it has strong expression throughout the epithelium although more intense in the cells located at the upper portions of the villi. In the colon, this gradient of moderate staining in the crypt base to intense staining at the luminal surface is roughly opposite to that of Bcl-2 (Krajewski et al., 1995). A brief overview of the current understanding of Bcl-2 family expression within the intestine is shown in Table 1 and Figure 1.5.

Table 1. Summary of findings from studies examining expression of Bcl-2 family proteins within the normal intestine.

Author	Bcl-2 family member	Function	Protein expression Small intestine	Protein expression Large intestine
Krajewski	Bcl-2	Anti-apoptotic	Villi – low/moderate Crypts – absent	Apical cells – low Basal cells – high
	Bax	Pro-apoptotic	Villi – moderate Crypts – high	Apical – high Basal – low
	Bcl-xL	Anti-apoptotic	Villi – moderate Crypts – moderate	Apical – moderate Basal – low
	Bak	Pro-apoptotic	Villi – high Crypts – high	Apical – high Basal – low
	Mcl-1	Anti-apoptotic	Villi – moderate Crypts – very low	Apical – moderate Basal – absent
Hirose	Bcl-2	Anti-apoptotic	Not investigated	Immunopositivity detected lower half of crypts
	Bcl-xL	Anti-apoptotic	Not investigated	Immunopositivity detected entire crypt length
	Bax	Pro-apoptotic	Not investigated	Weak immunopositivity detected apex of crypt
Krajewska	Bid	Pro-apoptotic	Staining present in absorptive epithelium	Not investigated
Wilson	Bax	Pro-apoptotic	Immunoreactivity strongest in crypt base	Immunoreactivity seen upper portion of crypts
	Bad	Pro-apoptotic	Low expression in villus tip and apical crypt cells	Immunoreactivity moderate in table region and absent from crypt base
O'Reilly	Bim	Pro-apoptotic	High expression in villi and crypt cells	Moderate expression in crypt cells
	Bcl-w	Anti-apoptotic	Moderate expression detected	Strong expression detected
Hockenbery	Bcl-2	Anti-apoptotic	Expression detected lower half of crypts	Expression detected lower half of crypts
Lu	Bcl-2	Anti-apoptotic	Bcl-2 positive cells not detected	Positive cells present in crypt base only

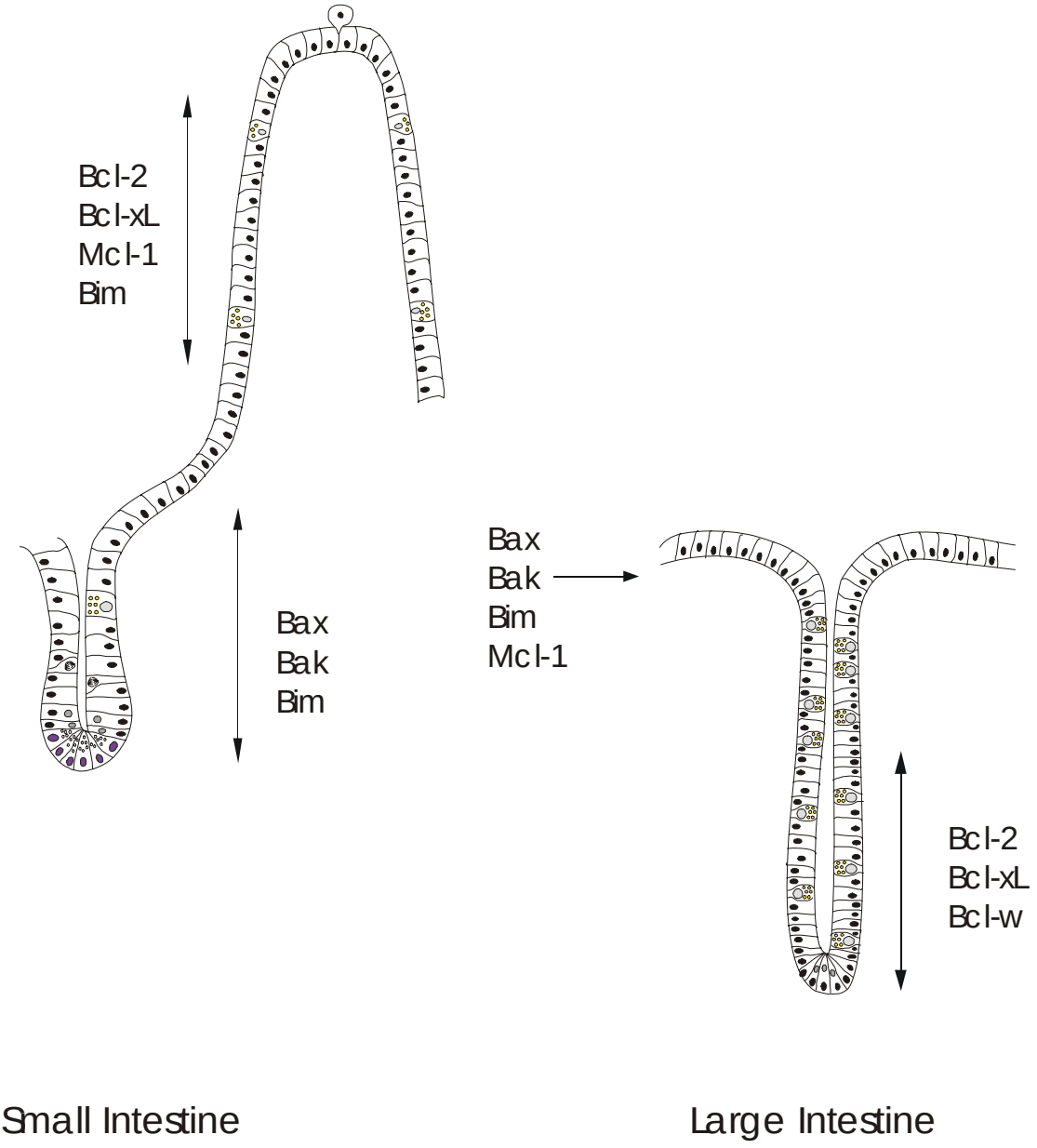

Figure 1.5. Diagram showing the distribution patterns of a selection of Bcl-2 family members in the small and large intestine, as investigated with immunohistochemistry by the authors summerised in table 1.

1.9.2 The role of Bcl-2 in damage-induced apoptosis in the intestine

Studies using gene-knockout mice have highlighted the importance of Bcl-2 family protein expression in the intestinal crypt's response to radiation and chemotherapy. Bcl-2-null mice have a greatly larger apoptotic response in the colonic crypts after radiation compared with wild-type litter-mates (Pritchard et al., 1999). While mice with no Bcl-w gene have much higher apoptosis levels in the crypts of the small intestine after treatment compared to control mice with an intact Bcl-w gene (Pritchard et al., 2000). In contrast, the intestinal crypts of Bax-null mice do not have a decreased apoptotic response compared to control mice (Pritchard et al., 1999). This may be due to other pro-apoptotic members of the Bcl-2 family substituting for Bax and taking over its role as the presumed quintessential apoptotic protein. Evidence to support this has come from experiments using Bax-null, Bak-null or both models which show that damage-induced apoptosis is only ameliorated when both genes are knocked-out (Wei, 2001). Thus it is apparent that apoptosis can be controlled by a number of different Bcl-2 family members, and the balance of expression may determine the response to chemotherapy in the crypts.

1.9.3 Differential sensitivity to apoptosis between small and large intestine

The small and large intestine has different susceptibility to spontaneous and damage induced apoptosis. Under normal conditions, approximately 1 apoptotic cell per villus can be seen in sections cut at 3 μm in the small intestine. Also, one cell in every 5 crypts (or less than 1% of crypt cells) will be undergoing apoptosis at any one time, although this can be as high as 10% within the stem cell region. In the large intestine it is very rare to see an apoptotic cell in the stem cell region with only occasional apoptotic cells seen scattered throughout the crypt and table region. Overall, spontaneous apoptosis occurs ten-fold less in the large intestine compared to the small intestine and this may contribute to the differential cancer incidence between the two tissues (Hickman et al., 1994; Potten et al., 1997b).

In studies examining the effect of radiation on the intestine, it was found that the small intestine is much more susceptible to damage induced apoptosis than the colon. This increased sensitivity has been attributed partly to the lack of expression of anti-apoptotic Bcl-2 within the crypts of the small intestine (Jones and Gores, 1997; Merritt et al., 1994; Merritt et al., 1995). The intestine responds with a dose dependent increase in apoptosis, which peaks approximately 3 to 6 hours after treatment. Increasing numbers of cells in the small intestine die up to a dose of approximately 1 Gy, where ~6 cells per crypt are killed.

Radiation primarily attacks at the site of the stem cell region of the crypts of the small intestine. Within the large intestine, an increasing number of cells die up to 6-8 Gy of radiation, but when specific doses are studied, apoptosis occurs at a lower level compared to the small intestine. Also, the site of apoptotic cells is not specifically located at the stem cell region within the colon but instead scattered throughout the crypt (Potten et al., 1997b).

Further studies have also examined the difference in sensitivity to apoptotic stimuli between the small and large intestine. After treatment with a number of pharmacological compounds that inhibit signal transduction molecules, it was found that in all cases there was a greater increase in apoptosis seen in the small intestine than the large intestine. It was concluded that segment-specific expression of Bcl-2 family members was at least in part responsible for cell survival within the colon after disruptions to signalling pathways (Gauthier et al., 2001a; Gauthier et al., 2001b).

1.10 Effect of chemotherapy agents on p53 and Bcl-2 expression

1.10.1 Chemotherapy and Bcl-2

Breast cancer cells treated with various cytotoxic agents to induce apoptosis upregulate Bax and downregulate Bcl-2 in a time-dependent and dose-dependent manner (Gibson et al., 1999; Leung and Wang, 1999). Similar experiments using colon cancer cell lines treated with 5-fluorouracil (5-FU) found that Bax and Bak expression was significantly increased without consistent change to other family members (Nita et al., 1998). An increase in Bax expression was observed in the intestinal crypts of mice, concurrent with sites of apoptosis following 5-FU treatment (Inomata et al., 2002). Many chemotherapy agents induce apoptosis in a p53-dependent manner which is known to critically involve the Bcl-2 family (Hickman et al., 1994; Lane et al., 1994; Merritt et al., 1994). Hence it is plausible that similar results could be seen in studies using normal intestinal tissue. A report by Kitada et al has shown that gamma-radiation increases Bax expression in mouse small intestine (Kitada et al., 1996). Recently it has also been shown that combined chemoradiotherapy (MTX + whole body irradiation) causes an increase in Bax, Bak and Bad RNA expression in the mouse intestine (Beck et al., 2004).

1.10.2 Chemotherapy and p53

The effect of chemotherapy treatment on p53 expression and subsequent apoptosis in the intestine has been thoroughly investigated compared to the Bcl-2 family. Activation of

p53 occurs in response to DNA damage and results in either the arrest of the cell cycle at one of its checkpoints or the induction of apoptosis (Benchimol, 2001). The activation of p53 is mainly at the post-translational level where the protein is stabilised through phosphorylation by a number of cell protein kinases. Possibly the most important activator of p53 is the protein kinase ATM, which recognises double-stranded DNA breaks (Bartek and Lukas, 2003). This stabilisation allows it to accumulate in the nucleus where it binds to and modulates transcription of genes including Bax and Bcl-2 (described above), and the cyclin dependent kinase inhibitor $p21^{waf1/cip1}$. The protein products of these genes regulate apoptosis and cell cycle progression respectively. The action on these genes in part explains the cells response to stress (Komarova and Gudkov, 2000). Enhanced transcription of the death receptor gene Fas by p53 also occurs after chemotherapy treatment, which enhances the sensitivity of the cell to apoptosis (Herr et al., 1997; Muller et al., 1998a; Muller et al., 1998b).

Transcriptional upregulation of effector genes is not the only way in which p53 can induce cell death. Recently it has been shown that cytoplasmic p53 can directly interact with members of the Bcl-2 family at the mitochondrial membrane to induce cytochrome c release ((Erster et al., 2004). Although the exact mechanism remains to be defined, it has been postulated that accumulation of p53 in the cytoplasm can function analogously to BH-3-only proteins (such as Bid), causing oligomerisation and membrane insertion of the pro-apoptotic proteins Bax and Bak (Chipuk et al., 2004). Alternatively, p53 could disrupt Bax/Bak heterodimers with anti-apoptotic family members and effectively become the dominant complex. This would release Bax and Bak to associate with the mitochondrial membrane. Evidence to support this is mitochondrial localised p53 has been shown to disrupt the Bak/Mcl-1 complex preceding caspase activation (Leu et al., 2004). As such it appears p53 has the ability to modulate apoptosis independently of new protein synthesis.

It is suggested that the amount of p53 protein present in the tissue determines its response to genotoxic stress (Komarova and Gudkov, 2000; Lane et al., 1994; Weller, 1998), and studies investigating the correlation between p53 status and radiosensitivity in the small and large intestine have supported this statement. Wilson and colleagues found that ionising radiation induced p53 expression in the crypts of the small intestine, and that sites of p53 immunopositivity were coincident with distribution of apoptotic cells (Wilson et al., 1998). Further to this, experiments using p53 null mice given whole body irradiation showed no difference in apoptosis levels compared to non-treated animals. Hence the

intestinal epithelial cells became radioresistant with loss of p53 (Merritt et al., 1994). Finally, a landmark study by Pritchard and colleagues showed that p53 is responsible for crypt damage after treatment with 5-FU. The experiment used $p53^{-/-}$ mice which after cytotoxic treatment had significantly reduced apoptosis and inhibition of cell cycle progression compared to $p53^{+/+}$ mice. In these mice, crypt integrity was maintained proving that the p53-dependent response to cell stress is responsible for gastrointestinal damage during chemotherapy (Pritchard et al., 1998). Thus both radiation and chemotherapy induce a p53-dependent apoptosis of crypt cells.

1.11 Prevention of mucositis, p53 and pifithrin-α

1.11.1 Anti-mucositis agents

Considerable effort has gone into developing ways to prevent intestinal mucositis, with studies investigating a wide range of possible therapeutical strategies. Growth factors including KGF, IGF and TGF-β act on the intestinal mucosa and have each been shown in different settings to reduce damage in intestinal tissue to some degree after chemotherapy treatment (Booth and Potten, 2001; Gibson et al., 2005; Gibson et al., 2002a; Gibson et al., 2002b; Howarth and Shoubridge, 2001). Worth noting is the recent approval of the use of recombinant human KGF (Palifemin, Amgen) in the prevention of oral mucositis during haematological malignancy treatment. The interleukins have wide ranging biological functions and interleukin-11 and -15 especially have shown potential as agents effective in amelioration of chemotherapy-induced intestinal damage (Cao et al., 1998a; Cao et al., 1998b; Gibson et al., 2002b). Recently a study using TGF-β2 has had modest success in preventing small intestinal side-effects of MTX treatment in rats possibly through modulation of stem cell cycle time (van't Land et al., 2002). Oral administration of anti-doxorubicin (doxorubicin is an anti-metabolite chemotherapy agent) monoclonal antibodies to mice has also had some success in reducing gastrointestinal toxicity. This treatment inhibited crypt cell apoptosis, weight loss and mortality after mice were given 12 mg/kg of doxorubicin (Morelli et al., 1996). A synthetic bacterial lipopeptide, JBT-3002 has shown to inhibit irinotecan-induced damage in the intestine by protecting the epithelium and lamina propria (Shinohara et al., 1998). In another study, an intestinal trophic peptide that is secreted by enteroendocrine cells in response to injury called glucagon-like peptide (GLP-2) was administered to mice before treatment with the chemotherapy drugs irinotecan hydrochloride and 5-FU. Mice that received GLP-2 showed significantly improved survival rates and attenuation of epithelial damage

compared with buffer treated animals (Boushey et al., 2001). In contrast to this, an experiment using lactoferrin to inhibit GLP-2-induced proliferation in the intestine was effective in reducing MTX-induced damage. The authors suggested that temporally arresting epithelial cell cycling in the intestine protected it from the deleterious side effects of the anticancer therapy (van't Land et al., 2004). A somewhat natural approach to limiting the gastrointestinal side effects of MTX treatment in the rat was investigated by Horie and colleagues, who used extracts of aged garlic. By measuring small intestinal permeability of the compound fluorescein-isothiocyanate-labeled dextran, they showed that rats fed with the aged garlic extract diet maintained a similar level of permeability to untreated rats, indicating they had ameliorated MTX-induced damage (Horie et al., 1999). Rats fed soybean extract also appeared to be somewhat protected from the gastrointestinal side effects of MTX treatment, with improved incidence of diarrhoea, anorexia and crypt cell death compared to animals fed a normal rat chow diet (Funk and Baker, 1991). While milk growth factors enriched from cheese whey reduce bacterial translocation and increase jejunal crypt area in rats following MTX treatment (Howarth et al., 1996). Other factors trialed as anti-mucotoxics include vitamin A, bombesin, intestinal trefoil factor, zinc, and glutamine (Beck et al., 2004; Chu et al., 1994; Nagai et al., 1993; Papaconstantinou et al., 2000; Tran et al., 2003). Many other studies not mentioned have attempted to find a way to prevent mucositis but currently there is no effective intestinal anti-mucositis treatment available.

1.11.2 p53 and pifithrin α

p53 is one of the major determinants of the side-effects of chemotherapy (Pritchard et al., 1998). Thus it seems likely that inhibiting the p53-dependent apoptotic response may effectively reduce damage in the intestine. Suppression of p53 as a method for overcoming the side effects of antitumour therapy is a relatively new idea. Previously efforts have concentrated on re-establishing p53 function in tumours rather than further suppressing p53 which was seen as too dangerous. However, over 50% of human cancers do not have functional p53, and so it may prove a useful therapy. Of course p53 suppression with molecules during chemotherapy is only suited to those patients already shown to lack active p53 in their cancer (Komarova and Gudkov, 1998; Komarova and Gudkov, 2000; Komarova and Gudkov, 2001).

Pifithrin-alpha (PFTα) is an anti-parasitic compound, effective in protecting cultured neurones from death induced by DNA-damaging topoisomerase I and II inhibitors. It has a

potential role in the prevention of neurodegenerative diseases such as Alzheimer's, Parkinson's and cerebrovascular stroke (Zhu et al., 2002). PFTα has also been shown to block activation of p53 in response to doxorubicin, ultraviolet and gamma radiation, etoposide, taxol, cytosine arabinoside, ischaemia and hyperthermia (Zhang et al., 2003). However, it is unable to prevent cell death due to trophic factor withdrawal which is a p53-independent form of cell death, proving its specificity to p53-mediated apoptosis (Zhu et al., 2002). Importantly, PFTα has been shown to be effective in saving mice from lethal doses of radiation, without promoting tumour formation (Komarov, 1999). No tumours were found in mice one year after treatment, therefore it does not appear to increase the risk of cancer development. Thus, temporary suppression of p53 is somewhat different from complete p53 deficiency in terms of cancer predisposition. The most interesting point from that study was that PFTα administered directly before high doses of gamma irradiation significantly abrogated apoptosis seen in crypts and villi of mice compared to untreated controls (Komarov, 1999). In experiments with p53-null mice, PFTα did not affect apoptosis incidence further proving its specificity to p53-dependent apoptosis. Other possible applications for PFTα could include hyperthermia stress, ischaemic diseases and brain degeneration (Komarova and Gudkov, 2001). This small, stable and lipophilic molecule has since been investigated for its potential to decrease neuronal death in a model of stroke and neurodegenerative disorders and also for acceleration of wound healing, with both having encouraging results (Culmsee et al., 2001; Vollmar et al., 2002). And more recently, PFTα has been used in numerous studies testing its ability to protect against cisplatin treatment, heat shock, glucocorticord signalling and endotoxin-induced cell death (Komarova et al., 2003; Schafer et al., 2003; Zhang et al., 2003).

It has been shown that PFTα works by inhibiting p53 DNA-binding activity and activation of Bax and p21, without affecting overall production of p53 protein in cells undergoing apoptosis. It has yet to be shown how PFTα affects expression of other members of the Bcl-2 family in response to damage. PFTα also stabilises mitochondrial function and suppresses caspase activation (Komarov, 1999), making it a promising candidate as an anti-mucositis agent. Pertaining to this, an experiment using both a single and a fractioned cumulative radiation dose which were relevant to clinical anticancer treatment doses protected mice and increased survival (Komarova et al., 2004). An outline of the apoptotic pathway and how PTFα modulates this is shown in Figure 1.6.

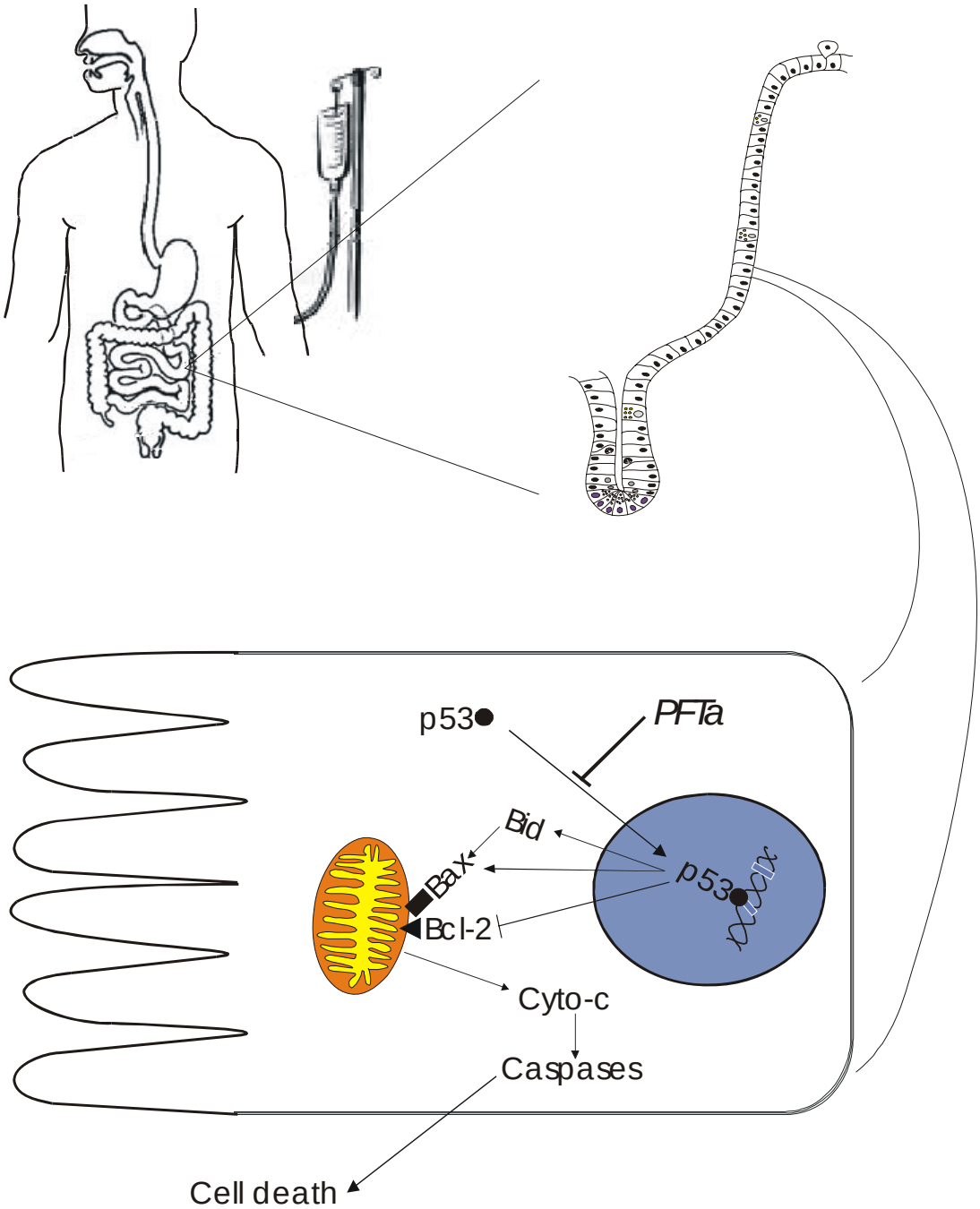

Figure 1.6. Diagram of the mitochondrial-regulated apoptosis pathway. Chemotherapy causes genotoxic damage which is recognised by p53. Translocation of p53 into the nucleus allows transcriptional regulation of multiple Bcl-2 family members. Insertion of Bax into the mitochondrial membrane induces release of cytochrome c, which in turn activates caspases. PFTa blocks movement of p53 into the nucleus to prevent initiation of cell death pathway.

1.12 Summary

Intestinal mucositis occurs as a consequence of cytotoxic treatment through complex interactions within the tissue, most notably crypt cell death and cytostasis. The molecular control of these actions although known to involve p53, the Bcl-2 family and caspases, is yet to be fully elucidated within the gastrointestinal epithelium. This review has attempted to provide an overview of the current research in the area and identify areas in which further elucidation is required. The work carried out in the following chapters has thus been designed to go some way to increase the understanding of the mechanisms responsible for small intestinal mucositis.

1.13 Specific aims and hypothesis

The hypothesis for this thesis is that the Bcl-2 family of proteins, under the control of p53, regulate apoptosis in the small intestine following chemotherapy and therefore contribute to mucositis severity.

Thus the specific aims of this PhD were:

1) To examine the protein and mRNA expression of Bcl-2 family members within intestinal crypts before and after chemotherapy
2) To identify correlations between changes in expression of specific Bcl-2 family members and apoptosis after chemotherapy and determine those primarily responsible for mucositis
3) To examine the role of p53 in modulation of proteins involved in intestinal cell death
4) To investigate the ability of PFTα to inhibit intestinal damage following irinotecan treatment in the rat with breast cancer.
5) To identify other genes possibly involved in the onset of intestinal mucositis in the rat with breast cancer.

Investigation of Bcl-2 family protein expression in the crypts of the small and large intestine of the DA rat with breast cancer.

2.0 Introduction

The gastrointestinal epithelium is a rapidly renewing tissue with a constant turnover of cells. Cells are produced within the crypts, the proliferative units of the gut, by stem cells (Potten and Loeffler, 1990). Daughter cells migrate up the crypt towards the villus in the small intestine and table region in the colon, differentiating as they do so. At the luminal surface, these cells are either extruded into the lumen or removed by apoptosis while still attached to the basement membrane (Hall et al., 1994; Potten et al., 1997a). This exfoliation ensures that the structure of the epithelium remains constant by removing cells which are no longer required. Spontaneous apoptosis also occurs in the stem cell region of the crypt, albeit at a relatively low level. This is thought to occur as a strategy to remove excess dividing cells, thus maintaining the appropriate rate of proliferation (Potten, 1992).

To date a discrepancy in the rate of spontaneous apoptosis that occurs in the small and large intestine has been noted (Gauthier et al., 2001b). It has been estimated that spontaneous apoptosis occurs at a ten-fold higher rate in the crypts of the small bowel compared to the colon (Potten et al., 1997b). This can not be accounted for by the respective number of stem cells in each region, which are approximately 4-16 in the small intestine, and 1-4 in the large intestine. This has implications for cancer as the incidence of neoplasia is far greater in the colon (Potten et al., 1992). Further to this, damage-induced apoptosis is often much greater in the crypts of the small bowel. This has been shown conclusively with the folate antagonist methotrexate, and irradiation (Gibson et al., 2005; Merritt et al., 1994; Potten and Grant, 1998). Studies using these cytotoxic agents have found that apoptosis is rapidly induced, peaks within 24 h, and is concentrated in the lower portion of the small intestinal crypt. In comparison, the colon has a lower response with apoptosis occurring at a lesser degree and which is distributed throughout the crypt rather than in a distinct site.

It has been proposed that basal expression levels of members of the Bcl-2 family are responsible for the differing levels of apoptosis (Gauthier et al., 2001a; Gauthier et al., 2001b). The Bcl-2 family play an integral role in the intrinsic apoptotic pathway. This pathway utilises the mitochondria as the central checkpoint following a death inducing stimulus, where by Bcl-2 family proteins dock and act to control the release of factors from the intra-mitochondrial space (Kroemer and Reed, 2000). These factors include pro-

caspases, AIF and importantly cytochrome c. Cytochrome c complexes with the adaptor protein APAF-1 and procaspase-9 to activate the caspase cascade and subsequent destruction of the cell (Kluck et al., 1997; van Loo et al., 2002). It has yet to be fully explained how the Bcl-2 family proteins act on the mitochondrial membrane, however the role of heterodimerisation of the opposing anti-apoptotic and pro-apoptotic members is critical in importance (Hanada et al., 1995; Sedlak et al., 1995). The BH-3 only proteins of the Bcl-2 family including, Bim, Bid and Noxa, have the highest affinity for anti-apoptotic members such as Bcl-2, Bcl-xL and Mcl-1 (Fleischer et al., 2003). The multiple domain pro-apoptotic members, such as Bax and Bak, have a lower binding affinity to anti-apoptotic members, but these still remain the dominant complex compared to homodimerisations between other members. When an anti-apoptotic member such as Bcl-2 is heterodimerised with a pro-apoptotic member such as Bax, the protein structure is in an inactive form, possibly due to the death-inducing BH-3 domain of Bax being hidden in this configuration. If this complex is disrupted or if all the anti-apoptotic proteins have been sequestered, Bax and Bak are left free to form homodimers which are toxic to the cell and induce the release of cytochrome c (Bouillet and Strasser, 2002; Eskes et al., 2000; Shimizu and Tsujimoto, 2000; Simonian et al., 1996; Zong et al., 2001). Therefore the respective levels of each protein in the cell are extremely important, particularly the pro- to anti-apoptotic ratio between members. Double gene knockout studies have highlighted this, with the requirement of at least Bax or Bak for apoptosis to occur following a cellular insult. BH-3-only family members do not induce apoptosis but rather sensitise cells to death (Wei, 2001; Zong et al., 2001).

To accurately investigate why apoptosis often occurs at a higher level in the small intestine compared to the large intestine, it seems appropriate that the basal level of expression of multiple Bcl-2 family proteins should first be described. Currently there exists little data on the expression levels of Bcl-2 family proteins in the rat intestine, with the vast majority of studies having been conducted in mice and more recently in human subjects. Also yet to be investigated is the expression of these proteins in an animal model with cancer. Therefore the primary aim of this study was to characterise the expression of Bcl-2 family proteins in the small and large intestine of the rat implanted with mammary adenocarcinoma. This was to investigate why the small intestine epithelium is susceptible to apoptosis and in was performed to provide a baseline for future comparison with samples treated with cytotoxic agents for cancer chemotherapy.

2.1 Methods and Materials

2.1.1 Laboratory animals

This study was approved by the Animal Ethics Committee of the Institute of Medical and Veterinary Sciences, Adelaide and complied with National Health and Research Council (Australia) Code of Practice for Animal Care in Research and Training (1997). Eleven female Dark Agouti (DA) rats, aged 6-8 weeks and weighing approximately 180 g, were purchased from the Institute of Medical and Veterinary Sciences MedVet Division, group housed and kept under a 12 h light/dark cycle with free access to food and water until the study commenced (approximately 2 weeks).

2.1.2 Preparation of tumour inoculum

All animals used in this and subsequent studies carried a subcutaneous tumour. The mammary adenocarcinoma for this study arose as a spontaneous tumour in the 1970s. It has been propagated since by passage through female DA rats. The tumour was donated by Dr. A. Rofe (Institute of Medical and Veterinary Sciences, Adelaide, South Australia) in 1996 to develop a model to assess small intestinal and tumour effects of chemoprevention (Keefe, 1998). This tumour has since been used extensively in our laboratory. One female donor rat was injected s.c. on both flanks with 0.2 ml (2.0×10^7 cells/ml) tumour inoculum 11 days prior to the study beginning. Over the subsequent days, these cells formed a tumour under the skin on both flanks. To harvest the tumour cells, rats were culled by CO_2 asphyxiation and cervical dislocation. Subcutaneous tumours were dissected and placed into ice cold sterile Phosphate Buffered Saline (PBS – 16% NaCl; 0.4% KCl; 0.4% KH_2PO_4; 2.3% Na_2HPO_4). The tumours were diced, homogenised and filtered through sterile gauze. The resultant cell suspension was spun at 250 g for 3 minutes. The supernate was removed and the cell pellet resuspended in fresh sterile PBS. This was repeated a further three times. A viable cell count was carried out using 0.4% w/v trypan blue.

2.1.3 Experimental design

Ten female DA rats (weighing approximately 200 g) were implanted with tumour inoculum of 4.0×10^6 cells in 0.2 ml of PBS s.c. into each flank. These tumours were allowed to grow for 9 days after which time the rats were culled by CO_2 asphyxiation and cervical dislocation. The gastrointestinal tract from the pyloric sphincter to the rectum was removed and flushed with 0.9% w/v saline. Two cm samples of small intestine (jejunum)

at 25% of the length of the small intestine from the pylorus and the mid colon were collected and placed into 10% neutral buffered formalin.

2.1.4 Immunohistochemistry for detection of Bcl-2 family proteins

For immunohistochemical detection of Bcl-2 family proteins, intestinal samples were opened longitudinally along the mesenteric boarder, placed in 10% neutral buffered formalin for 24 h before being routinely processed into paraffin wax. From tissue blocks, two consecutive 3 μm paraffin sections of jejunum and colon were cut onto Histogrip-treated (Zymed Laboratories, San Francisco, CA, USA) glass slides, dewaxed in xylene and rehydrated through graded alcohols to water. On each slide, one section was designated as the negative control and the other as the experimental section. Slides were washed with PBS before heat-mediated antigen retrieval in 10 mM citrate buffer (pH 6.0). Endogenous peroxidase activity was quenched with 3% hydrogen peroxide in methanol for 1 min, while non-specific antigens were blocked with normal serum for 20 mins. Elimination of endogenous avidin and biotin was carried out using a commercial avidin/biotin blocking kit (Vector Laboratories, Burlingame, CA USA) as per manufacturer's instructions. Experimental sections were incubated overnight at 4°C with the primary antibody (Santa Cruz Biotechnology, Santa Cruz, CA, USA, supplied as 200 μg in 1 ml stabilisation buffer) diluted in PBS with 2% serum (as described in Table 2.1). Negative control sections had the primary antibody omitted and were incubated with the dilution solution only. With stringent washes in PBS between each step, sections were incubated with a universal secondary antibody, followed by Ultra-Streptavidin conjugated to horseradish peroxidase and finally diaminobenzidine (DAB) chromogen in 0.03% hydrogen peroxide. Slides were then counterstained in diluted Lillie-Mayer's Haematoxylin, dehydrated and mounted.

2.1.5 Quantitative immunohistochemistry

Immunostaining was assessed as described by Matkowskyj and colleagues and adapted to the intestine (Matkowskyj et al., 2000). This method employs an algorithm that calculates the cumulative signal strength (pixel energy) of a digital file of the image in question. Firstly, staining in each section was visualised with the Nikon 800 research microscope and assessed using a x10 objective lens. A field was chosen which represented the general pattern of staining for the tissue and contained 10 well orientated mature crypts. In all cases staining was uniform and never focal. Then, focussing with a x60 dry lens, digital photomicrographs were taken of identical intestinal crypts in both the control and

experimental sections using a SPOT-RT camera (Diagnostic Instruments Inc, Michigan, Detroit, USA). A 49x49 pixel area of interest was selected over the cytoplasm of several identical crypt cell profiles located from cell positions 2 to 10 along the crypt axis using Image Pro Plus (Media Cybernetics, Silver Spring, MD, USA) in both the control and experimental sections and saved as TIFF files (Figure 2.1). Areas of interest were converted to image matrices, subtracted and normalised using matrix functions in Matlab (Mathworks Inc, Natick, MA, USA) using the algorithm below:

```
%ep;
a=double(imread('exp','tiff'));
b=double(imread('cont','tiff'));
ea=norm(a(:,:,1))+norm(a(:,:,2))+norm(a(:,:,3));
eb=norm(b(:,:,1))+norm(b(:,:,2))+norm(b(:,:,3));
et=abs(ea-eb);
en+sqrt(et^2/2401)
```

The intensity of staining was expressed as the difference in cumulative signal between the control and experimental matrices and given in units of pixel energy.

2.1.6 *Statistical analysis*

All statistical analysis was carried out using the Student's t test to identify differences in mean staining intensity between the jejunal and colonic crypts for each Bcl-2 family member. P-values <0.05 were considered statistically significant.

Table 2.1: The clone, source, dilution factor and positive control tissue used for immunohistochemical detection of Bcl-2 family proteins in the rat intestine.

	Antibody	**Species**	**Clone and Source**	**Dilution**	**Positive Control**
Anti-apoptotic	Bcl-2	Polyclonal, rabbit anti human	N-19, sc-492	1:1000	Spleen
	Bcl-xL	Polyclonal, rabbit anti human	H-62, sc-7195	1:800	Thymus
	Bcl-w	Polyclonal, goat anti human	N-19, sc-6172	1:300	Testis
	Mcl-1	Polyclonal, rabbit anti human	S-19, sc-819	1:5000	Spleen
Pro-apoptotic	Bax	Polyclonal, rabbit anti mouse	P-19, sc-526	1:1000	Thymus
	Bak	Polyclonal, goat anti human	G-23, sc-832	1:800	Stomach
	Bim	Polyclonal, goat anti human	N-20, sc-8265	1:800	Thymus
	Bid	Polyclonal, rabbit anti human	FL-195, sc-11243	1:2500	Spleen

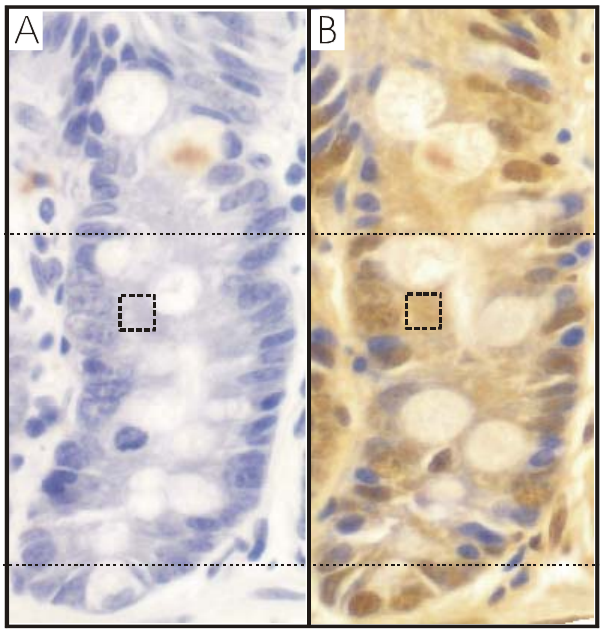

Figure 2.1: Photomicrographs of a serial A) control and B) experimental section showing quantification region overlayed with 49 x 49 area of interest box. Original magnification x600.

2.2 Results

2.2.1 Histology

At autopsy, both the small and large intestine appeared normal. Under microscopic inspection the jejunum and colon exhibited no deviation from expected histological parameters.

2.2.2 Bcl-2

Moderate Bcl-2 staining was found in villous enterocytes and lamina propria cells in all jejunal samples. Crypt staining was generally absent or occasionally very weak. In the colon, Bcl-2 staining occurred diffusely within lower crypt epithelium and also throughout the lamina propria. Staining was always cytoplasmic in nature. Matlab analysis of staining showed mean ± SE signal intensity of 42.1 ± 5.0 and 72.1 ± 12.9 pixels in the jejunal and colonic crypts, respectively.

2.2.3 Bcl-xL

Bcl-xL staining was present in the villous epithelium at a moderate intensity. A few strongly positive cells were also seen in the lamina propria. Jejunal crypts contained sporadic regions of moderate staining in the upper portions of the crypt but generally showed only very weak immunopositivity, especially in the lower section of the crypt. Staining was cytoplasmic and sometimes associated with the nuclear membrane. Matlab analysis of staining showed a mean ± SE signal intensity of 44.2 ± 7.8 and 71.3 ± 4.2 pixels in the jejunal and colonic crypts respectively.

2.2.4 Bcl-w

Staining for Bcl-w could not normally be detected in the crypts of the jejunum, except for very weak positivity seen occasionally in Paneth cells. Villous enterocytes showed weak staining for Bcl-w. In comparison, the crypts of the colon showed moderate staining with intensity increasing towards the apical region. Staining was always cytoplasmic in nature. Matlab analysis of staining showed a mean ± SE signal intensity of 34.2 ± 3.9 and 49.4 ± 4.6 pixels in the jejunal and colonic crypts respectively.

2.2.5 Mcl-1

Mcl-1 had a diffuse pattern of moderately intense staining throughout jejunal crypts. Villous epithelium showed weak to moderate staining while the lamina propria and muscle were not positively stained. The colon also showed moderate staining for Mcl-1 which

appeared even throughout the crypts. Staining was always cytoplasmic in nature. Matlab analysis of staining showed a mean ± SE signal intensity of 47.1 ± 5.2 and 49.8 ± 7.2 pixels in the jejunal and colonic crypts respectively.

2.2.6 Bax

There was strong staining for Bax throughout the jejunal epithelium. Immunostaining was especially strong within the crypts, while there appeared to be very little staining of other tissues such as the lamina propria. Bax staining in the colonic crypts showed a gradient of increasing intensity from absent/very weak at the crypt base to intense at the apical region. Lamina propria cells were often stained moderately. Staining was cytoplasmic. Matlab analysis of staining showed a mean ± SE signal intensity of 119.7 ± 7.8 and 48.9 ± 8.5 pixels in the jejunal and colonic crypts respectively.

2.2.7 Bak

Bak staining in the jejunum was intense at the base of the crypts and moderate in the remainder of the crypts and villus epithelium. Moderately stained cells also appeared in the lamina propria. Colonic crypts showed Bak staining predominantly within the upper half of the crypt with occasional moderately stained cells in the lower section. Lamina propria was also moderately stained as was muscle. Staining was always cytoplasmic in nature. Matlab analysis of staining showed a mean ± SE signal intensity of 84.2 ± 15.2 and 51.4 ± 7.8 pixels in the jejunal and colonic crypts respectively.

2.2.8 Bim

Villus epithelial cells had strong Bim staining in the jejunum. The lamina propria was moderately stained while the crypts showed weak staining. Single, individual cells intensely stained were also often present within the crypt epithelium. The colon had a gradient of staining for Bim along the crypt axis from absent at the crypt base to strong at the apical zone. The table region of the colon showed very intense staining for Bim. Staining was always cytoplasmic in nature. Matlab analysis of staining showed a mean ± SE signal intensity of 62.2 ± 9.4 and 39.0 ± 5.3 pixels in the jejunal and colonic crypts respectively.

2.2.9 Bid

Staining for Bid was strongest in the cells at the top of the jejunal crypts and villous base. The lower portion of the crypts had moderate to weak epithelial staining. Villus

enterocytes contained only weak staining and very few lamina propria cells contained moderate staining. Colonic crypts had very weak Bim staining in the lower half of the crypts and weak to moderate immunostaining in the top half of the crypts. Staining was cytoplasmic or associated with the nuclear membrane. Matlab analysis of staining showed a mean ± SE signal intensity of 71.6 ± 11.6 and 29.1 ± 3.2 pixels in the jejunal and colonic crypts respectively.

2.2.10 Small intestinal crypts v large intestinal crypts

Through extrapolation of cumulative signal values for staining of each family member investigated, it was found that expression of Bcl-2, Bcl-xL and Bcl-w was significantly lower in the crypts of the jejunum compared to the colon ($p<0.05$). Expression of Bax, Bak, Bim and Bid was significantly higher in the crypts of the jejunum compared to the colon ($p<0.05$). There was no significant difference in expression of Mcl-1 protein between jejunal and colonic crypts. Representative crypt staining for all antibodies shown in Figure 2.2 and 2.3. Staining intensity data shown in Figure 2.4 and 2.5.

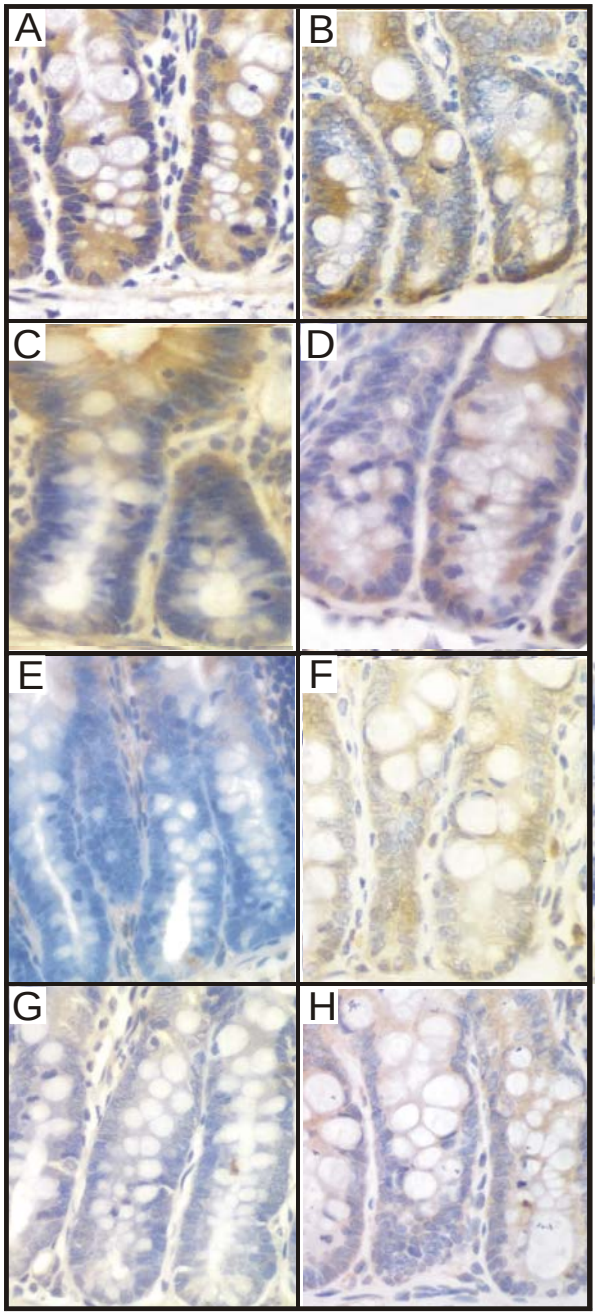

Figure 2.2. Photomicrographs of representative staining in jejunual crypts for A) Bax, B)Bak, C) Bim, D) Bid, E) Bcl-2, F) Bcl-xL, G) Bcl-w, and H) Mcl-1. Original magnification x400.

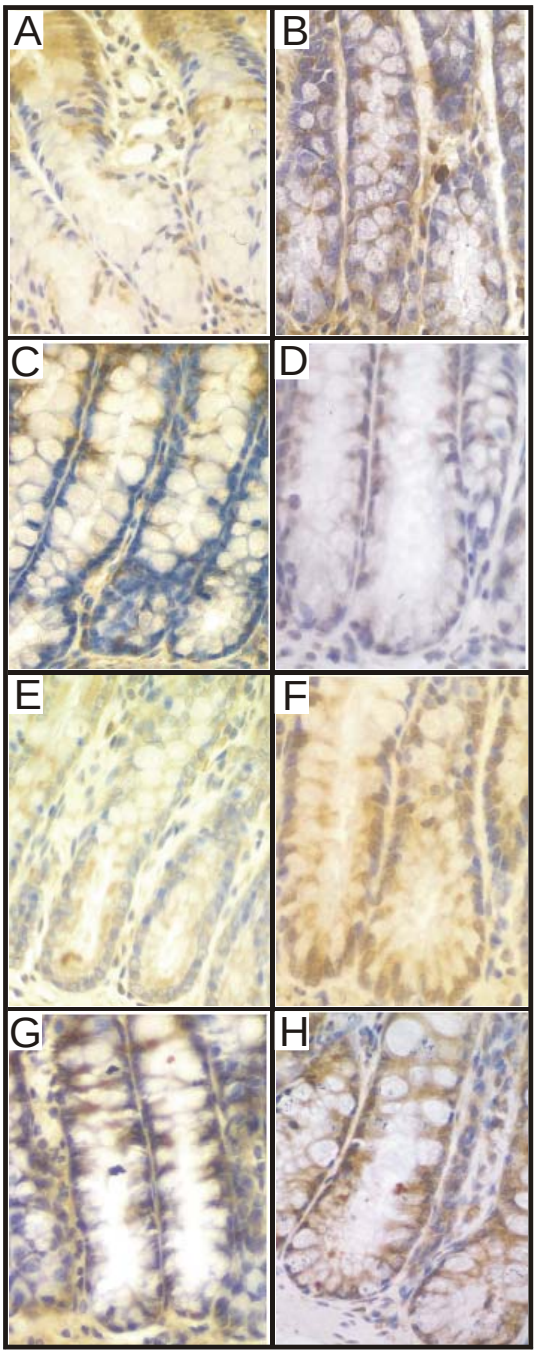

Figure 2.3. Photomicrographs of representative staining in rat colonic crypts for A) Bax,B) Bak, C) Bim, D) Bid, E) Bcl-2, F) Bcl-xL, G) Bcl-w and H) Mcl-1. Original magnification x400.

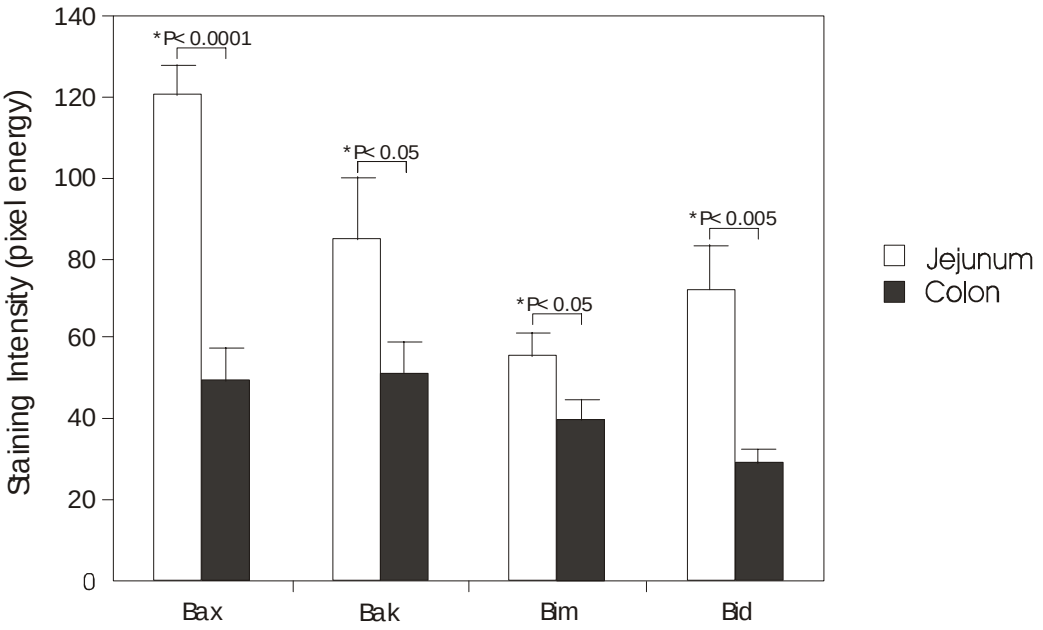

Figure 2.4. Differential protein expression in intestinal crypts of pro-apoptotic Bcl-2 family members. Results shown are group mean + SE (n = 10).

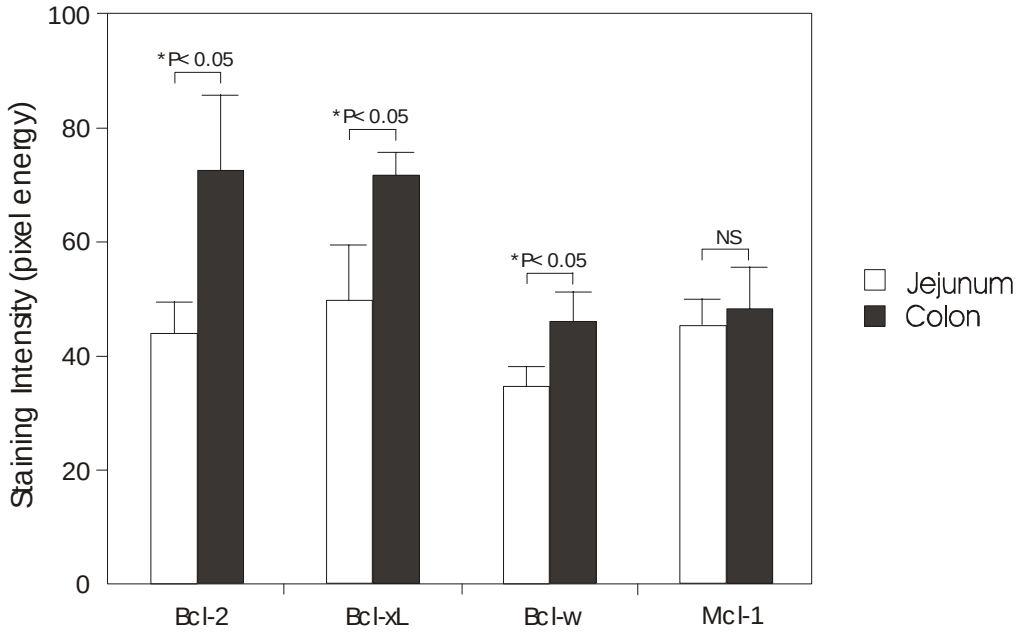

Figure 2.5. Differential protein expression in intestinal crypts of anti-apoptotic Bcl-2 family members. Results shown are group mean + SE (n = 10).

2.3 Discussion

The Bcl-2 family of proteins are well known for their regulatory control of the apoptotic pathway. They provide enhancing and inhibitory signals to the cell through the pro- and anti-apoptotic members respectively (Reed, 1998). During normal conditions, Bcl-2 proteins are found in the cytoplasm or loosely associated with intracellular membranes. During an apoptotic stimulus, these proteins transport primarily to the outer mitochondrial membrane and to a lesser extent the endoplasmic reticulum (Gross et al., 1999; Schinzel et al., 2004). Here they are integral in controlling the release of apoptogenic factors into the cytoplasm, with anti-apoptotic members such as Bcl-2 and Bcl-xL preventing their release and pro-apoptotic members Bax and Bak facilitating release, possibly through opening of ion selective channels (Ghribi et al., 2001; Narita et al., 1998; Tsujimoto and Shimizu, 2002). It is therefore assumed that the ratio of pro- to anti-apoptotic Bcl-2 proteins within the cell provides a rheostat for sensitivity to apoptosis induction (Oltvai et al., 1993; Raisova et al., 2001).

Studies of the small intestine have shown that spontaneous apoptosis occurs in the crypts at a relatively high rate compared to in the colon (Potten, 1998; Potten et al., 1997b). It has also been noted that damage-induced apoptosis is also higher in the small intestine compared to the colon after irradiation and methotrexate treatment (Cai et al., 1997; Gibson et al., 2005; Potten and Grant, 1998). As such, it is hypothesised that the difference in apoptotic sensitivity between the two regions is related to endogenous expression of Bcl-2 family proteins (Gauthier et al., 2001b; Merritt et al., 1995). Specifically, the presence of high levels of the pro-apoptotic protein Bax within jejunal crypts concurrently with low levels of anti-apoptotic protein Bcl-2. To test this, a quantitative immunohistochemistry technique was used to examine the relative expression levels of Bcl-2 family proteins in the small and large intestine of the rat implanted with breast cancer. This approach allows objective assessment of staining for multiple antibodies and produces precise arbitrary values. The technique was validated by the authors who developed the system (Matkowskyj et al., 2003). As expected, expression of Bcl-2 was very low in the crypts of the rat jejunum as indicated by weak to absent immunostaining. This has been documented previously in experiments using human and mouse samples to detect Bcl-2 (Krajewski et al., 1994; Lu et al., 1993). Conversely, moderate Bcl-2 staining was present within the crypts of the large intestine, especially towards the base of the crypt. There was a similar pattern seen for Bcl-xL, with the crypts of the colon having significantly higher levels of expression compared to the jejunum. The

stem cells for both regions are located close to the base of the crypt. These cells are sensitive to radiation and cytotoxic agents, however to a much greater degree in the small intestine (Booth et al., 2001). It is plausible that the protection conferred by endogenous expression of these anti-apoptotic proteins to the stem and their daughter cells in the colon is responsible for the lower level of apoptosis seen. Protection of stem cells or lack of apoptosis within the colon may also be responsible for neoplastic transformation, with the case of carcinomas in the large bowel greatly exceeding the number of cases in the small bowel (Potten et al., 1992). Bcl-w has been show to be important in control of damage induced apoptosis in the small bowel through knockout studies (Pritchard et al., 2000), however in this study could not be detected at any reasonable level in the crypts of the jejunum. Mcl-1 was the only anti-apoptotic family member investigated which had a similar expression profile in the small and large intestine. This protein showed moderate staining in nearly all crypt cells and could possible play a protective role (Krajewski et al., 1995).

The multi-domain pro-apoptotic Bcl-2 family members, Bax and Bak, showed variable expression in the crypts of the small and large intestine. In the jejunum, there was strong staining present, especially in the lower third of the crypt, while the colon staining was confined predominantly to the more apical zone of the crypt and table region. Strong Bax and Bak expression in the small intestinal crypt epithelium has been described previously (Krajewski et al., 1996; Krajewski et al., 1994; Moss et al., 1996) and in this study followed a similar pattern. The presence of these proteins in regions of high levels of apoptosis suggests an active role in tissue regulation in the rat as has been described in the mouse and human intestine. The BH3-only family member Bim was unique in that it had a reasonably similar pattern of staining in the small and large intestine. There appeared a gradient of expression from the base of the crypt to the absorptive surface. In the colon, there was an especially intense area of staining along the table region, indicating a role in epithelial cell extrusion. Sometimes present in the jejunal crypts were intensely stained individual cells which may have represented intraepithelial lymphocytes (personal communication A. Cummins). Bid was expressed in all epithelial crypt cells in the jejunum, while only a proportion of colonic cells expressed Bid. Bid has been implicated as a Bcl-2 family member that is involved in the extrinsic apoptotic pathway, providing a link to the intrinsic (mitochondrial) pathway (Eskes et al., 2000; Luo et al., 1998).

This study has shown that a balance favouring the pro-apoptotic proteins of the Bcl-2 family in the crypts of the small intestine in the rat exists. The expression of Bax, Bak, Bim and Bid were all found to be significantly greater in the crypts of the jejunum compared to the colon. Conversely, anti-apoptotic Bcl-2, Bcl-xL and Bcl-w were all expressed significantly higher in the colonic crypts compared to the jejunum. Together these findings are consistent with existing data describing Bcl-2 family expression patterns in other species and provides a platform to investigate changes in protein levels following cytotoxic treatment.

The effect of cancer chemotherapy treatment on expression of Bcl-2 family genes in the small intestine.

3.0 Introduction

The exact degree of individual and economic burden of mucositis is currently under investigation, however the harmful potential of high grade mucositis is already well known among patients and clinicians. Significant advances in the understanding of the mechanisms underlying mucositis development have occurred in the last decade. With this has come the realisation that effective therapeutic strategies need to be designed around specific pathobiological aspects of the disease. Considerable work has been carried out studying the effect of chemotherapeutic agents on individual cells, both cancerous and normal. This has allowed us to elucidate the well accepted pathway of cytotoxic drug-induced DNA damage, which leads to cytostasis and or apoptosis (Lane et al., 1994; Norbury and Zhivotovsky, 2004; Pritchard et al., 1998). Thus it seems reasonable that a better understanding of the genes involved in apoptosis and how they change following chemotherapy will help to better understand and ultimately to treat intestinal mucositis.

The Bcl-2 gene family, which consists of at least 20 members in mammalian species, controls apoptosis in response to a wide variety of stimuli that include chemotherapy (Adams and Cory, 1998; Gross et al., 1999; Herr and Debatin, 2001). The family contains both pro- and anti-apoptotic members, which are mainly involved in the intrinsic apoptotic pathway through regulation of mitochondrial membrane permeability and caspase activation. The transcription factor, p53, regulates these proteins by controlling expression of certain family members in response to cytotoxic treatment (Benchimol, 2001; el-Deiry, 1998; Gottlieb and Oren, 1998). Cleavage of the executioner caspase-3 occurs as a downstream event and is thought to represent a cellular commitment to death (Marshman et al., 2001; Slee et al., 1999). Pro-apoptotic family members include Bax, Bak, Bcl-xS, Bad, Bid, Bim, Noxa and Puma while anti-apoptotic family members include Bcl-2, Bcl-xL, Bcl-w, Mcl-1 and A1 (Green and Reed, 1998; Konopleva et al., 1999; Saini and Walker, 1998; Strasser et al., 2000). The ratio of pro- to anti-apoptotic family members within each cell is thought to be important for determining protein-protein interaction and ultimately the cellular sensitivity to an apoptotic stimulus (Kelekar and Thompson, 1998; Oltvai et al., 1993).

Many cancer treatment agents and regimens induce apoptosis in the gastrointestinal epithelium, and cause intestinal damage which is manifested in patients with symptoms

such as nausea, abdominal pain and diarrhoea (Decker-Baumann et al., 1999; Keefe et al., 2000). The small intestine is vulnerable to both chemotherapy and radiotherapy-induced damage and shows severe toxicity after treatment (Anilkumar et al., 1992; Pico et al., 1998). This was initially attributed to a high rate of cell proliferation, but expression of apoptosis regulating proteins seems to be a more important mechanism (Cai et al., 1997; Gauthier et al., 2001; Merritt et al., 1995). Apoptosis often occurs in the stem cell region at cell positions 4-6 in the crypts of the small intestine (Hickman et al., 1994; Potten, 1992; Potten et al., 1997). Thus, cytotoxic treatment in this case not only damages small intestinal crypts by apoptosis, but further compounds injury by damaging regenerative stem cells. The combination of apoptosis and reduced proliferation without concurrent reduction in epithelial cell migration causes significant alterations in crypt/villus morphology (Brittan and Wright, 2002; Potten et al., 1997). This reduction in morphometry contributes to malabsorption and anorexia (Carneiro-Filho et al., 2004; Pico et al., 1998; Smith et al., 1979). Apoptosis and cytostasis are not the only contributing factors in the development of mucositis in the small intestine, however to date these remain the best documented description of the cause of epithelial injury. Worth noting is the involvement of inflammatory mediators and damaging factors from tissues such as the endothelium , however further detail is outside the scope of this current study.

Previous studies have described high Bax and low Bcl-2 protein expression in intestinal crypts of murine and human small intestine and correlated this to high levels of apoptosis (Krajewski et al., 1994; Potten et al., 1992; Potten et al., 1997). However, previous studies have not investigated a combination of pro- and anti-apoptotic family members prior to and after chemotherapy *in vivo*. The aim of this study was therefore to investigate any change in relative expression of p53, caspase-3 and Bcl-2 family members following chemotherapy with cytotoxic agents. Expression was investigated in intestinal crypts of both rats and humans over various time points and with varying agents.

3.1 Methods and Materials

3.1.1 Laboratory animals

This study was approved by the Animal Ethics Committees of the Institute of Medical and Veterinary Sciences, Adelaide and of the University of Adelaide and complied with National Health and Research Council (Australia) Code of Practice for Animal Care in Research and Training (1997). Female Dark Agouti (DA) rats, aged 6-8 weeks and weighing approximately 160 g were purchased from the Institute of Medical and Veterinary Sciences MedVet Division. They were group housed and kept under a 12 h light/dark cycle with free access to food and water until the study commenced at approximately 2 weeks.

3.1.2 Preparation of tumour inoculum

All animals used in this study carry a subcutaneous (s.c.) tumour. The mammary adenocarcinoma for this study arose as a spontaneous tumour in the 1970s. It has been propagated since by passage through female DA rats. The tumour was donated by Dr. A. Rofe (Institute of Medical and Veterinary Sciences, Adelaide, South Australia) in 1996 to develop a model to assess small intestinal and tumour effects of chemoprevention (Keefe, 1998). This tumour has since been used extensively in our laboratory. One female donor rat was injected s.c. on both flanks with 0.2 ml (2.0×10^7 cells/ml) tumour inoculum at 11 days prior to the study beginning. Over the subsequent days, these cells formed a tumour under the skin on both flanks. To harvest the tumour cells, the rat was culled by CO_2 asphyxiation and cervical dislocation. Subcutaneous tumours were dissected and placed into ice cold sterile PBS. The tumours were diced, homogenised and filtered through sterile gauze. The resultant cell suspension was spun at 250 g for 3 minutes. The supernatant was removed and the cell pellet resuspended in fresh sterile PBS. This was repeated a further 3 times. A viable cell count was carried out using 0.4% w/v trypan blue.

3.1.3 Experimental design

Twenty four female DA rats (weighing approximately 180 g) were implanted with tumour inoculum of 4.0×10^6 cells in 0.2 ml of PBS s.c. into each flank. These tumours were allowed to grow for 9 days after which time the rats were given irinotecan (150 mg/kg i.p.) on two consecutive days to induce mucositis. Irinotecan was administered in a sorbitol/lactic acid buffer (45 mg/ml sorbitol/0.9 mg/ml lactic acid) that is required for activation of the drug. Rats also received 0.01 mg/kg s.c. atropine immediately prior to

irinotecan to reduce any cholinergic reaction to the treatment. Animals were culled by CO_2 asphyxiation and cervical dislocation 6, 24 and 48 h after the second injection. One further group of rats received buffer only and were designated as controls at time 0 h. The gastrointestinal tract from the pyloric sphincter to the rectum was removed and flushed with sterile 0.9% w/v saline. Two cm samples of small intestine (jejunum) at 25% of the length of the small intestine from the pylorus were collected, snap frozen in liquid nitrogen and stored at –70°C.

3.1.4 RNA extraction

Total RNA was isolated from 30 mg of homogenised whole jejunal tissue using TRIzol® Reagent (Invitrogen Life Technologies, Mulgrave, VIC). Avoiding contamination with RNases, frozen samples were disrupted by mortar and pestle, placed into 1.5 ml centrifuge tubes containing 500 µl TRIzol® and vortexed thoroughly. Samples were allowed to sit at room temperature for 5 mins before adding 100 µl chloroform. Tubes were hand shaken for 15 sec and left at room temperature (RT) for 3 mins. Samples were centrifuged at 12,000g for 15 mins a 4°C to separate aqueous and solvent phases. The upper aqueous phase was collected and placed into a new tube. An equal amount of 70% ethanol was added to change binding conditions of the RNA so as to be bind RNA to a silica gel membrane (Machery Nagel, Berlin, Germany). Following multiple washes of the membrane with ethanol, highly pure RNA was eluted in 60 µl RNase-free sterile water. Finally, RNA was treated with DNAse 1 (Ambion, Austin, TX, USA) to remove genomic DNA. In a new sterile tube, 3 µl of (10x) DNAse 1 buffer (0.1 volume) and 1 µl of DNAse 1 (2 units) was added to 30 µl of RNA. This was mixed gently and incubated for 20 mins at 37°C. The reaction was halted by addition of 5 µl of the DNAse inactivation reagent slurry. After 2 mins incubation at RT, the tubes were centrifuged at 10,000g for 1 min to pellet the slurry. RNA supernate was removed to a new tube and re-frozen until use.

3.1.5 Nucleic acid quantification

RNA concentration was quantified by diluting 1:20 with diethyl pyrocarbonate (DEPC) (Sigma)-treated H_2O and measuring the absorption at 260 nm and 280 nm on a spectrophotometer. Concentration of RNA was determined by the formula:

$$A_{260} \times 40 \times 20 = \text{RNA ng/µl}$$

(assuming that an optical density reading of 1.0 represents 40 µg/ml of RNA). Quality of RNA was checked by A_{260}/A_{280} ratio of samples.

3.1.6 cDNA synthesis

cDNA was synthesised from 2 μg of RNA prepared from rat jejunum using M-MLV reverse transcriptase (Invitrogen, VIC, Australia). Firstly, 100 ng of $PD(N)_6$ primers (Amersham Pharmacia Biotech, Sydney, NSW) were added to the RNA and DEPC-treated H_2O was used to make a final volume of 15 μl. This reaction mixture was heated at 90°C for 5 mins and chilled on ice for 3 mins to denature RNA. Secondly, an assay mixture containing 6 μl of (5x) first strand buffer, 3 μl of deoxyncleotide-triphosphate (dNTP) solution (10 mM of each; dATP, dTTP, dCTP, dGTP), 3 μl of 0.1 M DTT, 2 μl of DEPC water and 1 μl of M-MLV (200 U/μl) was then added to each $PD(N)_6$ reaction tube and incubated for 90 mins at 37°C. cDNA was stored at -20°C until experimentation.

3.1.7 Primer design

Oligonucleotide primers were designed for each of the 8 Bcl-2 family members using the published sequences (as listed in Entrez Nucleotide) for rat. The sequences were inserted into the GeneFisher primer design program to identify possible primer pairs (R. Giegerich et al., 1996). This program listed the best 8 pairs and stated the product length, difference in melting temperature, and priming position in the sequence for each. Theoretical primer pairs were checked for stability, primer dimers and cross priming using the Amplify program. Primers were synthesised by GeneWorks (Adelaide, SA) and resuspended with sterile H_2O to a working concentration of 50 ng/μl. A list of each of the primer pairs is shown in Table 3.1.

Table 3.1. Bcl-2 family primer pairs used in RT-PCR analysis.

	Forward Primer	***Reverse Primer***
Bax	GGTTTCATCCAGGATCGAGCAGAG	CCAGACAAGCAGCCGCTCAC
Bak	CTGTTGGGCCAATTTGTGGTACAC	CTGACTTTGGGCAGAGCGGATG
Bid	AGCATCCAGCCCACAC	CCAGGCAGTTCCTTTTG
Bim	CCCTACCTCCCTACA	CCTGAGACTGCCTTAT
Bcl-2	GGGACGCGAAGTGCTA	TGCAGCTGACTGGACA
Bcl-xL	AAGCCCCAGAAGAAACTG	TCCTTGTCTACGCTTTCC
Mcl-1	TATTTCTTTTGGTGCCTTTG	CCCAGCCTCTTTGTTTCA
Bcl-w	CAGCAACGCTTCACC	GCACTTGTCCCACCA

3.1.8 Polymerase chain reaction

Presence of Bcl-2 family member mRNA in the rodent intestine was confirmed, and changes in mRNA expression after treatment was investigated by multiplex RT-PCR. Taq DNA polymerase (Promega, Madison, WI, USA) was used for reverse transcriptase (RT)-PCR analysis. DNA was amplified in a 25 μl reaction containing 13.3 μl sterile water, 2.5 μl Taq polymerase buffer (100 mM Tri HCL, 1% TritonX-100, 500 mM/L KCl, pH 9.0), 2 μl of primers (50 ng of each forward and reverse primer), 0.5 μl dNTPs, 0.1 μl Taq (1 Unit), 2 μl of 18S rRNA primers plus competimers (QuantumRNA™ kit, Ambion, Austin Texas, USA) and 2 μl of cDNA.

The 18S and Competimers were included in each PCR to act as an internal standard for relative quantification. Initially, using a positive control tissue, a series of dilution ratios of 18S and competimers (i.e. 0:10, 1:9, 2:8, 3:7, 4:6, 5:5) were added to the master mix to establish a concentration that resulted in a band ratio of 1 for the respective 18S and Bcl-2 family member product band. Relative PCRs were optimised so that specific PCR primer and 18S products were in a linear exponential phase of amplification verses cycle number. Cycle number ranged from 28 to 36 dependent on primer pair used. Reactions were carried out in a thermal cycler with a heated lid and were subjected to an initial denaturing step for 5 min at 95°C, and then the appropriate number of cycles of 45 sec denaturation at 95°C, 45 sec primer annealing at temperatures between 42 and 60°C (dependent on primer pair) and 1 min primer extension at 72°C. A final 7 min primer extension step at 72°C was also included. PCR products were run on agarose gels and visualised with ethidium bromide. Resultant band intensity was evaluated by a gel documentation system (Kodak, Rochester, NY). Data are given as the ratio of Bcl-2 member to 18S rRNA.

3.1.9 Intestinal samples for investigation of protein expression

Blocks of archive tissue from previous studies carried out in the laboratory were retrieved to investigate changes in protein expression in a variety of species with differing treatments. All samples had been formalin fixed and were routinely processed to paraffin.

a) *DA rat:* Groups of 6 rats were treated with 1.5 mg/kg methotrexate (MTX) on two consecutive days to induce mucositis and killed from 6 to 72 h following chemotherapy. It had been found that apoptosis and intestinal damage peak at 6 and 48 h, respectively, in this model after MTX treatment (Gibson et al., 2002).

b) *Human:* Biopsies from the third part of the duodenum were collected from subjects with cancer who were investigated for apoptosis in the intestine after chemotherapy. These were collected either immediately prior to, or at day 1 or 3 following treatment. Each group had 6 to 8 members. Individual malignancies and treatment have been described elsewhere (Keefe, 1998). Apoptosis peaked at day 1 following chemotherapy in these samples.

3.1.10 Immunohistochemistry for detection of Bcl-2 family proteins

Two consecutive 3 μm paraffin sections of small intestine were cut onto 3-aminopropyltriethoxy-silane-treated (Sigma Aldrich, Steinheim, Germany) glass slides, dewaxed in xylene and rehydrated through graded alcohols to water. Of the two sections on each slide, one was designated the negative control and the other the experimental section. Slides were washed with PBS before heat mediated antigen retrieval in 10 mM citrate buffer (pH 6.0). Endogenous peroxidase activity was quenched with 3% hydrogen peroxide in methanol for 1 min, while non-specific antigens were blocked with normal serum for 20 mins. Elimination of endogenous avidin and biotin was carried out using a commercial avidin/biotin blocking kit (Vector Laboratories, Burlingame, CA USA) as per manufacturer's instructions. Experimental sections were incubated overnight at 4°C with the primary antibody for respective Bcl-2 family proteins and caspase-3 (Santa Cruz Biotechnology, Santa Cruz, CA, USA) and p53 (Novocastra Laboratories, UK) diluted in a solution of PBS with 2% serum (as described in Table 3.2). Negative control sections had the primary antibody omitted and were incubated with the dilution solution only. With stringent washes in PBS between each step, sections were incubated with a universal secondary antibody, followed by Ultra-Streptavidin conjugated to horseradish peroxidase and finally diaminobenzidine (DAB) chromogen in 0.03% hydrogen peroxide (Signet Laboratories, MA, USA). Slides were counterstained in diluted Lillie-Mayer's Haematoxylin, dehydrated and mounted.

3.1.11 Quantitative immunohistochemistry

Immunostaining was assessed as described by Matkowskyj and colleagues and adapted to the intestine (Matkowskyj et al., 2000). This method employs an algorithm that calculates the cumulative signal strength (pixel energy) of a digital file of the image in question. Firstly, staining in each section was visualised with the Nikon 800 research microscope and assessed using a x10 objective lens. A field was chosen which represented the general pattern of staining for the tissue and contained 10 well orientated mature crypts. In all

cases staining was uniform and never focal. Then, focussing with a x60 dry lens, a digital photograph was taken of the identical intestinal crypts in both the control and experimental sections using a SPOT-RT camera (Diagnostic Instruments Inc, Michigan, Detroit, USA). A 49x49 pixel area of interest was selected over the cytoplasm of several identical crypt cell profiles located from cell positions 2 to 10 along the crypt axis using Image Pro Plus (Media Cybernetics, Silver Spring, MD, USA) in both the control and experimental sections and saved as TIFF files. Areas of interest were converted to image matrices, subtracted and normalised using matrix functions in Matlab (Mathworks Inc, Natick, MA, USA) using the algorithm previously described. The intensity of staining was expressed as the difference in cumulative signal between the control and experimental matrices and given in units of pixel energy. Furthermore, the accuracy of this method of quantification in our model of intestinal damage was tested as follows: Marshmen et al have shown that detecting and quantifying apoptosis by immunostaining for active caspase-3 compares favourably with the traditional TUNEL assay (Marshman et al., 2001). Thus, using archival colon tissue blocks which were collected and processed in an identical manner to all other blocks, they were stained for caspase-3, and the staining quantified as described above. Tissue blocks were from rats that had received either saline, 1.5 mg/kg or 2.5 mg/kg MTX and killed at 6 h. These samples showed a dose-dependent increase in apoptosis as detected by the TUNEL assay, described previously (Gibson et al., 2005). We found that caspase-3 staining also increased dose dependently in the MTX-treated groups, with the 2.5 mg/kg group having the highest level recorded. Results shown in Figure 3.0.

3.1.12 Qualitative assessment of staining

The degree of immunostaining for each rat section was also evaluated while blinded to treatment and scored according to intensity as follows; 0 = negative, 1 = weak, 2 = moderate, 3 = strong, 4 = very intense. Slides were re-analysed by another investigator (RG) and the results presented are of the combined assessment.

3.1.13 Statistical analysis

All statistical analysis was carried out using the Peritz F-test or one way ANOVA with Tukey's post hoc test to identify changes in mean staining and band intensity over time for each Bcl-2 family member plus p53 and caspase-3. P-values <0.05 were considered statistically significant.

Table 3.2. Immunohistochemistry information for sections of rat intestine immunostaining

	Antibody	Species	Clone and Source	Dilution	Positive Control
Anti-apoptotic	Bcl-2	Polyclonal, rabbit anti human	N-19 sc-492	1:1000	Spleen
	Bcl-xL	Polyclonal, rabbit anti human	H-62 sc-7195	1:800	Thymus
	Bcl-w	Polyclonal, goat anti human	N-19 sc-6172	1:300	Testis
	Mcl-1	Polyclonal, rabbit anti human	S-19 sc-819	1:5000	Spleen
Pro-apoptotic	Bax	Polyclonal, rabbit anti mouse	P-19 sc-526	1:1000	Thymus
	Bak	Polyclonal, goat anti human	G-23 sc-832	1:800	Stomach
	Bim	Polyclonal, goat anti human	N-20 sc-8265	1:800	Thymus
	Bid	Polyclonal, rabbit anti human	FL-195 sc-11243	1:2500	Spleen
	p53	Monoclonal mouse	NCL-p53-240	1:50	Tumour
	Caspase-3	Polyclonal, goat anti human	K-19 sc-1224	1:1500	Spleen

Table 3.3. Immunohistochemistry information for sections of human intestine immunostaining

	Antibody	Species	Clone and Source	Dilution	Positive Control
Anti-apoptotic	Bcl-2	Polyclonal, rabbit anti human	N-19 sc-492	1:1500	Tonsil
	Bcl-xL	Polyclonal, rabbit anti human	H-62 sc-7195	1:850	Thymus
	Bcl-w	Polyclonal, goat anti human	N-19 sc-6172	1:500	Testis
	Mcl-1	Polyclonal, rabbit anti human	S-19 sc-819	1:7000	Spleen
Pro-apoptotic	Bax	Polyclonal, rabbit anti mouse	P-19 sc-526	1:1300	Tonsil
	Bak	Polyclonal, goat anti human	G-23 sc-832	1:1400	Tonsil
	Bim	Polyclonal, goat anti human	N-20 sc-8265	1:2000	Tonsil
	Bid	Polyclonal, rabbit anti human	FL-195 sc-11243	1:4000	Spleen

A

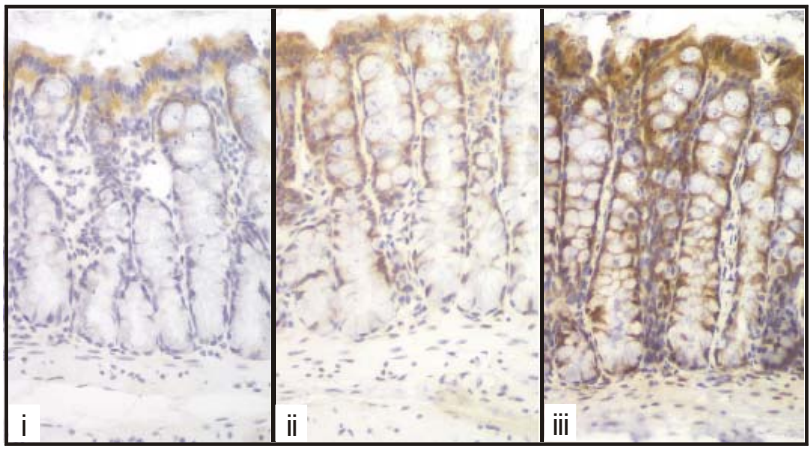

B

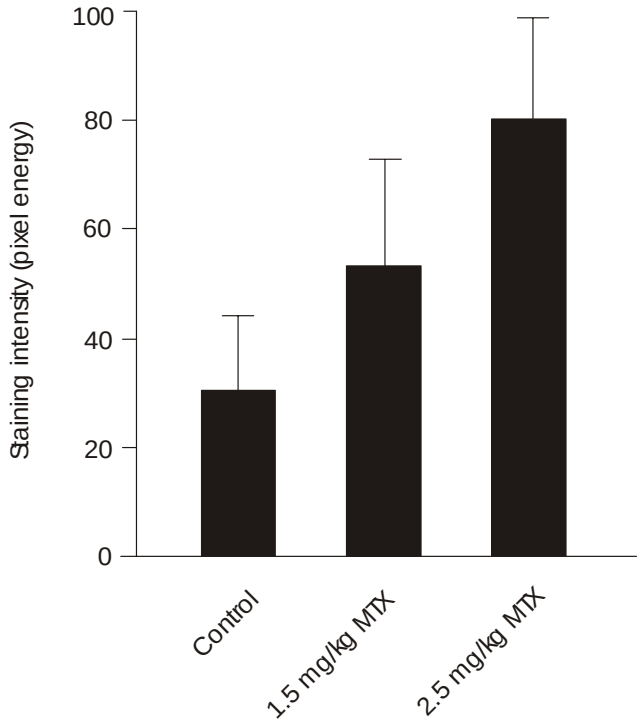

Figure 3.0. Results of caspase-3 staining in the rat colon to validate use of Matlab analysis. A) Photomicrographs of i) control, ii) 1.5 mg/kg MTX 6 h and iii) 2.5 mg/kg MTX 6 h. Original magnification x200. B) Graph of results, data shown is group mean + SEM (n = 6).

3.2 Results

3.2.1 RNA expression

The mRNA levels of eight Bcl-2 family members were detected by RT-PCR in jejunal samples from rats treated with irinotecan at 0, 6, 24 and 48 h. Bcl-2, Bcl-xL, Bcl-w, Mcl-1, Bid and Bim expression remained relatively constant at each time point investigated and showed no significant change following irinotecan treatment. Bax and Bak band intensity and therefore expression was increased 2-fold at 6 h following treatment. The mRNA levels were not significantly different at any other time point, however Bax remained somewhat elevated for the remainder of the study compared to controls. Representative gels and band intensity graphs are shown in Figure 3.1 and 3.2 respectively.

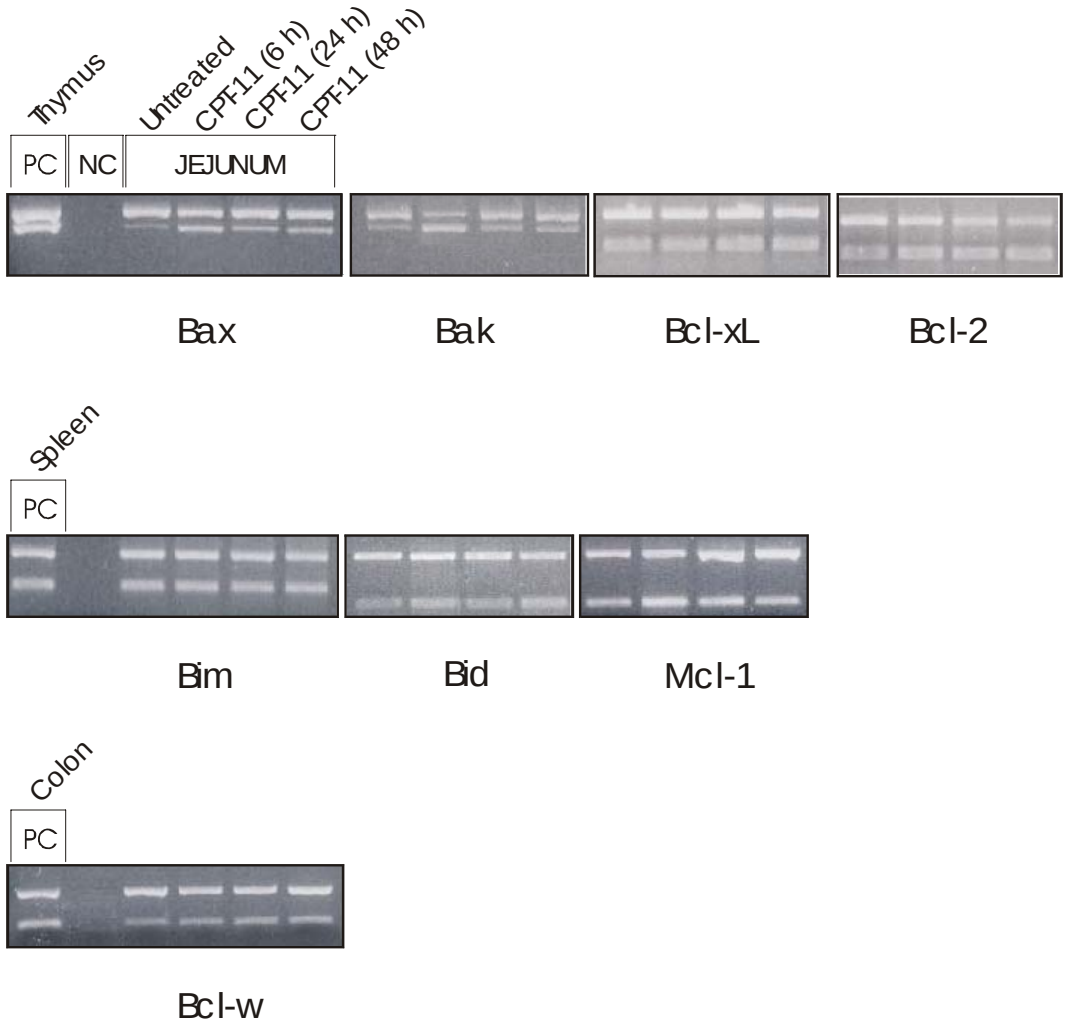

Figure 3.1. Representative agarose gel images showing PCR products of each Bcl-2 family member. PC = positive control tissue, NC = negative control (no cDNA in master mix).

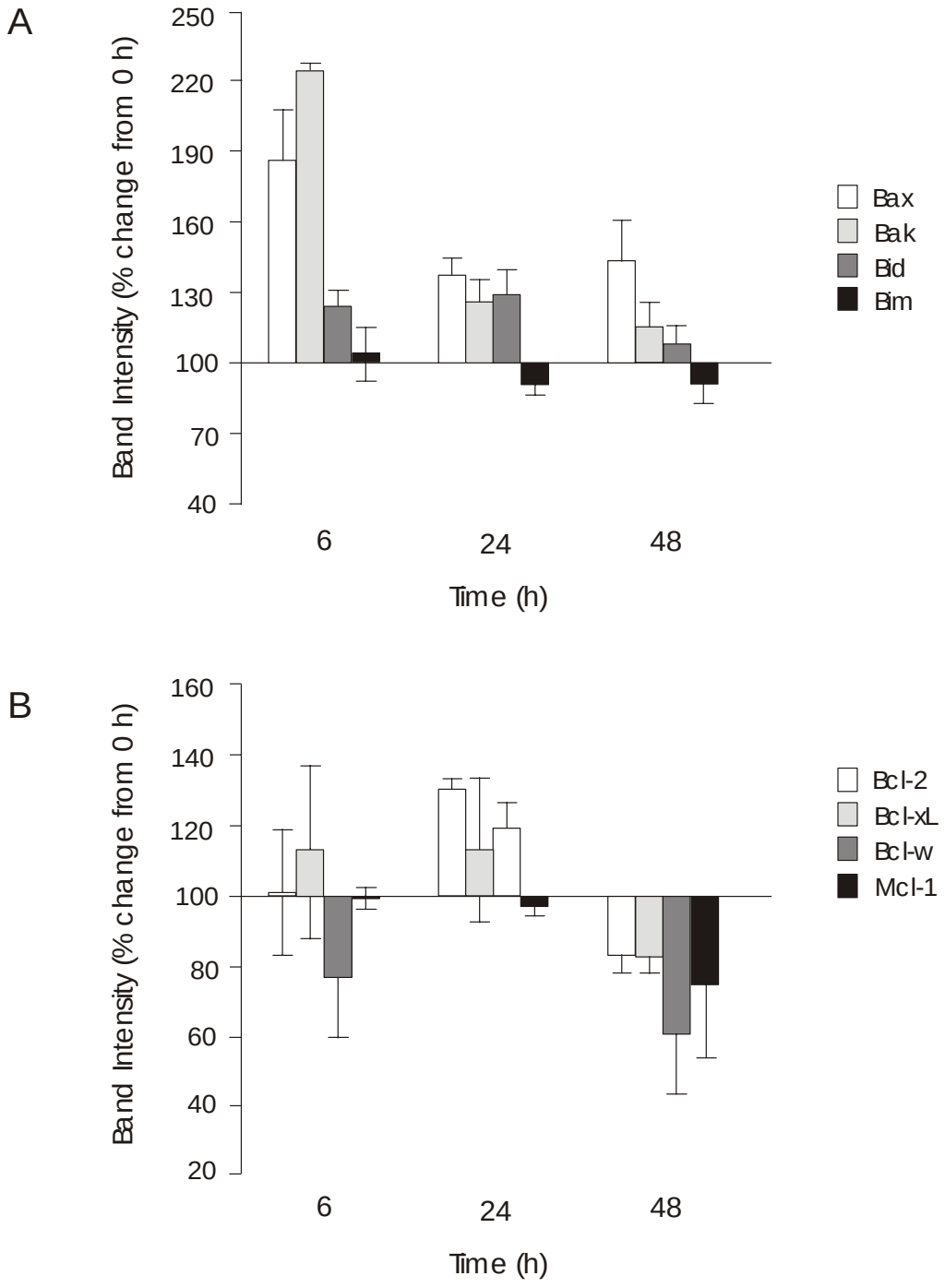

Figure 3.2. Graph of results for RT-PCR analysis of Bcl-2 family members in rat jejunum following chemotherapy. A) Pro-apoptotic Bax, Bak, Bid and Bim. B) Anti-apoptotic Bcl-2, Bcl-xL, Bcl-w and Mcl-1. Data shown is group mean +/- SE (n = 6).

3.2.2 Protein expression in rat

The protein levels of eight Bcl-2 family members, p53 and caspase-3 were detected by immunohistochemistry in jejunal crypts of rats treated with methotrexate at 0, 6, 24, 48 and 72 h. Staining of p53 was minimal in untreated crypts, with only occasional individual cells exhibiting strong staining. At 6 h following MTX, crypt staining increased 3.4-fold, with most cells being positive for nuclear p53. Expression of p53 reduced over time, and returned to control levels by 72 h. Caspase-3 staining also increased following MTX treatment, peaking at 6 h with a 3.9-fold rise in staining intensity. Positive staining was seen in both the cytoplasm and nucleus. The reduction in caspase-3 over later time points closely followed the pattern of p53. (Figs 3.3. and 3.4.) Bcl-2 family member proteins showed cytoplasmic staining only. Pro-apoptotic proteins Bax and Bak increased after MTX with a 2.4 and 2.5-fold peak increase (respectively) in staining at 6 h. By 24 h, staining returned to control values and remained constant for the remainder of the experiment. Bid expression was reduced by 70% between 6 and 24 h after MTX treatment. Staining for Bid did not return to control values until 72 h. The anti-apoptotic protein Mcl-1 was also decreased following MTX. Staining was reduced maximally at 24 h by 57%, and this returned to control levels by 72 h. (Figs 3.5 and 3.6.) No significant change in expression was seen for the other Bcl-2 family proteins at any time point. Staining intensity values for each of the proteins investigated at each time point is shown in Table 3.3 and qualitative assessment of staining is shown in Table 3.4.

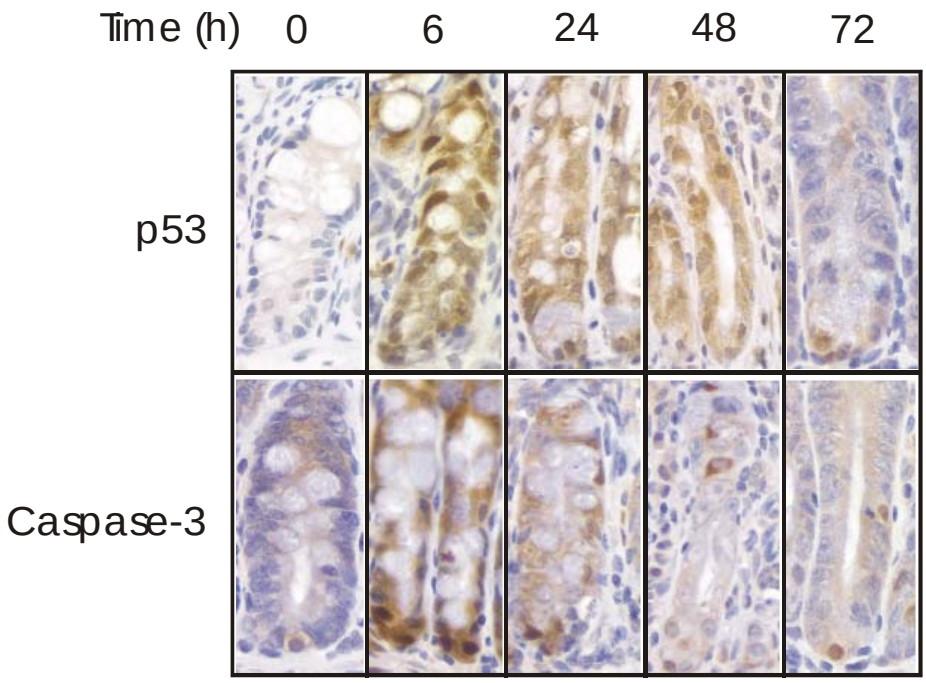

Figure 3.3. Photomicrographs of crypt staining for p53 and caspase-3 following MTX treatment. Original magnification x600.

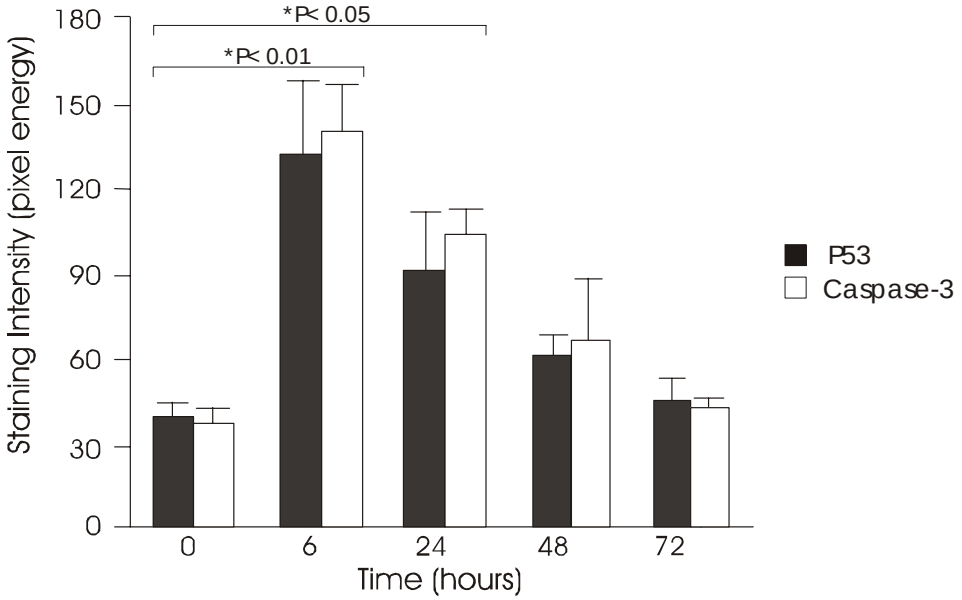

Figure 3.4. Graph of results for protein expression of p53 and caspase-3 in rat jejunual crypts following chemotherapy. Data shown is group mean + SEM (n = 6).

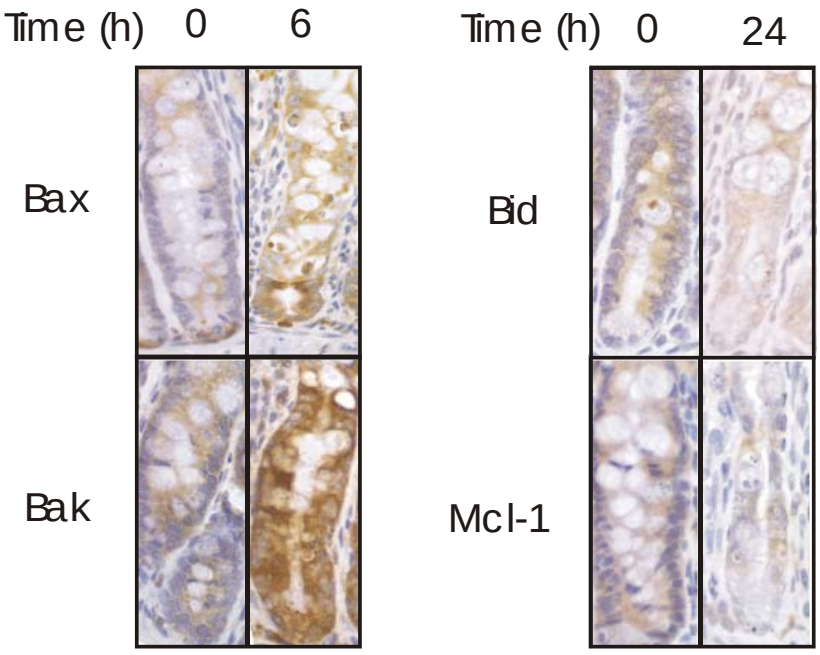

Figure 3.5. Photomicrographs of crypt staining for Bcl-2 family members, Bax, Bak, Bid and Mcl-1. Original magnification x600.

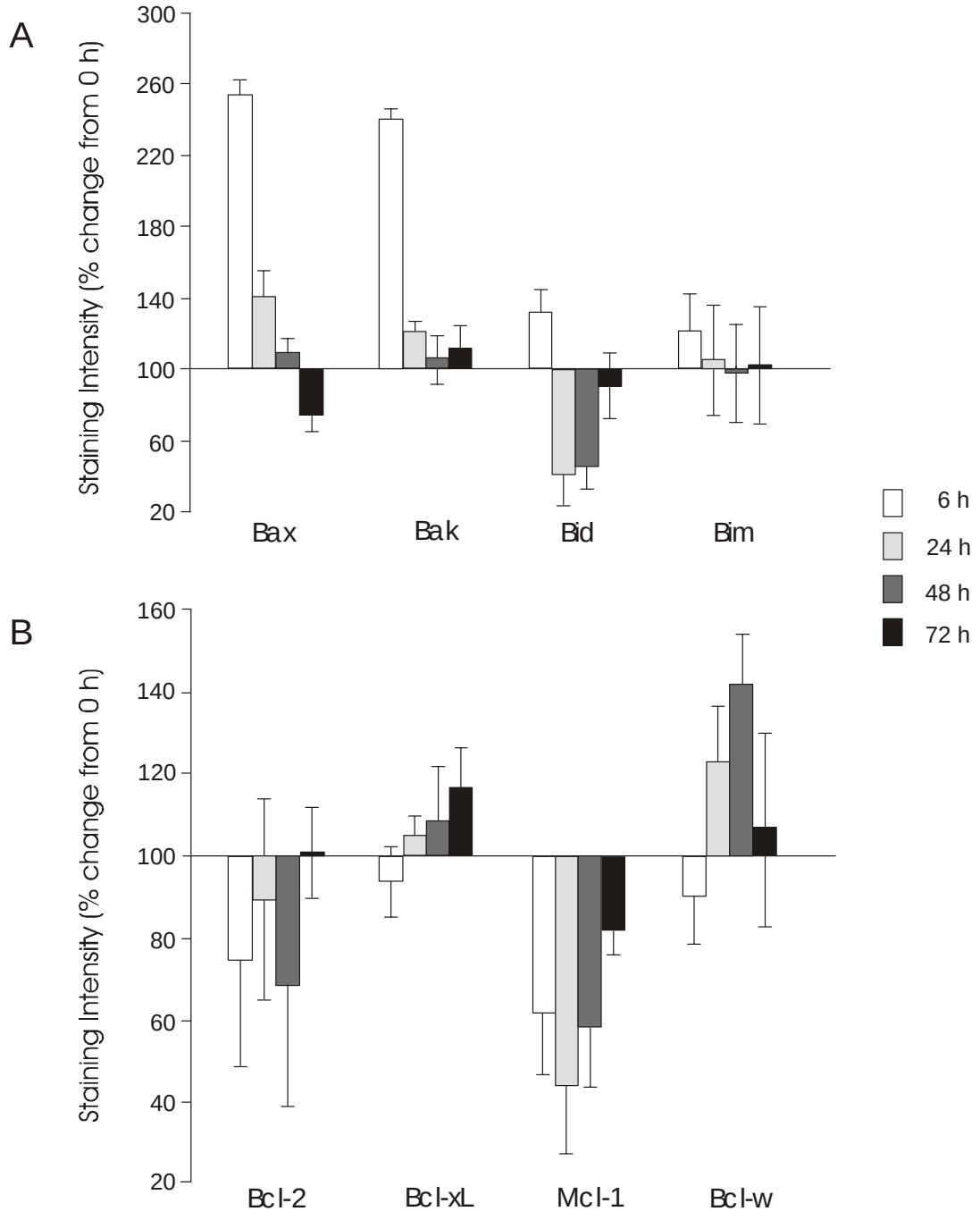

Figure 3.6. Graph of results for Bcl-2 family protein expression in rat jejunal crypts following chemotherapy treatment. A) Pro-apoptotic Bax, Bak, Bid and Bim. B) Anti-apoptotic Bcl-2, Bcl-xL, Mcl-1 and Bcl-w. Data shown is of group mean +/- SE (n = 6).

Table 3.3. Results of immunohistochemistry on rat jejunal sections. Staining intensity was determined by Matlab program and data shows mean ± SE cumulative signal in units of pixel energy (n = 6). * indicates significant change from 0 h control (P<0.05), ** P<0.005.

	0 h	**6 h**	**24 h**	**48 h**	**72 h**
p53	38.0 ± 9.7	131.8 ± 32.0**	90.9 ± 21.2*	60.8 ± 7.1	45.2 ± 8.6
Caspase-3	35.7 ± 6.6	139.3 ± 18.1**	103.1 ± 9.7*	65.3 ± 24.4	41.7 ± 3.3
Bax	121.9 ± 22.3	308.9 ± 25.3**	171.9 ± 25.0	132.7 ± 11.4	91.9 ± 9.4
Bak	100.9 ± 4.8	237.5 ± 16.8**	118.2 ± 7.5	107.8 ± 19.3	112.6 ± 22.8
Bim	61.3 ± 30.6	73.8 ± 24.1	60.0 ± 23.5	62.4 ± 29.7	51.8 ± 29.9
Bid	65.9 ± 22.0	87.2 ± 11.0	26.7 ± 4.7*	29.4 ± 3.6*	59.7 ± 11.2
Bcl-2	53.9 ± 11.5	48.1 ± 12.4	57.4 ± 12.0	44.5 ± 11.6	66.2 ± 9.8
Bcl-xL	80.45 ± 20.0	74.7 ± 8.2	85.64 ± 5.3	89.78 ± 18.0	87.5 ± 10.5
Bcl-w	21.0 ± 14.5	19.9 ± 5.4	26.0 ± 3.0	30.5 ± 6.7	22.5 ± 9.6
Mcl-1	92.04 ± 14.1	56.5 ± 8.6	40.6 ± 6.6**	53.8 ± 7.6	75.6 ± 7.8

Table 3.4. Qualitative assessment of immunostaining in rat jejunal crypts before and after MTX treatment.

	0 h	**6 h**	**24 h**	**48 h**	**72 h**
p53	0 - 3	4	2 - 4	3	2
Caspase-3	1 - 2	4	2 - 3	1 – 3	1 - 2
Bax	2	4	2 - 3	2	2
Bak	2	4	2 - 3	2 – 3	2 - 4
Bim	2	2	2	2	2
Bid	2	2 - 3	1	1	2
Bcl-2	1 - 2	1	1	1	2
Bcl-xL	2	2	2	2	2
Bcl-w	0 - 1	0 - 1	0 - 1	0 – 1	0 - 1
Mcl-1	3	2 - 3	2	2	

3.2.3 Protein expression in patients

Distribution of intestinal crypt Bcl-2 family protein expression was also investigated in human duodenal biopsies of patients treated for cancer.

Firstly, the pattern of Bax staining in pre-treatment samples was different to that seen previously in the rat tissue. Specifically, crypts had weaker staining often with no cells positive for Bax present. Conversely, the lamina propria contained a much higher percentage of strongly stained cells.

This was also the case for Bak which appeared to have constitutive staining throughout the lamina propria. Following treatment there was a highly significant increase in Bax and Bak staining within crypts. Strong to intensely stained cells were predominantly seen within the lower half region of the crypt on day 1. Crypt damage was evident by day 3 and staining for these pro-apoptotic proteins significantly decreased from day 1 but did not return to pre-treatment levels at this time point.

Bid levels were variable in patients. Of the 6 patient samples tested from the pre-treatment group, 3 had minimal staining for Bid within crypts with only a very few positively stained cells present, while the other 3 had diffuse moderate intensity cytoplasmic staining along the length of the crypts. On day one, 2 out of the 6 samples tested had multiple strongly stained cells within crypts, while the remaining 4 showed no difference in staining when compared to the 3 weakly stained samples from the pre-treatment group. The staining on day 3 was somewhat more uniform among patients. Generally it was seen that crypts had few to multiple individual cells moderately to strongly stained for Bid, not unlike the pre-treatment samples. This appeared to be irrespective of whether the patients were undergoing standard or high dose chemotherapy. There was no significant difference in staining intensity values for any group.

The final pro-apoptotic Bcl-2 family member investigated, Bim, also showed variable staining within different patients. In pre-treatment samples all crypts showed cytoplasmic staining along entire crypt length, however the intensity varied from weak to strong between patients. There was also considerable levels of Bim expression in the lamina propria. Samples collected on day 1 following chemotherapy had only one example of strongly stained entire crypts, while the remaining sections had only minimal Bim expression. Crypt staining on day 3 was generally more consistent and comprised of

few to multiple strongly positive cells distributed evenly throughout. There was no significant difference in staining detected at any time point. Although there was variability between patients, individuals showed similar staining patterns before and after treatment.

The anti-apoptotic protein Bcl-2 was present within duodenal biopsies taken from patients directly before starting their chemotherapy cycle. Staining within the crypt varied from completely absent to weak-moderate staining along length of crypt. More notably, lamina propria staining for Bcl-2 was always present at a moderate to strong level. Biopsy sections on day 1 showed overall slightly less positive staining for Bcl-2. Positively staining cells retracted to a few discreet cells within crypt epithelium. Staining within lamina propria was also reduced. Day 3 biopsy sections showed similar staining to day 1. There was no significant difference in staining intensity found between groups.

For Bcl-xL, there was overall less crypt staining seen in human duodenal biopsies compared to rat small intestine, combined with more predominant lamina propria positive staining. Of the eight patients investigated pre chemotherapy, only one had more than 10% of crypt cells positively stained for Bcl-xL. This patient also showed strong staining at day 3. Day 1 biopsies stained similarly to the pre chemotherapy sections with generally only one to two positively staining cells per crypt and weak to moderate staining in the lamina propria. Staining of biopsies on day 3 was typically unchanged compared to pre chemotherapy staining and as such no significant difference was found between any group.

Bcl-w staining was confined to crypt epithelium in biopsy sections. At each time point staining was weak to undetectable. There was slight variation in intensity among patients, however no significant difference between groups.

Finally, Mcl-1 protein expression was analysed in each of the groups. Pre-chemotherapy biopsies all showed moderate to strong staining throughout crypt epithelium. At day 1 there was a significant decrease in number of positively stained cells in each crypt, often with Mcl-1 becoming undetectable in multiple crypts. This was maintained on day 3, albeit with a slight return towards positive staining within crypts. There was also a notable increase in staining within the lamina propria at this time point for 2 out of the 6 biopsies investigated. Representative staining shown in Figure 3.7 with graph of Matlab values in figure F.8.

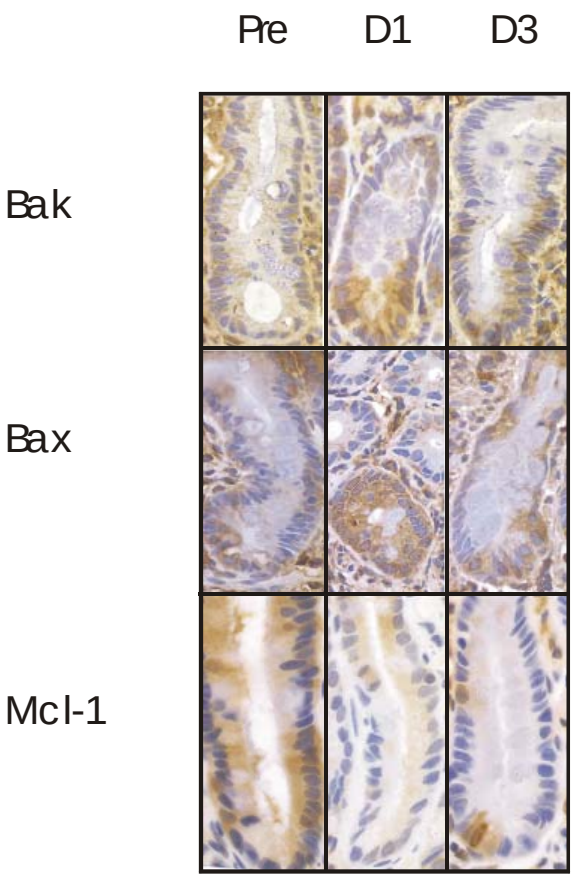

Figure 3.7. Photomicrpgraphs of human small intestinal crypts immunostained for Bcl-2 family members Bax, Bak and Mcl-1 before and on day 1 and day 3 following.chemotherapy. Original magnification x600.

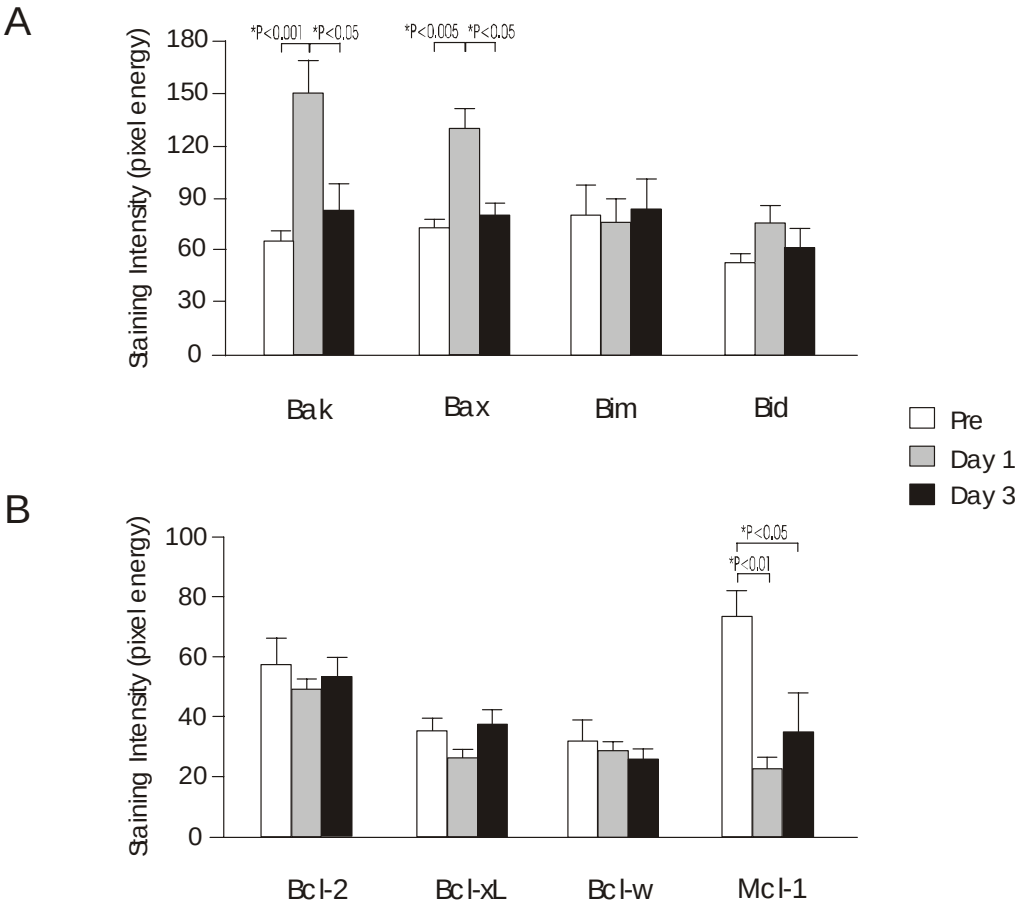

Figure 3.8. Graph of results for Bcl-2 family members protein expression in human duodenal crypts following chemotherapy. A) Pro-apoptotic Bax, Bak, Bim and Bid. B) Anti-apoptotic Bcl-2, Bcl-xL, Bcl-w and Mcl-1. Data shown is group mean + SE (n = 6).

3.3 Discussion

Chemotherapy-induced mucosal damage has gained interest in the previous few years, with a considerable body of literature now existing describing the pathobiology behind this type of tissue injury. This study has furthered our knowledge by investigating the effects of a range of chemotherapy regimens on the small intestinal expression of apoptosis-related genes over varying time points in both rats and humans.

The proximal small bowel is exquisitely sensitive to cytotoxic-induced damage. Studies examining mucosal damage following MTX treatment in the rat and in the human have led the way in our understanding of how the epithelium responds to this insult (Taminiau et al., 1980; Trier, 1962). It is well known that increased apoptosis and crypt hypoplasia lead to changes in intestinal structure and function and the symptoms of mucositis. The area which remains yet to be fully explained though is how genes involved in apoptosis react to chemotherapy within the intestine. Specifically, which genes are up and down-regulated and at what time in the sequelae of damage. The DA rat model of mucositis provides an ideal example to investigate changes in the small intestine after treatment, and has been shown to follow the clinical presentation of patients, albeit slightly faster. In this study, we found that pro-apoptotic Bax and Bak are upregulated by MTX at both the RNA and protein level at 6 h in crypt epithelium, while the full length Bid protein is decreased by 24 h. The anti-apoptotic protein, Mcl-1, was markedly reduced also at 24 h. At 6 h there was also maximal increases seen in p53 and caspase-3 proteins.

The increase in p53 following insult and its relationship to apoptosis in the intestine has been widely examined and thoroughly documented (Arai et al., 1996; Merritt et al., 1994; Pritchard et al., 1998), as too the link between caspase-3 activity and the cellular commitment to death (Grutter, 2000; Marshman et al., 2001). Thus, the increase in p53 and caspase-3 that was observed in this study was expected and strengthens previous conclusions. The current theory of how apoptosis is controlled in the small bowel consists of the p53 pathway of cell death and its transcriptional control of downstream effector genes (Benchimol, 2001; el-Deiry, 1998; Lane et al., 1994; Smith et al., 2003). These downstream genes include multiple members of the Bcl-2 family (Kannan et al., 2001; Miyashita et al., 1994a; Miyashita et al., 1994b; Miyashita and Reed, 1995). Recently, non-transcriptional functions of p53 have also been shown to play a role in regulation of apoptosis. Most notably the direct cytoplasmic interaction of p53 with both pro- and anti-

apoptotic members of the Bcl-2 family (Chipuk et al., 2004; Erster et al., 2004; Leu et al., 2004; Mihara et al., 2003).

Previous studies investigating the changes in Bcl-2 family expression that occur within intestinal epithelial cells following cytotoxic treatment are not as abundant as for p53 but include a number conducted in cancer cell lines and mice. Breast cancer cells treated with various cytotoxic agents to induce apoptosis upregulate Bax and downregulate Bcl-2 in a time-dependent and dose-dependent manner (Gibson et al., 1999; Leung and Wang, 1999). Similar experiments using colon cancer cell lines treated with 5-fluorouracil (5-FU) have found that Bax and Bak expression is significantly increased without consistent changes to other family members (Nita et al., 1998). While, an increase in Bax expression has been observed in the intestinal crypts of mice, concurrent with sites of apoptosis following 5-FU treatment (Inomata et al., 2002), gamma-radiation (Kitada et al., 1996) and chemoradiation (MTX + whole body irradiation) (Beck et al., 2004). This study has confirmed the effect of cytotoxic agents on members of the Bcl-2 family in rat small intestinal crypt epithelium.

The investigation into changes in Bcl-2 family expression following chemotherapy in the human provided similar results as those seen in the rat. The increase in Bax and Bak was consistent, as too the decrease in Mcl-1. The variation in staining for other Bcl-2 family proteins seen among patients may possibly have contributed to the lack of further significant results over the time points. Due to the nature of patients trials, and the natural variation in age, sex and intestinal health of each person, it is therefore possible that larger recruited numbers per group may have provided more meaningful results. Other limitations and possible confounding factors for this part of the study included a lack of detailed history for each patient. Missing data included the cycle number at time of biopsy and the exact type or location of malignancy. Animal trials are as such better suited to these types of examinations with much superior control conditions and reproducability.

These results show that the two multi-domain pro-apoptotic members of the Bcl-2 family, Bax and Bak, are consistently upregulated following chemotherapy treatment regardless of type of drug used or species. This upregulation is rapid, occurring within 24 h, and transient, resolving by 72 h. It coincides with increases in p53, caspase-3 and apoptosis which all occur before overt tissue damage. Mcl-1 was the only anti-apoptotic Bcl-2 family member altered by chemotherapy treatment and this only occurred at the protein level, leaving the effect of p53 on it unclear. Post-transcriptional regulation of this protein may occur via interaction with the p53 protein within the cytoplasm (Leu et al., 2004).

However, Mcl-1 has an extremely short half life, and so cellular protein levels are more likely reduced due to drug-induced cell hypoproliferation (Iglesias-Serret et al., 2003). Surprising was the lack of changes seen for the other anti-apoptotic genes. Although Bid was only significantly changed following chemotherapy in the rat samples, it still provides an interesting example of how intestinal epithelium respond to treatment. Bid is a BH-3 domain-only member of the Bcl-2 family which has been described as the link between the extrinsic and intrinsic apoptotic pathways (Luo et al., 1998). In response to a death stimulus from the FADD receptor pathway, Bid is truncated, allowing it to interact with Bax and induce Bax insertion into the mitochondrial membrane (Eskes et al., 2000). This is seen as an initiating event, occurring upstream of mitochondrial membrane permeabilisation, the centre point of the intrinsic apoptotic pathway (Desagher et al., 1999). Bid is a direct transcriptional target of p53 (Sax et al., 2002). However in this present study, the changes seen in Bid protein levels occurred after the peak increases in Bax and Bak expression and apoptosis, and therefore does not indicate a central role for Bid in this model of intestinal damage. Recently PUMA and NOXA which are also BH-3 CE_TYPE><ACCESSION_NUMBER>12667443</ACCESSION_NUMBER><VOLUM E>11</VOLUME><NUMB p53 in response to chemo-radiotherapy and are also involved in apoptosis regulation in the intestine. These proteins all contain p53 responsive elements within regions of the gene (Fei et al., 2002; Nakano and Vousden, 2001; Shibue et al., 2003) and provide interesting pathway information for p53/Bcl-2 family apoptosis regulation.

In conclusion, this study has highlighted a common pathway of death, involving p53, the Bcl-2 family and caspase-3 which is maintained from rodents to humans within the small intestine. In that, regardless of the chemotherapy drug used to initiate the injury, or the species, the upregulation of these particular genes is consistent and hence may provide an exploitable therapeutic target against intestinal damage.

Effect of chemotherapy treatment on apoptosis, proliferation and protein expression in intestinal cells

4.0 Introduction

Intestinal crypts are uniquely adapted to their functional role as proliferative units. The small intestinal epithelium is replaced every 3-5 days due to the constant turnover of cells (Potten and Loeffler, 1990; Westcarr et al., 1999). This occurs as stems cells located near the base of the crypt produce one of the four intestinal cell lineages to replace the differentiated villus tip cells that are sloughed into the lumen (Grossmann et al., 2001; Potten et al., 1997). Expression of apoptosis regulators in the small intestine is such that an environment of exquisite sensitivity to genotoxic damage prevails (Jones and Gores, 1997; Merritt et al., 1994; Merritt et al., 1995). It is believed that following even minor genetic challenge to stem cells, apoptosis is initiated without any attempt to undertake repair (Duncan and Grant, 2003; Potten et al., 2003). This is to avoid cells remaining to replicate with mutations that could develop into neoplasia. This commitment to apoptosis without repair following genotoxic damage only applies to the small intestine, as reflected by the large intestine's much higher incidence of tumours (Potten, 1992; Potten et al., 1992).

Expression of the tumour suppressor protein, p53, has been shown to increase following a range of cellular insults including chemotherapy and irradiation (Lane et al., 1994; Merritt et al., 1994; Muller et al., 1998; Weller, 1998; Wilson et al., 1998). It acts as a transcription factor in the nucleus, activating a number of downstream genes to induce apoptosis, halt the cell cycle or both depending on the cell type and stimulus (Smith et al., 2003). The p53-dependent pathway leading to apoptosis following DNA damage is believed to be initiated by the ATM kinase, which recognises strand breaks. This leads to stabilisation of p53 through phosphorylation and movement into the nucleus, where its binds via a sequence-specific consensus element to multiple gene promotor regions (Gottlieb and Oren, 1998; Norbury and Zhivotovsky, 2004; Slee et al., 2004). Genes including pro-apoptotic members of the Bcl-2 family, Bax, Bak, Bid, Noxa and Puma are then upregulated, tipping the balance in favour of cell death. Other genes associated with apoptosis that are upregulated by p53 include Pidd, Killer/DR5, Fas/Apo-1 and p53Aip1 and are involved in both the intrinsic and extrinsic pathways (Bouvard et al., 2000; el-Deiry, 1998; Kannan et al., 2001). Repression of genes by p53 also further enhances its apoptotic effect (Harris and Levine, 2005; Ho and Benchimol, 2003). The anti-apoptotic

proteins, Bcl-2, Bcl-xL and Survivin, are all downregulated. However, the precise mechanism by which p53 carries this out remains undetermined. Apart from its transcriptional abilities, p53 also regulates apoptosis through transcription-independent mechanisms. (Erster et al., 2004; Mihara et al., 2003; Moll and Zaika, 2001) It has been shown that p53 can act at the mitochondrial membrane to activate Bak through interactions with its binding protein, Mcl-1. It can also signal within the cytoplasm to activate Bax, in a role that is similar to BH3-domain members of the Bcl-2 family (Chipuk et al., 2004; Leu et al., 2004). To halt the cell cycle and maintain cells in G_1 phase, p53 upregulates the cyclin dependent kinase inhibitor, $p21^{waf\text{-}1/cip1}$. P53 is also able to arrest cells in G_2, and does this through target genes, 14-3-3 sigma, Gadd45 and B99 (Ho and Benchimol, 2003; Moucadel et al., 2002). It is thought that the combination of apoptosis and reduced proliferation contribute to loss of epithelial integrity in the intestine following cytotoxic therapy for cancer (Keefe, 1998).

The intestine has a predictable pattern of p53 induction following DNA-damaging treatment. P53 increases from very low levels to a peak by 24 h of a stimulus, becomes, concentrated within crypt epithelial cells and this coincides with induction of apoptosis (Arai et al., 1996; Merritt et al., 1997; Wilson et al., 1998). The effect of cytotoxic treatment on p53 expression and apoptosis in established intestinal cell lines has not been described in as much detail. Therefore, this study investigated the effect of the chemotherapeutic agents methotrexate (MTX), irinotecan (CPT-11) and doxorubicin (DOX) on cellular viability and protein expression in three epithelial cell lines, two intestinal and one tumour-derived. The effect of temporary inhibition of p53 using pifithrin alpha (PFT) on subsequent cell viability was also examined. Cell lines were used so that the effect of chemotherapy on a single intestinal cell type could be examined in detail, and also to assess the similarities between an *in vitro* and the established *in vivo* model of intestinal damage.

4.1 Methods and Materials

4.1.1 Cell lines

Both the IEC-6 (IEC) and FHs 74 (FHs) epithelial cell lines were obtained from the American Type Culture Collection (Rockville, MD, USA), while MCF-7 (MCF) cells were a kind gift from Professor M. Brown (Royal Adelaide Hospital, South Australia). IEC cells are derived from adult rat jejunum and display immunohistochemical markers characteristic of an undifferentiated crypt cell type. Assays using this cell line were carried out between passages 15 and 22. The FHs cells are derived from human foetal small intestine and may contain some mesenchymal characteristics. Experiments were carried out on these cells between passages 24 and 30. MCF cells are derived from a human breast carcinoma and were used within 6 passages of initial thawing of the cell line. All cell lines retained their original morphology and growth characteristics over the range of passages used.

4.1.2 Cell culture

The IEC cell line was maintained in Dulbecco's modified Eagle's media supplemented to contain 1.5 g/L sodium bicarbonate, 4.5 g/L glucose, 50 U/ml penicillin, 50 μg/ml gentamycin, 1 μg/ml fungizone, 4 mM L-glutamine, 10 μg/ml bovine insulin and 10% foetal calf serum (FCS). The FHs cell line was maintained in Dulbecco's modified Eagle's media supplemented to contain 1.5 g/L sodium bicarbonate, 4.5 g/L glucose, 50 U/ml penicillin, 50 μg/ml gentamycin, 1 μg/ml fungizome, 2 mM L-glutamine, 0.9x non essential amino acid solution, 0.9 mM sodium pyruvate, 1 mM oxaloacetic acid, 10 μg/ml recombinant human insulin, 30 ng/ml EGF and 10% FCS. The MCF-7 cell line was maintained in RPMI media supplemented with 2 mM L-glutamine and 10% FCS. Stock cells were kept in 75 cm^2 or 150 cm^2 sterile plastic culture flasks in a humidified atmosphere of 95% air with 5% CO_2 at 37°C. Experimental cell cultures were grown in sterile multi-well tissue culture plates under identical growth conditions. Media and supplements were purchased from Gibco BRL (Breda, The Netherlands).

Cell lines were routinely passaged when culture monolayers reached approximately 80% confluence. Cells were subcultured at ratios between 1:3 and 1:6 in fresh growth medium. Monolayers were detached by aspirating growth medium and rinsing once with Trypsin-EDTA solution (0.05% trypsin, 0.53 mM EDTA). This was followed by covering cells with fresh trypsin/EDTA and incubating at 37°C for 10 mins. The reaction was neutralised

by addition of growth medium and cells were sub-cultured for experimentation or continuation of passage. For experimental use, trypsinised cell suspensions were centrifuged at 250 x g for 5 mins, the supernate removed, and then resuspended in 10 ml of fresh growth medium. An assessment of cell number was carried out by addition of 0.4% trypan blue to an aliquot of cell suspension at a ratio of 1:1 and counted on a haemocytometer. The remaining cell suspension was then centrifuged once again, the supernate removed and resuspended in fresh media to obtain a cell density of 1 x 10^5 cells/ml.

4.1.3 Drug treatment

The chemotherapeutic agents methotrexate (MTX) and doxorubicin (DOX) were obtained from the Royal Adelaide Hospital pharmacy and were supplied as 25 mg/ml and 2 mg/ml in sterile water respectively. Irinotecan (CPT-11) was a generous donation from Pharmacia (Kalamazoo, MI) and kept at a concentration of 20 mg/ml diluted in a sorbitol/lactic acid buffer as described in previous Chapters. Drugs were stored at 4°C in a light-proof container under sterile conditions. MTX and DOX were diluted in saline immediately prior to addition to cells. All further dilutions of CPT-11 were in sorbitol/lactic acid buffer and carried out immediately prior to experimental use.

4.1.4 Cell viability assessment

To assess response of epithelial cells to differing doses of cytotoxic agents, a trypan blue assay was employed. Cell culture suspensions were seeded into 6-well plastic tissue culture plates at a density of 2 x 10^5 cells per well in 2 ml of growth medium. Cells were allowed to attach and begin exponential growth for 36 h after which time cytotoxic agents were added to culture media for 6 to 24 h. Media from each well was collected and transferred to labelled 10 ml centrifuge tubes. Cell monolayers were detached with trypsin/EDTA solution and transferred to appropriate tubes. Following centrifugation at 250 x g for 5 mins, cells were resuspended in 1 ml of fresh media. Viable cell counts were performed with addition of 0.4% trypan blue at a 1:1 ratio to cell suspension, visualised with a haemocytometer and shown as a percentage of cells capable of excluding the dye. Cells which take up the dye are believed to be undergoing late stage cell death.

4.1.5 Cell number assessment

To measure drug toxicity in epithelial cells, the methylene blue dye binding assay was used to estimate adherent cell number. Cells were sub-cultured into 96-well plastic tissue

culture plates at a density of 5000, 10000 and 15000 cells/well for MCF, IEC and FHs respectively in 200 μl of growth medium. The first row of wells were designated controls and received 200 μl of medium without cells. After an initial 36 h incubation, drugs were added to wells at differing concentrations ± 10 μM PFT for 24 h. At the end of each assay, cells were immediately washed twice with saline to remove all traces of medium. Cells were then fixed with 100% methanol for 10 mins before being covered with 10 mg/ml methylene blue (Sigma) in 0.01 M sodium tetraborate (pH 8.5) for 30 mins. Wells were then washed three times with 0.01 M sodium tetraborate (pH 8.5) to remove unbound dye. The bound dye was eluted by adding 100 μl of 0.1 M HCl/100% ETOH(1:1) ethanol to each well and then quantified with an automated plate reader at the absorbance wave length of 630 nm (Coulter). The inhibitory concentration was calculated as:

Inhibitory concentration (%) = ((1–A_{630} value treated) ÷ A_{630} value control) x 100

4.1.6 Cell proliferation assessment

To measure the proportion of cycling cells following drug treatment, the XTT assay (Bohringer Manheim, Germany) was carried out in multiwell reactions. Cells were subcultured into 96-well plastic tissue culture plates at the aforementioned cell densities in 200 μl of growth medium. After an initial 36 h incubation, drugs were added to all wells at differing concentrations ± 10 μM PFT for 24 h. At the end of the treatment period, the media was aspirated and replaced with 100 μl of fresh growth medium. Each well also received 50 μl of freshly prepared XTT labelling mixture (tetrazolium salt XTT and electron coupling reagent). Metabolically active cells cleave XTT to a soluble formazan dye which was quantitated after 6 h using a scanning multiwell spectrophotometer at the absorbance wave length of 490 nm. Inhibition of cell cycling was calculated as:

$$\text{Cytostasis (\%)} = \frac{(A_{490}\text{ value control} - A_{490}\text{ value treated})}{A_{490}\text{ value control}} \times 100$$

4.1.7 Immunohistochemistry on intestinal cells

To visualise changes in protein expression patterns following cytotoxic treatment, cells were subcultured onto 8-chamber glass slides (TissueTek, Naperville, IL, USA) at a density of 4 x 10^4 cells/well in 400 μl of growth medium. Cells were treated with 20 μg/ml CPT-11 or 0.5 μg/ml DOX ± 10 μM PFT for 24 h. At completion of each experiment, growth medium was removed and chambers washed twice with sterile PBS. Chambers were then removed before fixation of cells in freshly made 4%

paraformaldehyde for 30 min at 4°C. Fixed cells were washed twice in PBS before being incubated with 3% H_2O_2 in PBS for 10 min. Slides were rinsed in PBS before undertaking a blocking step with 20% goat serum in PBS for 20 min. Following this incubation, the excess was removed and replaced with primary antibodies against Bax, Bak, Bcl-xL and Mcl-1 diluted in PBS. Slides were incubated for 1 h at RT followed by three washes in PBS. Slides were incubated with a biotinylated secondary antibody, followed by Ultra-Streptavidin conjugated to horseradish peroxidase and finally diaminobenzidine (DAB) chromogen in 0.03% hydrogen peroxide. Slides were then counterstained in diluted Lillie-Mayer's Haematoxylin, dehydrated and mounted.

4.1.8 Protein extraction

To investigate overall protein expression, cells were grown to 80% confluency in 10 cm diameter sterile plastic tissue culture dishes. Cells were washed and given 10 ml of fresh media with or without a cytotoxic drug and incubated for 24 h. Following treatment, cells were washed twice with cold PBS and then harvested into cold lysis buffer (10 mM Tris, 150 mM NaCl, 1 mM EDTA, 1% Triton X-100 + protease inhibitor cocktail, Sigma and Roche Diagnostics) by gentle scraping of monolayer with rubber policeman. Cells were drawn up through 23 G needle and expelled into a 1.5 cm centrifuge tube on ice. This was repeated 10 times to disrupt cell membranes. Cell suspensions were spun at 10,000 rpm for 15 mins at 4°C and the supernate was collected and aliquoted to be stored at -70°C.

4.1.9 Determination of protein concentration

All samples were quantified by the Bradford Protein Assay using BioRad Protein Assay Reagent (BioRad), where bovine serum albumin (BSA) was used as the standard. All samples and standards were completed in duplicate. A 1 mg/ml BSA standard was prepared from 10 mg/ml BSA stock. The dilution series of BSA standard samples were prepared by placing 799, 798, 796, 792 and 784 µl Baxter water in sterile 5 ml tubes. 1 µl, 2 µl, 4 µl, 8 µl and 16 µl of 1 mg/ml BSA solution plus 200 µl of BioRad assay reagent was added to the water respectively to provide protein standards. Experimental protein samples were prepared by placing 2 µl of each unknown protein solution plus 200 µl of BioRad assay reagent to 798 µl aliquots of water in sterile 5 ml tubes. All tubes were vortexed and incubated for 5 min at room temperature. The protein concentration for all samples was determined on a Beckman Coulter DU 530 spectrophotometer (Life Science) at a wave length of 595 nm.

4.1.10 Western Blotting

Cell lysates were prepared, normalised for total protein content and 10 - 30 µg of protein was fractionated by SDS-PAGE before being electroblotted onto nitrocellulose membranes. Membranes were blocked with 3% skim milk in PBS containing 0.1% Tween 20 for 1 h prior to immunoblotting. Membranes were probed with anti-p53 monoclonal and p21 polyclonal Abs (1 µg/ml) overnight at 4^{o}C. This was followed by rabbit anti-mouse and goat anti-rabbit IgG Ab respectively conjugated to HRP (DAKOcytomatics) and detection by enhanced chemiluminescence (ECL; Amersham Pharmacia). Membranes were also probed with anti-ß actin monoclonal Ab (Sigma) followed by rabbit anti-mouse secondary conjugated to HRP (Dako) to control for actual protein concentration loaded.

4.1.11 Statistical analysis

Statistical analysis was carried out using the repeated measures ANOVA with post hoc test and Kruskil Wallis test to identify differences between groups. P-values <0.05 were considered statistically significant.

4.2 Results

4.2.1 Initial dose-finding experiments

IEC-6 cells were used to optimise chemotherapy agent dosing. Cells were treated with MTX, CPT-11 and DOX at various concentrations and for differing lengths of time to assess toxicity of each agent. Cells were found to be resistant to MTX, as shown by continued trypan blue exclusion following high dose treatment and lack of reduction in adherent cell number shown by methylene blue assay (Figure 4.1). As a consequence, MTX use was discontinued for all further experiments. Through trypan blue exclusion assays, it was shown that CPT-11 and DOX cause a modest and marked dose-dependent decrease in cell viability, respectively. Concentrations above 10 μg/ml for CPT-11 and 0.5 μg/ml for DOX caused significant cell death at 24 h (Figure 4.2). To determine the kinetics of cell death, IEC-6 cells were treated for either 18 or 36 h. At high drug concentrations, cell death was significantly increased at the later time point, while cell viability was similar between time points at low concentrations indicating a peak increase in apoptosis occurs within 24 h when intestinal cells are treated with low doses of chemotherapy (Figure 4.3).

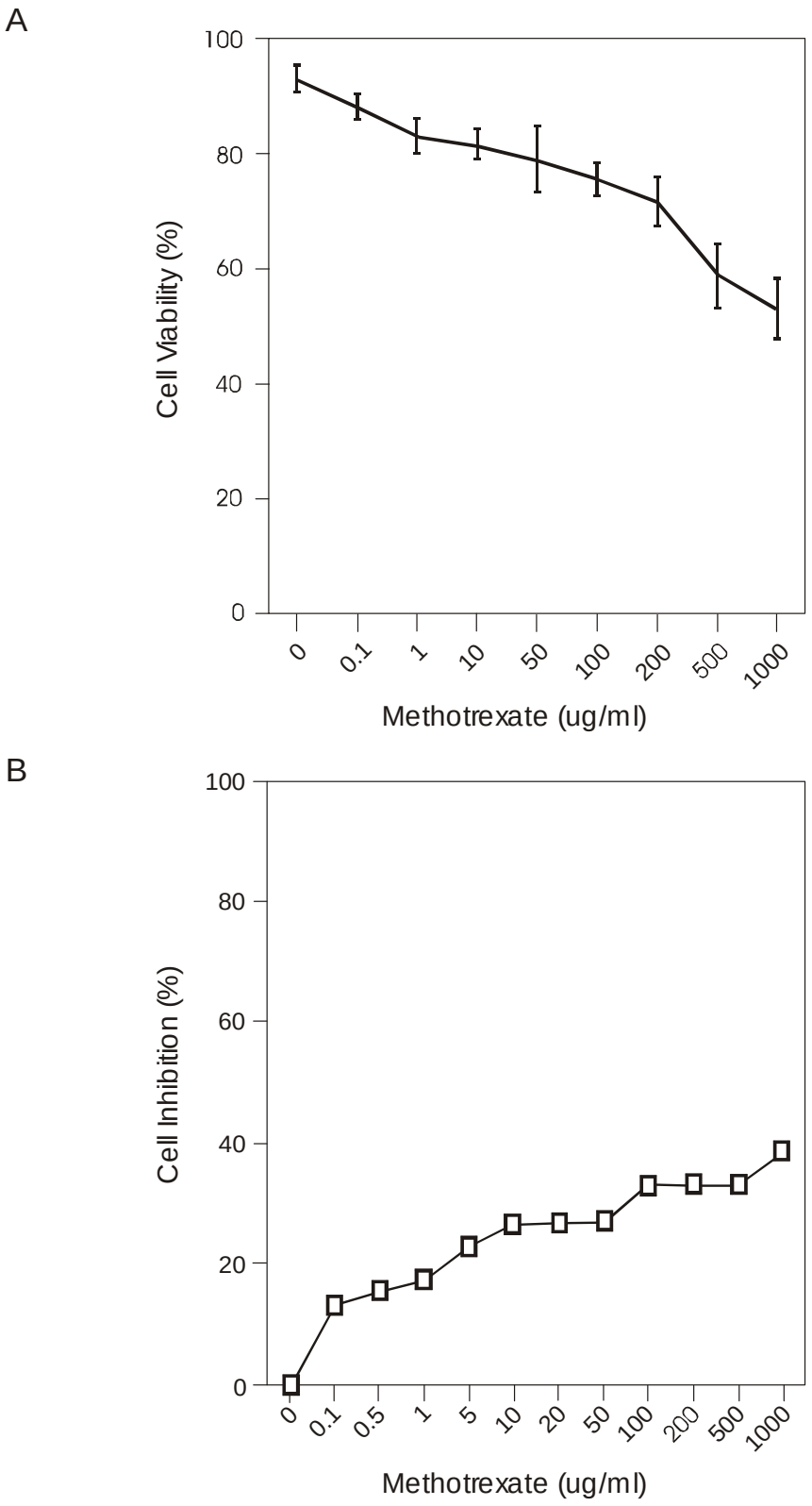

Figure 4.1. The effect of methotrexate treatment on IEC-6 cells. A) Results of trypan blue assay, data shown group mean +/- SE. B) Results of methylene blue assay, data shown group mean. Each experiment was repeated 3 times with 4 replications in each (n = 12).

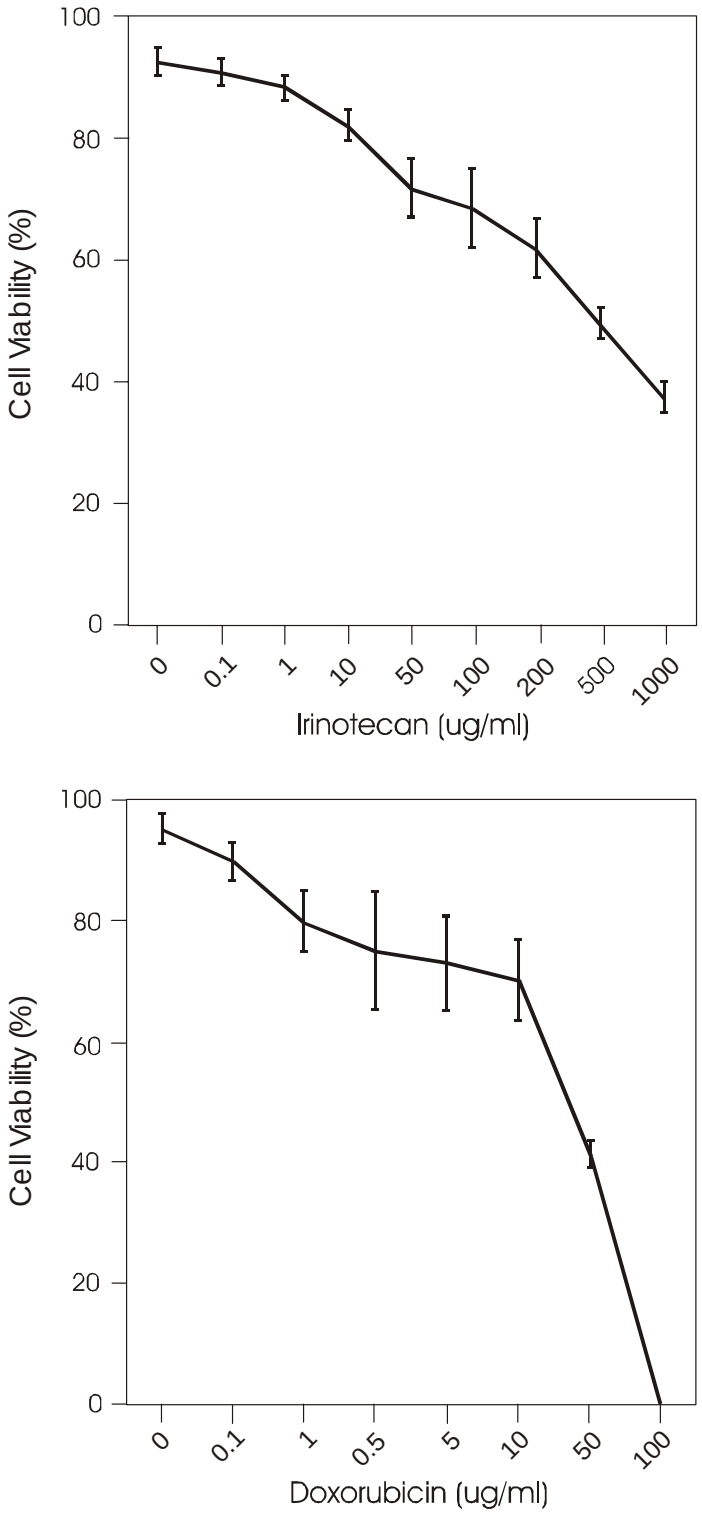

Figure 4.2. The effect of cytotoxic treatment on IEC-6 cells as assessed by trypan blue exclusion. Each experiment was repeated 3 times with 4 replications in each (n = 12). Data presented is of group means +/- SE.

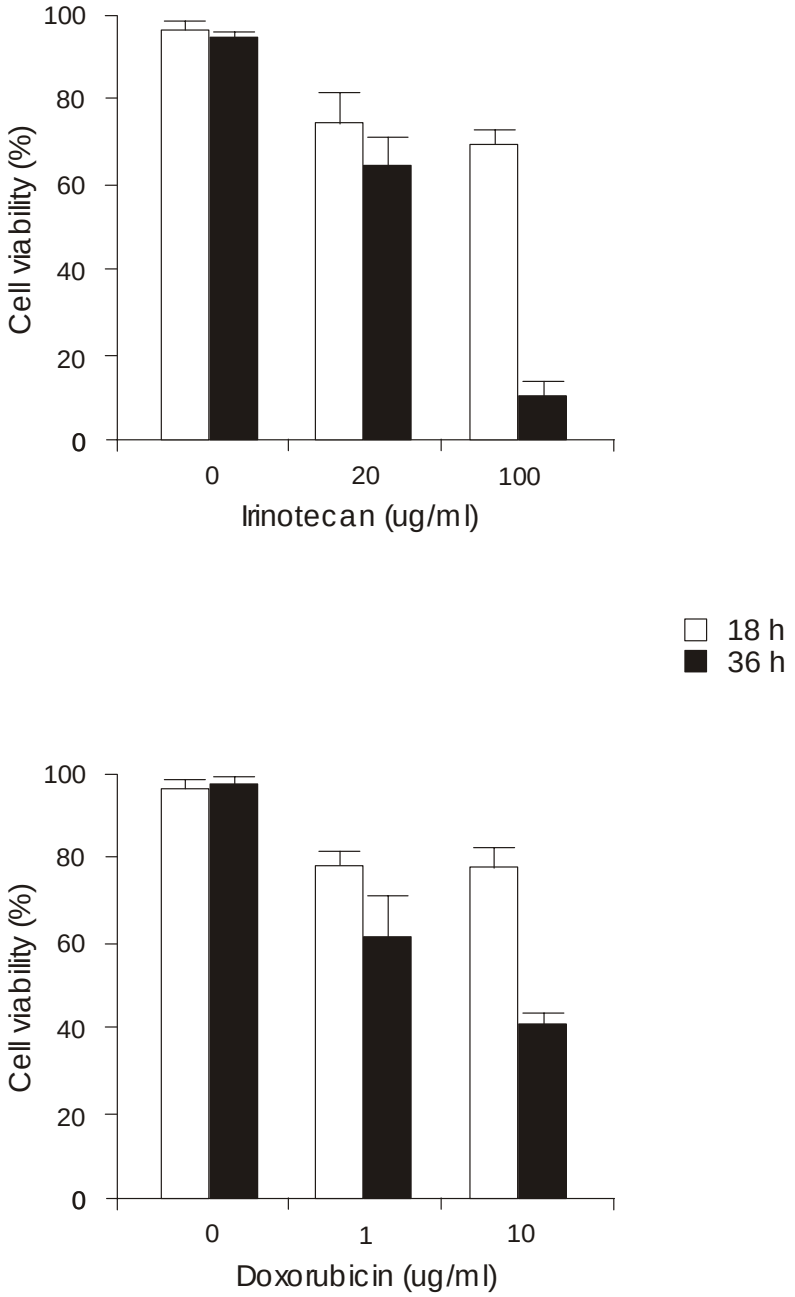

Figure 4.3. The effect of drug exposure time on IEC-6 cells. Experiments were repeated 3 times with 2 replications in each (n=6). Data presented is of group means + SE.

4.2.2 Effect of chemotherapy on cell adherence

Methylene blue assays were carried out on each cell line to determine the effect of cytotoxic agents on adherent cell number. Firstly, 24 h CPT-11 treatment caused a dose-dependent decrease in IEC-6 cell number, reaching a plateau in cell loss for concentrations above 50 μg/ml. DOX treatment for 24 h induced a more striking effect on IEC-6 cell number at low doses, with a plateau in cell loss being reached for concentrations over 1 μg/ml (Figure 4.4). The FHs 74 cell line showed a similar response to CPT-11. There was a dose-dependent decrease in adherent cells which plateau at concentrations above 100 μg/ml. Doses below 5 μg/ml did not induce cell lose. DOX treatment caused a somewhat different response in FHs compared to IEC, whereby doses below 0.05 μg/ml had no effect on cell number. A plateau in cell loss was also only noticed at concentrations above 10 μg/ml indicating a slightly better resistance to DOX in the human cell line (Figure 4.5). Treatment of the human breast carcinoma cell line, MCF-7, with CPT-11 did not cause significant cell loss at concentrations below 40 μg/ml. A sharp decrease in adherent cell number was seen between 50 and 200 μg/ml after which a plateau was noted for higher doses. A dose dependent decrease in cell number was seen for MCF-7 treated with DOX at each concentration. No plateau was observed, instead a linear relationship existed between dose and cell number up to the highest dose investigated, 20 μg/ml (Figure 4.6).

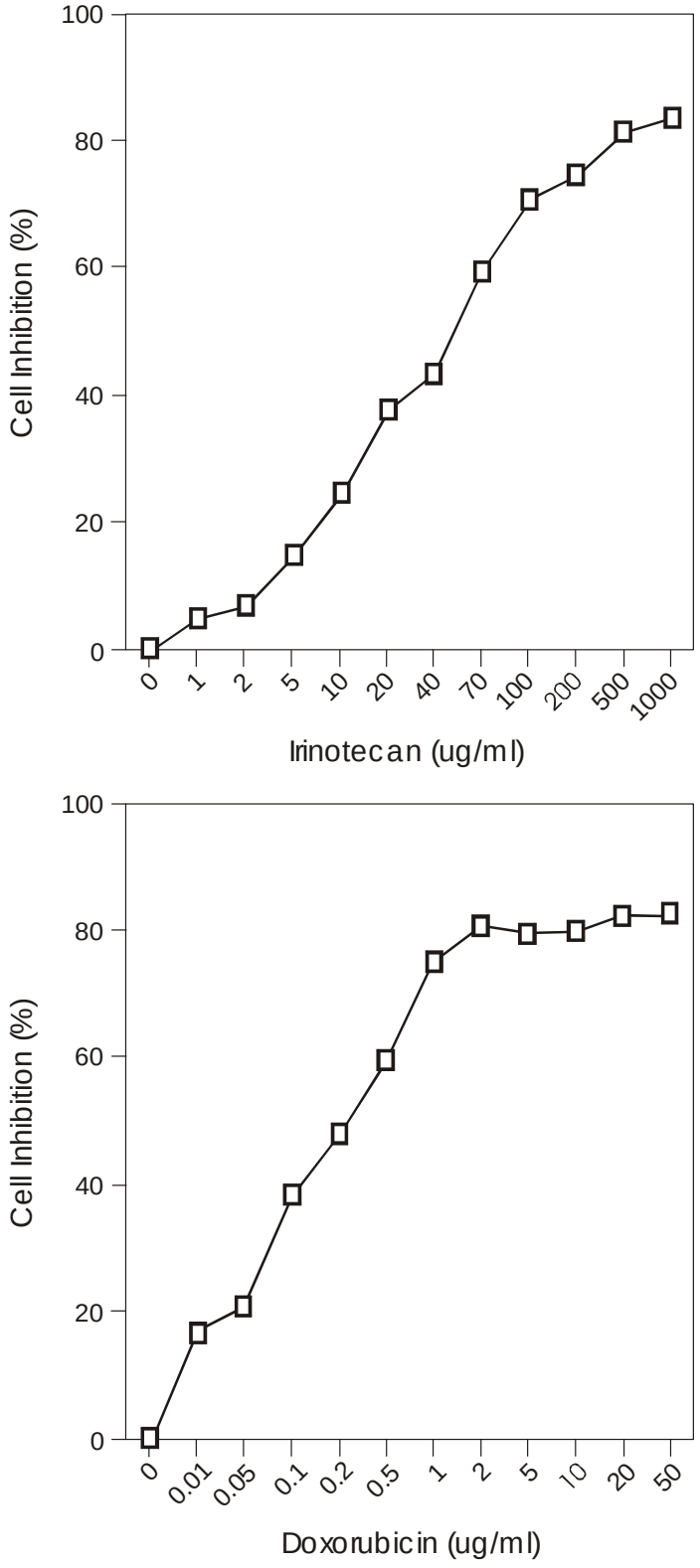

Figure 4.4. The effect of cytotoxic drug treatment on adherent cell number in IEC-6 cells, as assessed by methylene blue assay. Each experiment was repeated 3 times with 4 replications in each (n = 12). Data presented is of group means.

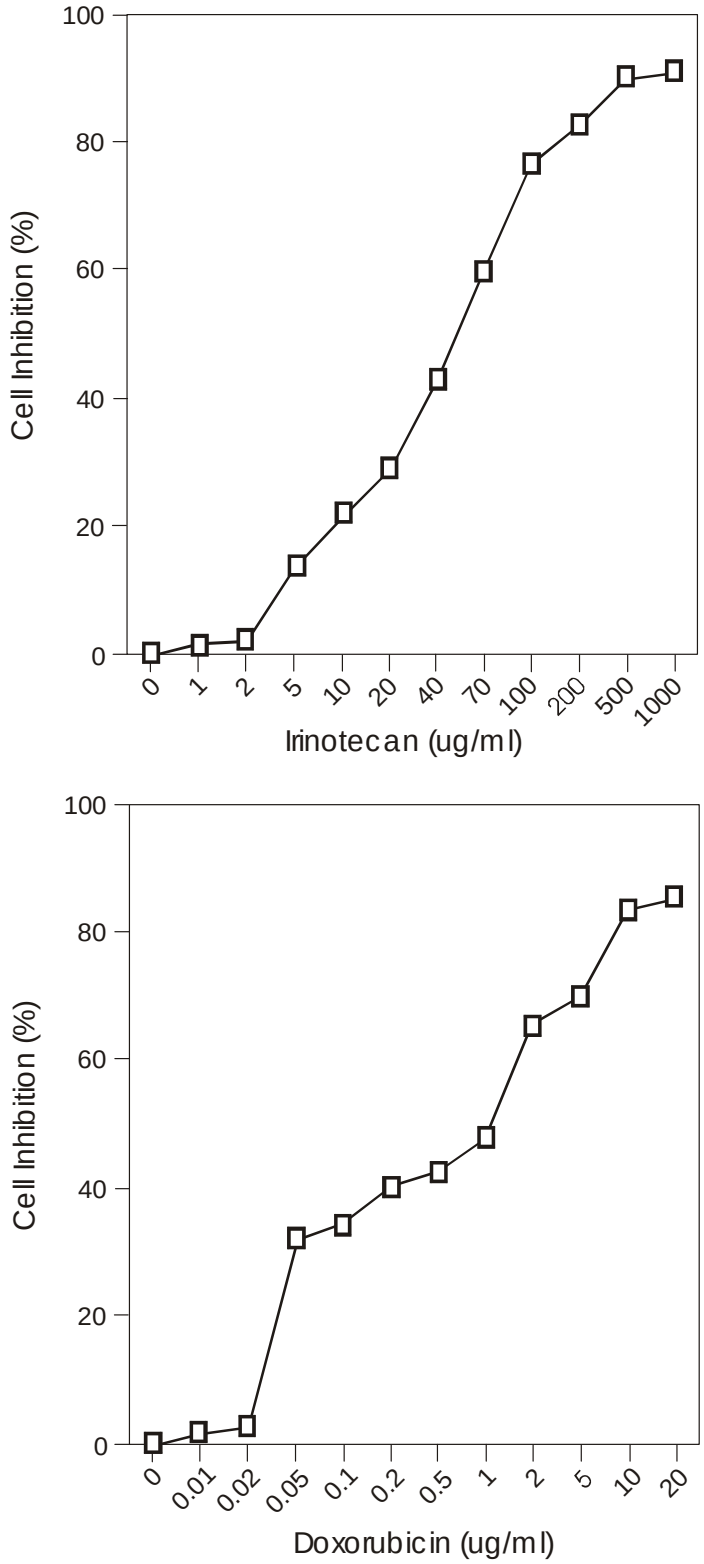

Figure 4.5. The effect of cytotoxic drug treatment on adherent cell number in FHs 74 cells, as assessed by methylene blue assay. Each experiment was repeated 3 times with 4 replications in each (n = 12). Data presented is of group means.

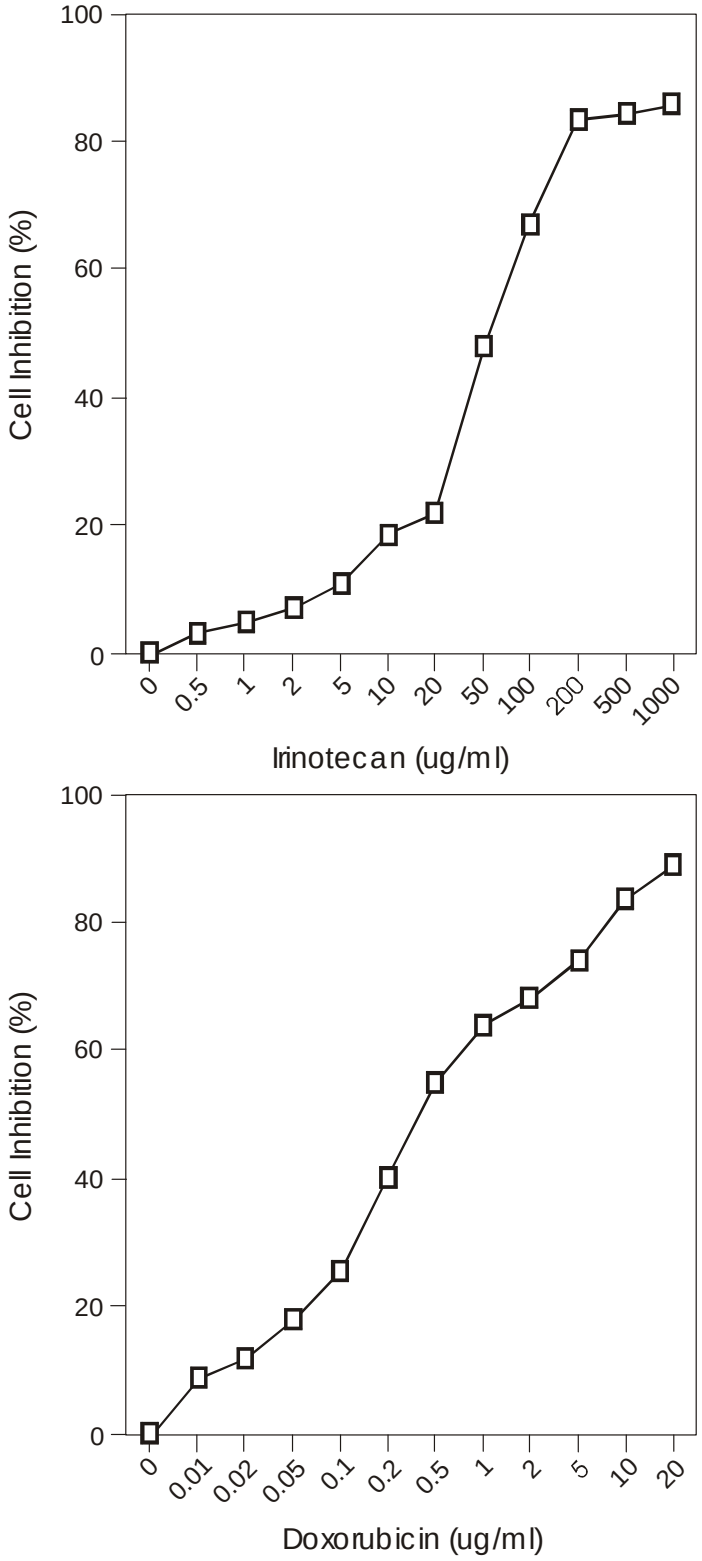

Figure 4.6. The effect of cytotoxic drug treatment on adherent cell number in MCF-7 cells, as assessed by methylene blue assay. Each experiment was repeated 3 times with 4 replications in each (n = 12). Data presented is of group means.

4.2.3 Effect of pifithrin alpha on cell survival

The nature of cell death induced by CPT-11 and DOX was investigated by temporary suppression of the transcriptional activity of p53 to determine whether a p53-dependent pathway was being utilised. During methylene blue assays, addition of 10 μM PFT immediately prior to 24 h cytotoxic drug incubation resulted in no significant improvement in cell number for either IEC-6 or FHs cell lines (Figures 4.7 and 4.8). MCF cells were protected against cell loss at high doses of CPT-11 and over a range of DOX concentrations by the addition of PFT (Figure 4.9). This indicates that cell death in the intestinal and cancerous cell lines is differentially regulated. To assess the proportion of cells that remain metabolically active following CPT-11 treatment the XTT assay was employed. CPT-11 caused a dose dependent decrease in cell cycling in each of the cell lines. PFT did not provide significant protection against cytostasis in any cell line (Figure 4.10). Of note, the relative decrease in metabolically active cells was markedly lower for the MCF cell line compared to intestinal cells, indicating the induction of apoptosis without cellular senescence in response to cytotoxic treatment in the cancerous cell line.

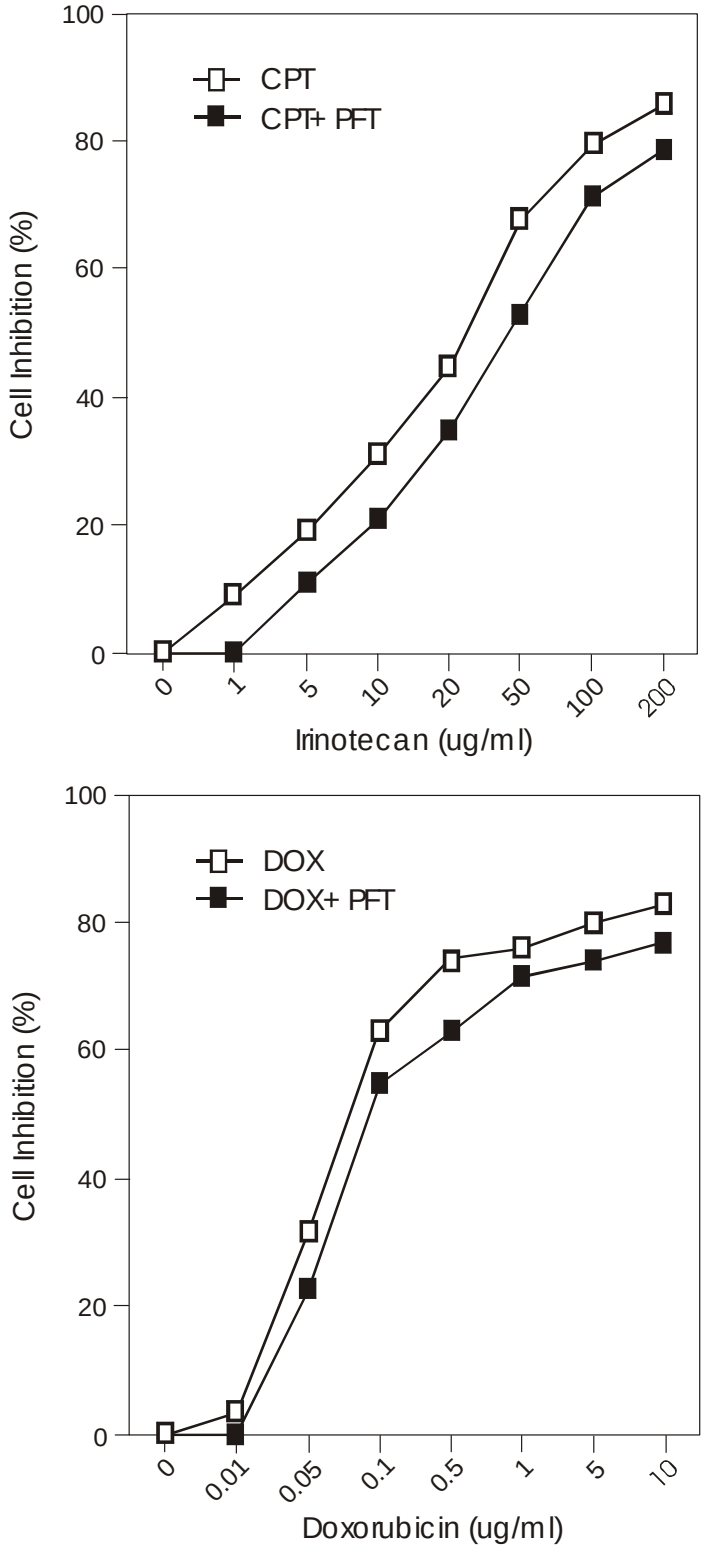

Figure 4.7. The effect of PFT on adherent cell number following cytotoxic drug treatment in IEC-6 cells. Each experiment was repeated 3 times with 4 replications in each (n = 12). Data presented is of group means.

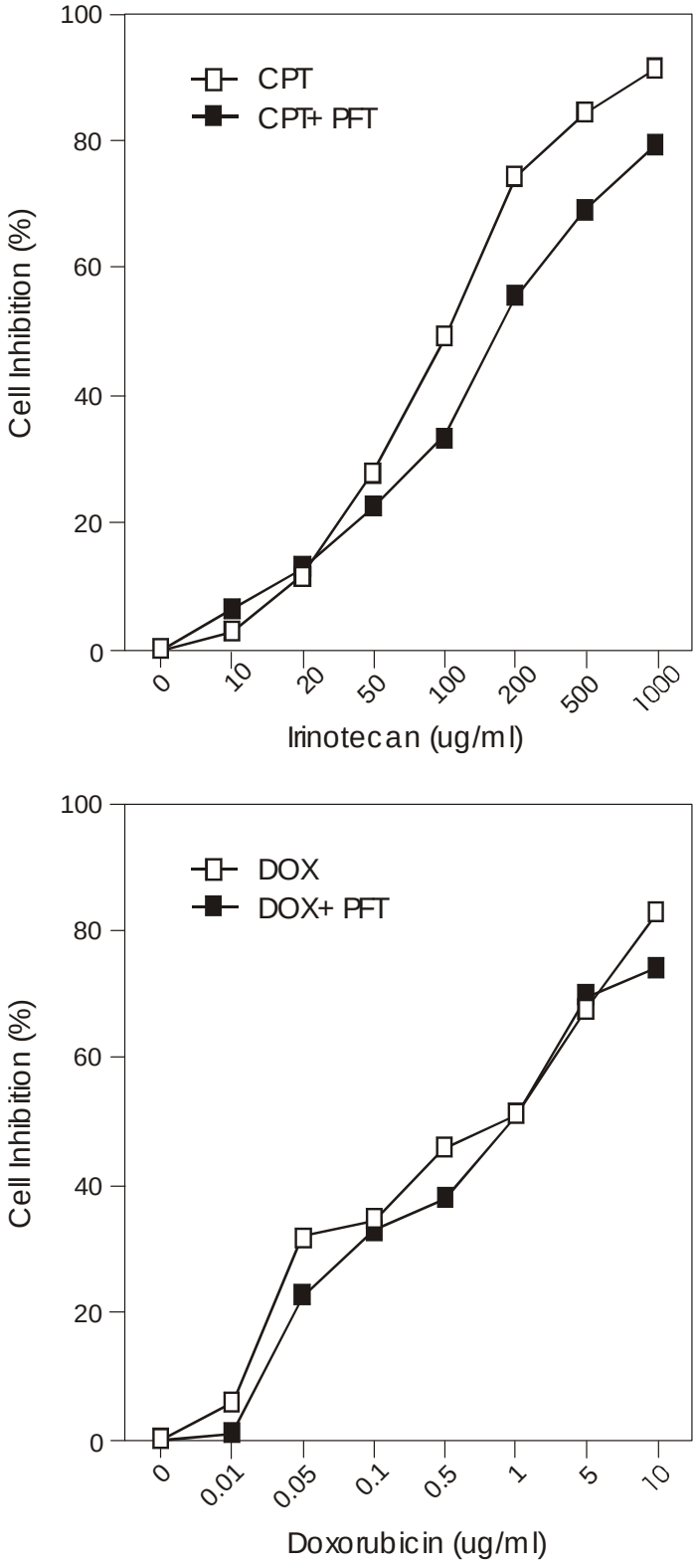

Figure 4.8. The effect of PFT on adherent cell number following cytotoxic drug treatment in FHs 74 cells. Each experiment was repeated 3 times with 4 replications in each (n = 12). Data presented is of group means.

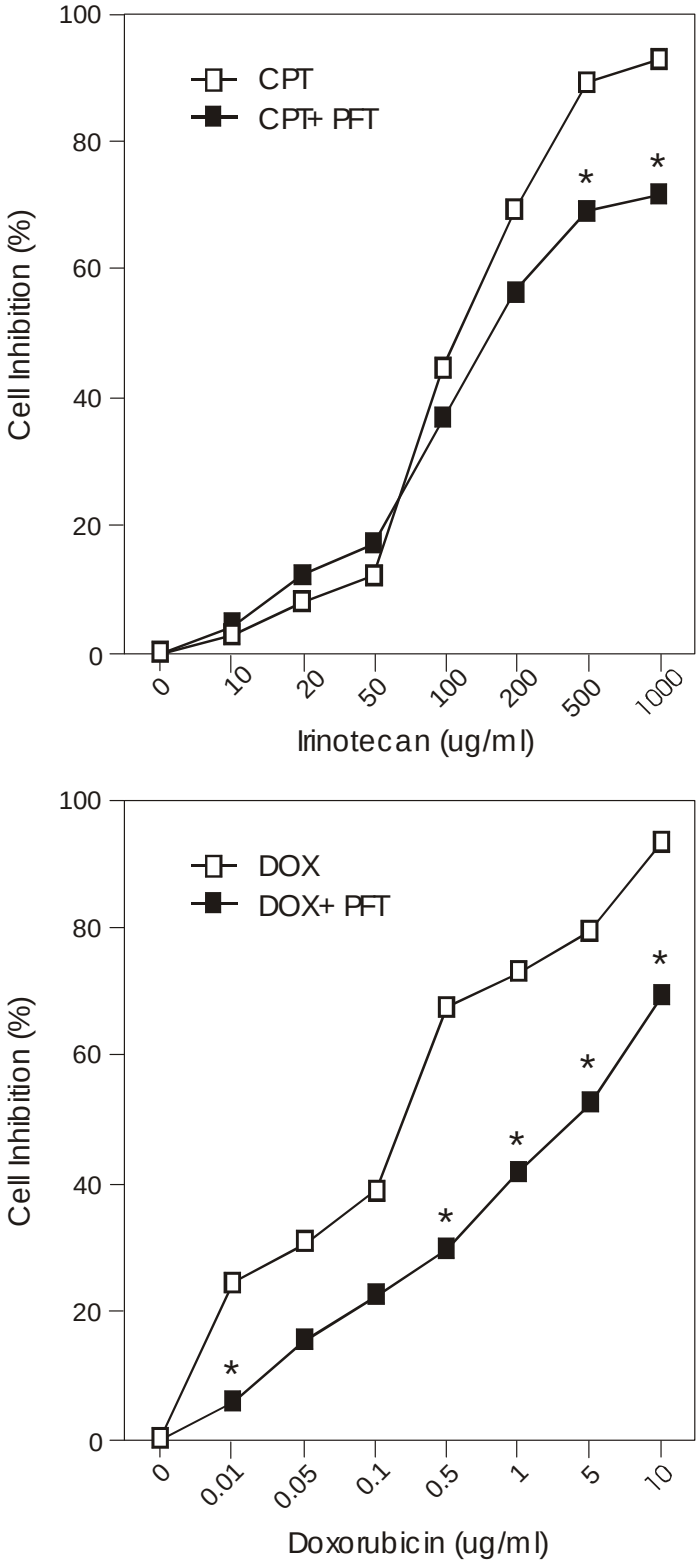

Figure 4.9. The effect of PFT on adherent cell number following cytotoxic drug treatment in MCF-7 cells. Each experiment was repeated 3 times with 4 replications in each (n = 12). Data presented is of group means.

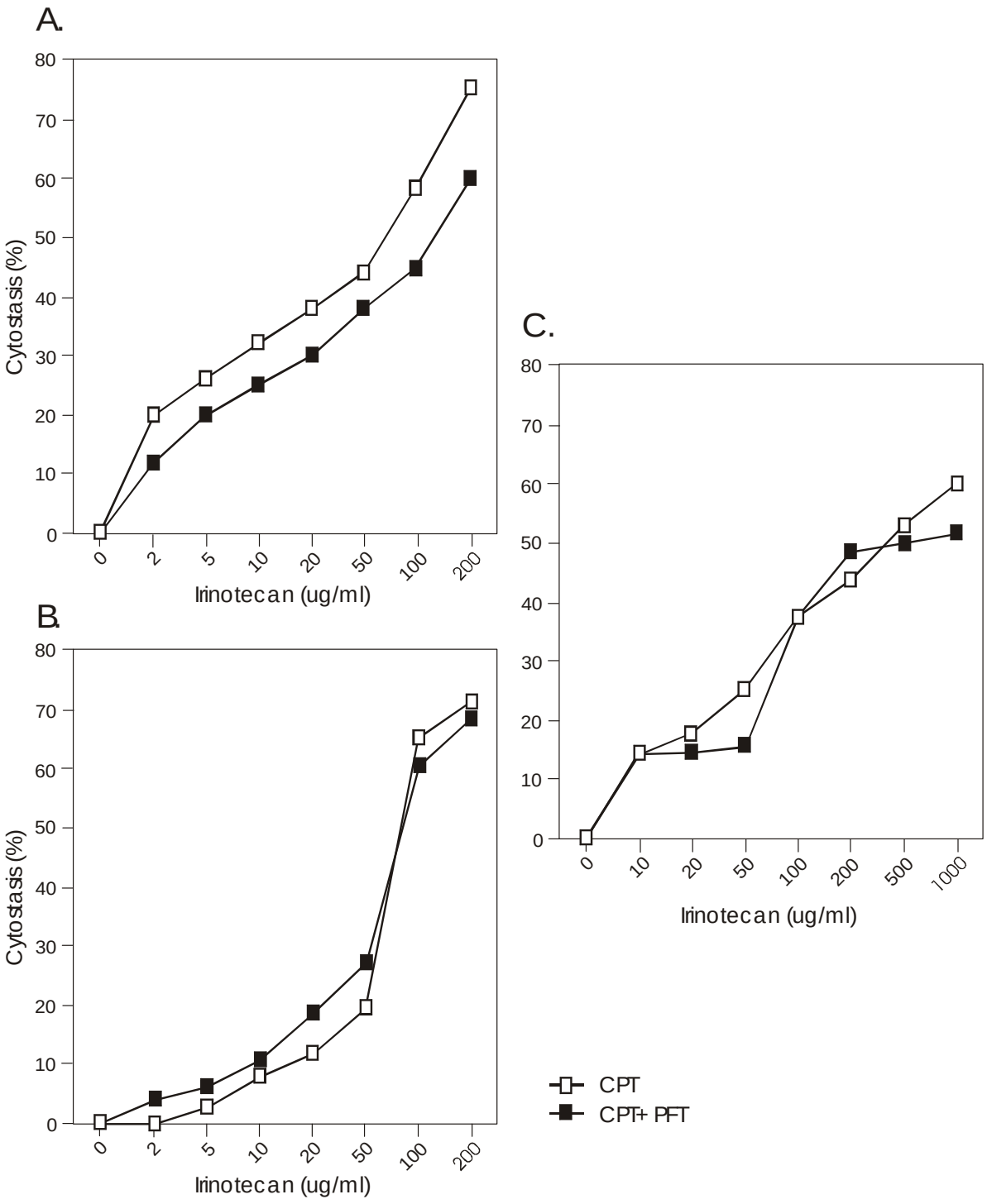

Figure 4.10. The effect of PFT on proliferation after cytotoxic drug treatment in epithelial cell lines; A) IEC-6, B) FHs 74 and C) MCF-7. Each experiment was repeated 3 times with 4 replications in each (n = 12). Data presented is of group means.

4.2.4 Effect of cytotoxic treatment on p53 and p21 expression

Through western blott detection it was found that treatment of MCF cells with DOX caused a marked increase in p53 expression, while treatment with CPT-11 was considerably weaker. DOX also induced strong upregulation of p21 in MCF cells, with only a modest increase seen following CPT-11. PFT blocks the movement of p53 into the nucleus following a death stimulus but does not affect overall cellular levels of the protein. This was evident as p53 expression was similar in MCF cells treated with DOX + PFT and DOX only. Conversely, PFT treatment reduced p21 expression in MCF cells when administered in conjunction with DOX. It did not however cause a significant reduction in p21 expression compared to CPT-11 alone treated cells. The expression of p53 and p21 was not increased in IEC or FHs cells by CPT-11 or DOX treatment (Figure 4.11).

4.2.5 Effect of cytotoxic treatment on Bcl-2 family expression in intestinal cells

IEC and FHs cells were grown on glass slides and subjected to immunohistochemistry to detect Bcl-2 family proteins. MCF cells were only weakly adherent following growth in chambers slides and as such unsuitable for immunohistochemistry. Treatment with both DOX and CPT-11 caused a marked increase in Bax and Bak expression in IEC cells with an increase from <20% cells stained to >80% of cells stained (Figure 4.12 and 4.13). A marginal increase in Bak staining was noted for FHs cells following DOX treatment, while a strong increase was seen for Bax. Treatment with CPT-11 did not cause a significant change in either Bax or Bak expression in FHs cells. There was weak cytoplasmic staining of Bcl-xL in approximately 50% of FHs cells which was unchanged by CPT-11 or DOX. Less than 20% of IEC cells were positive for Bcl-xL. They too had very weak cytoplasmic staining which was unaltered following any treatment. Finally, Mcl-1 expression was reduced by CPT-11 in IEC cells, with a decrease from around 40% positively stained cells to <10% following treatment, however was unchanged in FHs cells. Treatment of either cell line with PFT alone resulted in no change in expression of Bcl-2 family proteins compared to controls.

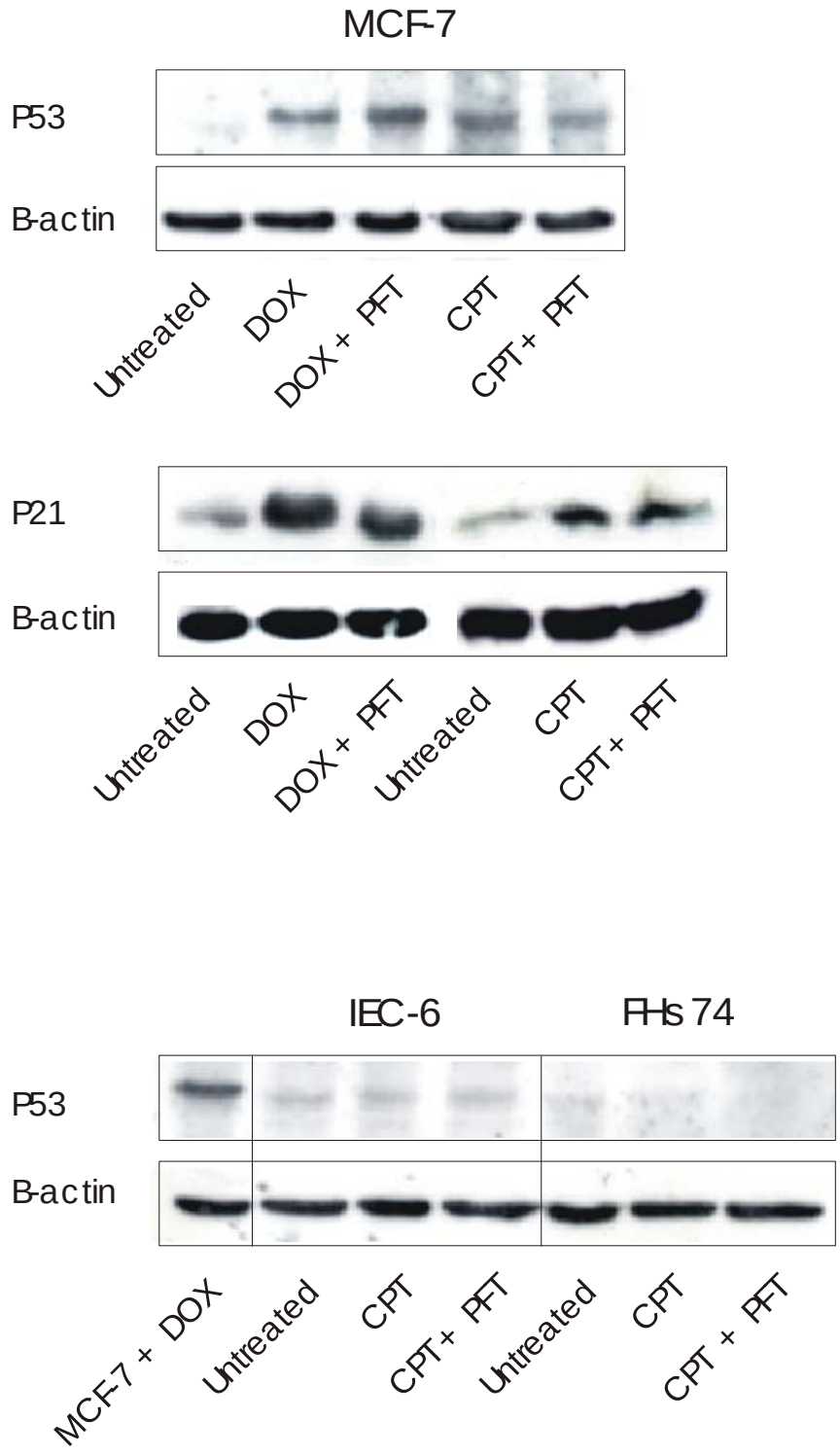

Figure 4.11. The effect of PFT and cytotoxic drug treatment on protein expression in epithelial cell lines. Each experiment was repeated 3 times. Results presented in each case is of a typical Western Blott experiment.

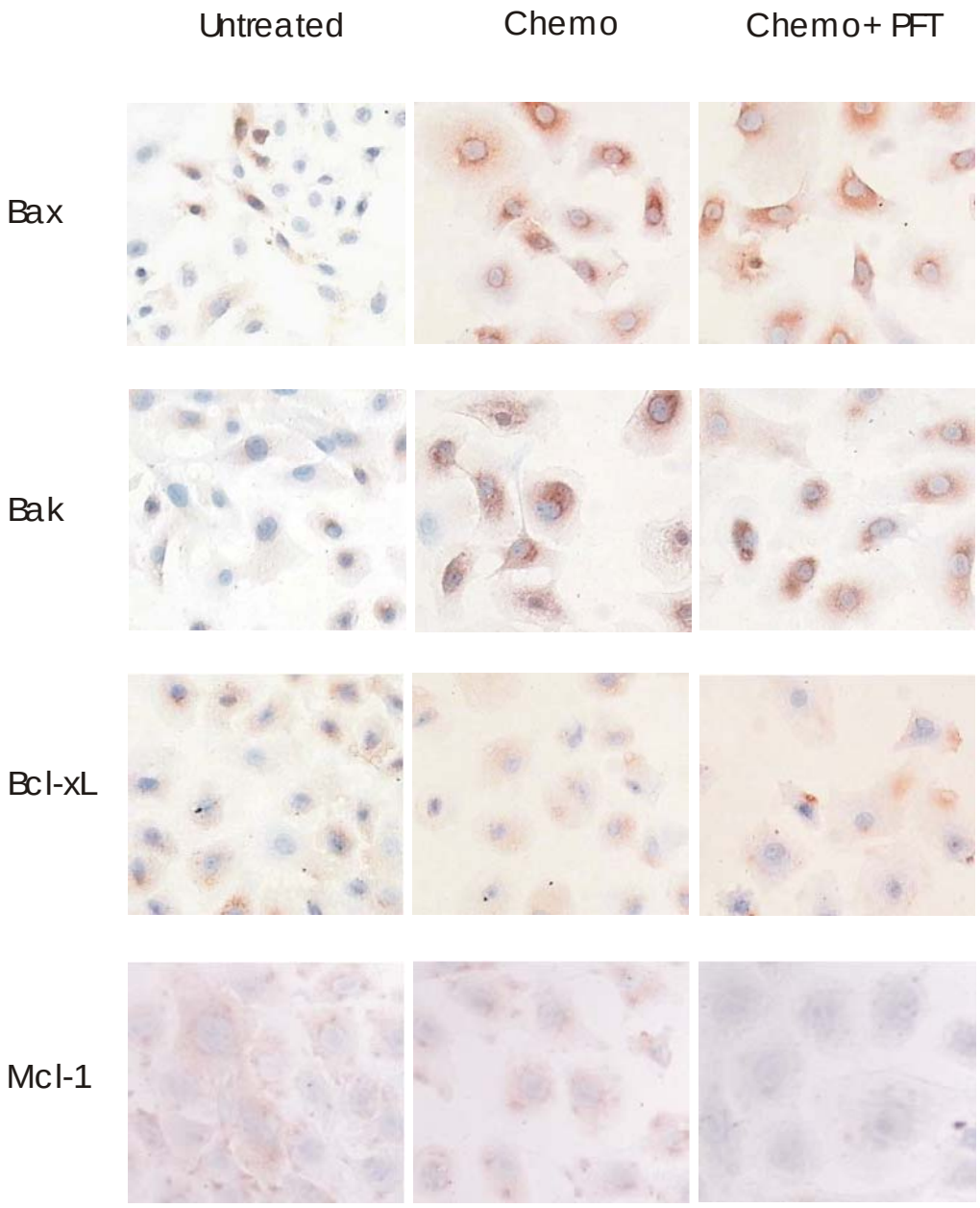

Figure 4.12. The effect of PFT and DOX treatment on Bcl-2 family protein expression in IEC-6 cells. Each experiment was repeated 3 times. Photomicrographs are of typical staining in each case. Original magnification x400

.

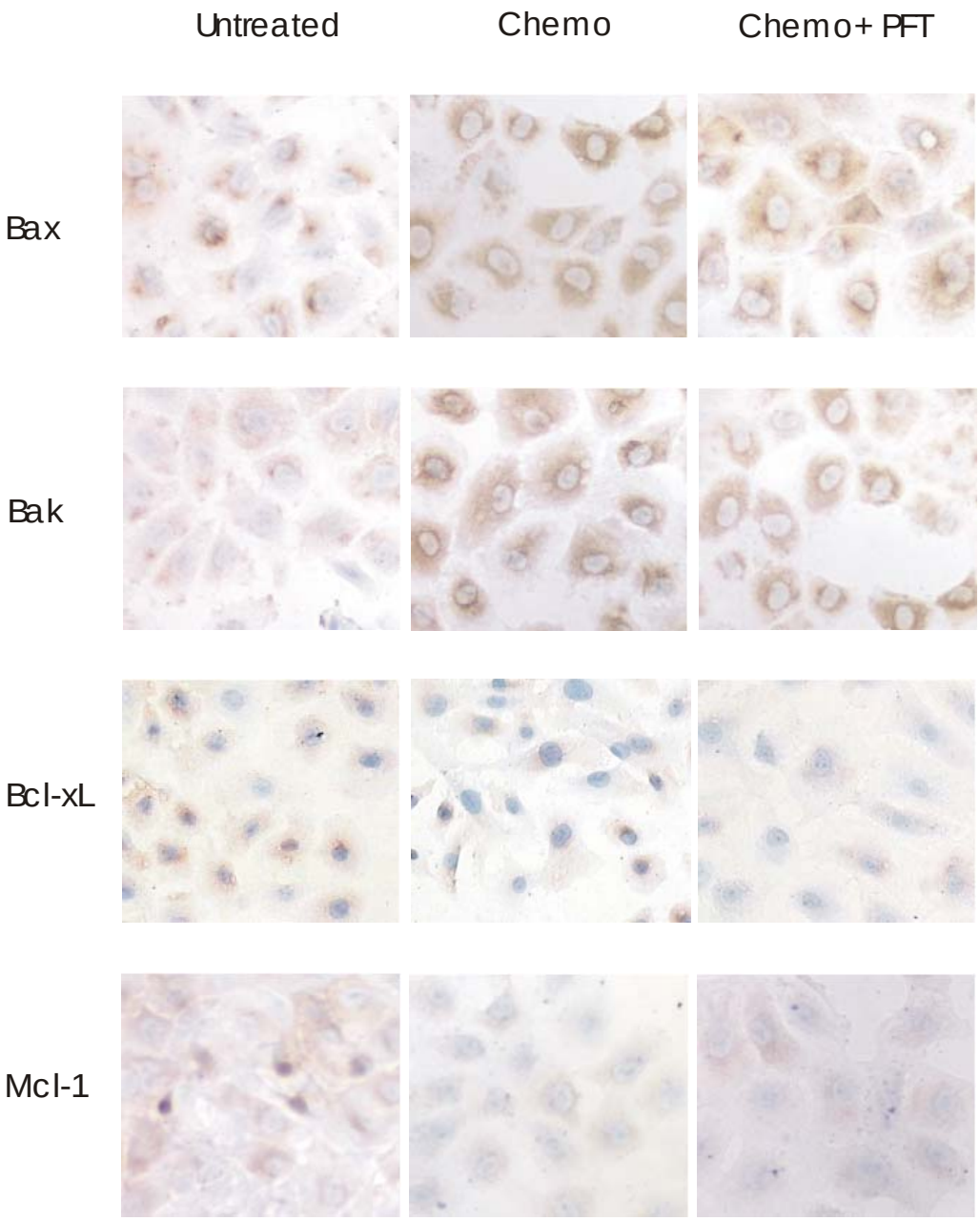

Figure 4.13. The effect of PFT and CPT treatment on Bcl-2 family protein expression in IEC-6 cells. Each experiment was repeated 3 times. Photomicrographs are of typical staining in each case. Original magnification x400

.

4.3 Discussion

Cancer treatment agents damage the lining of the intestine and cause significant alterations in architecture and barrier function along with changes in gene expression (Gibson et al., 2005; Keefe et al., 2000). The result of these changes is mucositis, a severe dose-limiting toxicity and potentially life threatening condition (Pico et al., 1998; Sonis et al., 2001). To date, our understanding of the pathobiology of mucositis has been limited, and this has been partly caused by the intestine being a relatively difficult organ to investigate due to its location and complex tissue structure inhibiting the number of studies. However, the development of non-transformed intestinal cell lines has provided us with an ability to examine epithelial cells in isolation and their response to chemotherapy agents without the restrictions caused by whole tissue harvesting.

A wide range of cancer treatment agents, including chemotherapy drugs and radiotherapy, have been shown to induce apoptosis and restrict proliferation in epithelial crypts in the small and large intestine (Clavijo et al., 2004; Keefe et al., 2000; Potten, 2004; Potten et al., 1997; Wilson et al., 1998). It has been postulated that these changes culminate in mucosal barrier injury. As such, the effect of irinotecan (CPT-11) and doxorubicin (DOX) on levels of apoptosis and cell cycling in epithelial cell lines was investigated, as too the nature of these cytotoxic effects through examination of associated changes in gene expression. This study has been the first to investigate multiple effects of CPT-11 and DOX treatment in normal intestinal cells and has shown that they both cause a dose-dependent decrease in cell viability which is associated with increases in pro-apoptotic Bax and Bak protein expression. A previous study using the IEC-6 cell line also found that CPT-11 decreases cell viability (Shinohara et al., 1999), however this experiment differed from the current study in that cell number was quantified only after a 96 h incubation with a very low concentration of the drug. In that experiment the MTT assay, which is similar in principle to the XTT assay, showed a 60% cytostasis induced by CPT-11 treatment. The current trial found that CPT-11 induced a 20% cytostasis at the equivalent concentration after only 24 h which was markedly increased with escalating doses. This shows that intestinal cells are affected by both the dose and duration of exposure to chemotherapy agents which correlates well to damage seen *in vivo*. No previous reports could be found describing the effects of doxorubicin on IEC-6 or FHs 74 cells.

The two drugs used in this study, CPT-11 and DOX, act on the cell by inhibiting topoisomerase I and topoisomerase II enzymes respectively and hence are potent

antiproliferative agents (Ando and Hasegawa, 2005; Lorenzo et al., 2002). It is unknown however if these drugs activate a p53-dependent apoptosis pathway in intestinal cells. The MCF-7 cell line was derived from a human breast epithelial carcinoma and has been shown to undergo p53-dependent apoptosis in response to a number of agents including DOX (Troester et al., 2004; Wang et al., 2004; Zhu et al., 2001). For this reason it was included as an internal control for the study and was again shown to upregulate p53 and p21 following treatment. To determine the role of p53 in chemotherapy-induced cell death in intestinal cells a temporary p53-inhibitor, pifithrin alpha (PFT), was included in a series of experiments. PFT was firstly shown to inhibit apoptosis in response to DOX in MCF cells and also CPT-11 at high concentrations, however did not prove effective in either intestinal cell line. This indicates that the normal and cancerous cell lines in this study activate a different apoptotic pathway following chemotherapy. This was confirmed by the lack of p53 expression in response to treatment in both intestinal cell lines, compared to strong p53 activation in the MCF-7 cell line. This phenomenon has been reported previously (Wang et al., 2004).

Thus the question remains, if apoptosis is occurring in a predominantly p53-independent fashion in response to chemotherapy treatment with these agents in intestinal epithelial cells, then what is responsible for cell death in this setting? It is likely that generation of reactive oxygen species (ROS) in combination with direct DNA damage contribute to cellular injury. Activation of the transcription factor NFκB and its mediators by ROS has been implicated in the induction of mucositis (van't Land et al., 2004; Yeoh et al., 2005). Furthermore, a role for NFκB is likely since PFT has no effect on its activation, unlike p53 (Komarova et al., 2003) which may partly explain PFT's limited effects within the study. The pro-apoptotic role of NFκB in mucosal toxicity in cancer patients is a field currently under intense investigation (Sonis, 2002). The possibility of intestinal cell lines carrying a p53 mutation was not investigated in this study, although this would explain the lack of activation following cytotoxic insult. The IEC-6 cell line has previously been reported to have normal p53 (Ray et al., 2001; Ray et al., 1999), while no reports exist for FHs 74.

The intestinal epithelium is a unique and complex tissue which carries out multiple functions simultaneously. When these functions are altered following cancer therapy, systemic disturbances are the result. Investigations using epithelial cell lines will improve our understanding of the biological consequences of cytotoxic treatment and ultimately prevent these toxicities. This study has provided evidence of a p53-independent pathway,

utilising Bcl-2 family apoptotic proteins, in intestinal cell death following two chemotherapy agents. This correlates well with the established *in vivo* model of intestinal damage seen in the DA rat. Continued studies with cell lines are required to elucidate the exact mechanisms of cancer therapy-induced epithelial damage and mucosal barrier injury. However, further animal work will also be required due to the epithelial-subepithelial interactions *in vivo*.

The effect of irinotecan on the intestine in the rat with breast cancer.

5.0 Introduction

Some degree of alimentary mucositis occurs in 40% of patients undergoing standard dose cancer treatment and in 100% of patients receiving high dose chemotherapy with autologous cell transplantation (Keefe et al., 2004). Despite this, it remains without a truly effective treatment or preventative solution. This has led to a number of studies investigating the effectiveness of potential antimucotoxics in the laboratory and clinic. The hallmark histological features of intestinal mucositis include apoptosis, crypt hypoplasia, reduction in villous morphometry and increased permeability with or without inflammation (Keefe, 1998; Keefe et al., 2000). At the patient level, symptoms include diarrhoea, abdominal pain, nausea, vomiting and ulceration (Keefe, 1998; Pico et al., 1998). It is still yet to be completely elucidated which morphological and functional changes in the gut contribute to patient symptoms, however it is imperative that preventative therapies are designed in response to increased understanding of the pathogenesis of mucositis. Recently, Palifermin (human recombinant keratinocyte growth factor, Amgen) has become the first cytokine approved in the use of preventing oral mucositis in patients with haematological malignancies receiving myelotoxic therapy requiring stem cell transplantation. It may also work in solid tumours in patients receiving chemotherapy, however this has yet to be fully tested. As such, the search for an effective broad spectrum anti-mucotoxic continues.

Irinotecan is a relatively new chemotherapy agent which is used commonly in the treatment of colorectal cancer. It is a topoisomerase I inhibitor and acts on the DNA complex to disrupt replication and induce cell death (Ando and Hasegawa, 2005; Ikuno et al., 1995; Yu et al., 2005). Although effective against tumours, it also causes severe gastrointestinal mucositis in a large proportion of patients, with the most frequent toxicity being severe diarrhoea (Abigerges et al., 1994; Gibson et al., 2003). The biochemical mechanisms for early and late-onset diarrhoea induced by irinotecan differ and are thought to involve adverse cholinergic effects and direct mucosal damage respectively. Furthermore, pathological changes may also include activation of COX-2 expression and TNF-α secretion, both of which play an important role in causing colonic damage and inflammation (Alimonti et al., 2004; Gibson et al., 2005b; Yang et al., 2005). Irinotecan has gained much interest for intestinal mucositis research and a number of novel preventative agents have been trialed with varying degrees of success. These have

included growth factors (Boushey et al., 2001; Gibson et al., 2005b; Hecht, 1998), cytokines and their modulators (Cao et al., 1998; Govindarajan et al., 2000; Shinohara et al., 1998; Zhao et al., 2004), COX-2 inhibitors (Trifan et al., 2002) and antibiotics (Takasuna et al., 1998).

Traditionally, investigations into the morphological effect of irinotecan on the intestine have been conducted in rodent models receiving multiple doses of irinotecan to induce mucositis (Cao et al., 1998; Gibson et al., 2003; Gibson et al., 2005b; Ikuno et al., 1995; Trifan et al., 2002). From these studies, it is known that irinotecan causes apoptosis early, which is followed by epithelial crypt loss. Apoptosis is activated in response to DNA damage which can be controlled by the transcription factor, p53 (Benchimol, 2001; Lowe et al., 1993; Merritt et al., 1994; Weller, 1998). The p53 protein regulates a number of downstream genes that act on the intrinsic and extrinsic apoptotic pathways. Targets along the intrinsic pathway include multiple members of the Bcl-2 family (Bax, Bak, Noxa, Puma, Bcl-2 and Bcl-xL) (el-Deiry, 1998; Hershko and Ginsberg, 2004; Muller et al., 1998; Nita et al., 1998; Norbury and Zhivotovsky, 2004; Reinke and Lozano, 1997; Sax et al., 2002; Shibue et al., 2003). It is believed alterations in expression ratios of pro-apoptotic and anti-apoptotic members of the Bcl-2 family control sensitivity of the cell to cytotoxic stimuli and ultimately its survival (Miyashita et al., 1994; Miyashita and Reed, 1995; Raisova et al., 2001; Upadhyay et al., 1995; Zong et al., 2001). Another function of p53 is to activate genes required to arrest the cell cycle, namely, $p21^{waf/cip-1}$ and 14-3-3 sigma (Fei et al., 2002; Vousden and Lu, 2002). The p21 protein is a cyclin dependent kinase inhibitor and once activated holds cells in G_1 phase (Harris and Levine, 2005). The requirement of p53 to transcriptionally activate genes to induce apoptosis and halt cell cycling can be exploited through blockade by chemical compounds (Kannan et al., 2001; Komarova and Gudkov, 2001). The small anti-parasitic compound, pifithrin α (1-[4-Methylphenyl]-2-[4,5,6,7-tetrahydro-2-imino-3(2H)-benzothiazoly]-ethane monohydrobromide), was identified as a temporary inhibitor of p53 that prevents movement of p53 into the nucleus following cytotoxic stimuli hence rendering it unable to act as a transcription factor (Gudkov and Komarova, 2003; Gudkov and Komarova, 2005; Komarov, 1999). It has since been tested in various models of cancer treatment induced cell death and shown to be effective at ameliorating damage (Culmsee et al., 2001; Komarova et al., 2003; Schafer et al., 2003; Vollmar et al., 2002; Zhang et al., 2003).

This study was designed to answer a number of questions relating to the mechanism of irinotecan-induced damage in the intestine. Firstly, the effect of a single dose of irinotecan on apoptosis and crypt damage has not previously been investigated in the DAMA rat model and hence was chosen to characterise these changes at early time-points following treatment. Secondly, it is unknown whether apoptosis seen within crypts following irinotecan occurs through activation of p53 and if so, what the expression profile is. And thirdly, this study aimed to determine if blockade of p53 is effective at ameliorating irinotecan-induced mucositis in the rat with breast cancer.

5.1 Methods and Materials

5.1.1 Laboratory animals

This study was approved by the Animal Ethics' Committees of the Institute of Medical and Veterinary Sciences, Adelaide and of the University of Adelaide and complied with National Health and Research Council (Australia) Code of Practice for Animal Care in Research and Training (1997). Female Dark Agouti (DA) rats, aged 6-8 weeks and weighing approximately 160 g were purchased from the Institute of Medical and Veterinary Sciences MedVet division, group housed and kept under a 12 h light/dark cycle with free access to food and water until the study commenced (approximately 2 weeks).

5.1.2 Preparation of tumour inoculum

All animals used in this study carried a subcutaneous tumour. The mammary adenocarcinoma for this study arose as a spontaneous tumour in the 1970s. It has been propagated since by passage through female DA rats. The tumour was donated by Dr. A. Rofe (Institute of Medical and Veterinary Sciences, Adelaide, South Australia) in 1996 to develop a model to assess small intestinal and tumour effects of chemoprevention (Keefe, 1998). This tumour has since been used extensively in our laboratory. One female donor rat was injected s.c. on both flanks with 0.2 ml (2.0×10^7 cells/ml) tumour inoculum 11 days prior to the study beginning. Over the subsequent days these cells form a tumour under the skin on both flanks. To harvest the tumour cells the rat is culled by CO_2 asphyxiation and cervical dislocation. Subcutaneous tumours are dissected and placed into ice cold sterile PBS. The tumours are diced, homogenised and filtered through sterile gauze. The resultant cell suspension is spun at 250 g for 3 minutes. The supernate is removed and the cell pellet resuspended in fresh sterile PBS. This is repeated a further 3 times. A viable cell count is carried out using 0.4% w/v trypan blue.

5.1.3 Experimental design

Forty female DA rats (weighing approximately 180 g) were implanted with tumour inoculum of 4.0×10^6 cells in 0.2 ml of PBS s.c. into each flank and divided into 8 groups as follows; 1) control day 0, 2) CPT-11 only day 0, 3) CPT-11 + PFT day 0, 4) PFT only day 2, 5) control day 2, 6) CPT-11 only day 2, 7) CPT-11 + PFT day 2 and 8) PFT only day 2. Tumours were allowed to grow for 9 days after which time rats in CPT-11 treated groups (2, 3, 6 and 7) were given an injection of irinotecan (200 mg/kg i.p.) to induce mucositis. Irinotecan was administered in a sorbitol/lactic acid buffer (45 mg/ml

sorbitol/0.9 mg/ml lactic acid) that is required for activation of the drug. Rats also received 0.01 mg/kg s.c. atropine immediately prior to irinotecan to reduce any cholinergic reaction to the treatment. The rats in groups receiving PFT (3, 4, 7 and 8) were administered the compound diluted in DMSO (2.2 mg/kg i.p.) immediately prior to CPT-11. Control group rats (1 and 5) received DMSO injection only. Daily body weight was recorded along with 4x daily assessment of reaction to treatment. Animals were culled by CO_2 asphyxiation and cervical dislocation at 6 and 48 h after treatment. The gastrointestinal tract from the pyloric sphincter to the rectum was removed and flushed with sterile 0.9% w/v saline and the weight of the small and large intestine recorded. Two cm samples of small intestine (jejunum) at 25% of the length of the small intestine from the pylorus and from the mid colon were collected, and fixed in 10% neutral buffered formalin or in Clarke's fixative for further analysis.

5.1.4 Histological examination

Samples of jejunum and colon were collected and formalin fixed overnight for routine histological examination. Tissue was paraffin embedded before being sectioned at 4 μm and baked onto glass microscope slides. Following dewaxing in xylene and rehydration of tissue, sections were stained in Mayer's haematoxylin for 10 mins. Following differentiation in 1% acid alcohol and blueing of sections in Scott's tap water, sections were counterstained with eosin for 3 mins. Sections were dehydrated and cleared before being mounted. Slides were sent to specialist veterinary pathologist, Dr. John Finnie, of the Institute of Medical and Veterinary Sciences, South Australia, for expert reporting.

5.1.5 Intestinal morphometry

Sections of jejunum and colon were opened onto cardboard and fixed for 24 h in Clarke's fixative, before being transferred to 70% ethanol for storage. To investigate intestinal morphometry, tissues were firstly removed from cardboard, rehydrated gradually and then hydrolysed in 1M HCl for 7 mins at 60°C. Tissue was then washed twice with double distilled water and stained in Schiff's reagent. After 45 mins, the tissue was washed once more with double distilled water before being microdisssected using a cataract knife and stereomicroscope under 20x magnification. Microdissected tissue was mounted in 45% (v/v) acetic acid to measure villous area and crypt lengths using a calibrated graticule. Villous area was calculated as a trapezoid approximation by measuring villous height and apical and basal width. Villous area and crypt length correlate with villus and crypt epithelial cell populations, respectively (Cummins et al., 1990).

5.1.6 Apoptosis measurement

Sections of jejunum and colon were fixed in 10% neutral buffered formalin for 24 h. Tissue was routinely processed through ethanols and xylene and embedded into paraffin wax. Sections of intestine were cut at 4 μm and subjected to TUNEL (TdT-mediated dUTP neck end labelling) assay by the In Situ cell death detection kit AP (Roche, Mannheim, Germany) according to manufacturer's instructions. The methodology employed for labelling apoptotic cells was similar to that of Gavrieli (Gavrieli et al., 1992). After dewaxing, slides were rehydrated to water before being immersed in 0.1% TX-100 in 0.1% (w/v) sodium citrate buffer for 8 mins. Sections were rinsed twice in PBS and then covered with a TUNEL buffer solution (150mM Tris; 0.7M NaCaCo; 10mM $CoCl_2$; 10% BSA and sterile H_2O) for 10 mins. The buffer was removed without rinsing, and slides were immediately incubated with reaction mixture for 3 hours at 37°C in an humidified chamber. Following stringent washes in PBS, slides were incubated with Converter-AP solution for a further 60 mins at 37°C in an humidified chamber. Slides were then subjected to another series of washes in PBS before Fast Red chromogen (Roche) was applied for 15 mins. The reaction was halted by washing slides in 2 changes of PBS. Slides were counterstained with Mayer's haematoxylin and mounted with glycerol aqueous medium. Apoptotic bodies were counted and recorded per crypt per 4 μm section.

5.1.7 Immunohistochemical detection of proteins

Two consecutive 4 μm paraffin sections of jejunum and colon were cut onto 3-aminopropyltriethoxy-silane-treated (Sigma Aldrich, Steinheim, Germany) glass slides, dewaxed in xylene and rehydrated through graded alcohols to water. Of the two sections on each slide, one was designated as the negative control and the other as the experimental section. Slides were washed with PBS before heat mediated antigen retrieval in 10 mM citrate buffer (pH 6.0). Endogenous peroxidase activity was quenched with 3% hydrogen peroxide in methanol for 1 min, while non-specific antigens were blocked with normal serum for 20 mins. Elimination of endogenous avidin and biotin was carried out using a commercial avidin/biotin blocking kit (Vector Laboratories, Burlingame, CA USA) as per manufacturer's instructions. Experimental sections were incubated overnight at 4°C with the primary antibody for Bcl-xL, Bax, Bak, Bid, p21 (Santa Cruz Biotechnology, Santa Cruz, CA, USA) and p53 and PCNA (Novocastra Laboratories, UK) diluted in a solution of PBS with 2% serum (as described in Table 5.1). Negative control sections had the

primary antibody omitted and were incubated with the dilution buffer only. After stringent washes in PBS between each step, sections were incubated with a biotinylated secondary antibody, followed by Ultra-Streptavidin conjugated to horseradish peroxidase and finally diaminobenzidine (DAB) chromogen in 0.03% hydrogen peroxide. Slides were counterstained in diluted Lillie-Mayer's Haematoxylin, dehydrated and mounted.

5.1.8 Statistical analysis

All statistical analysis was carried out using the one way ANOVA with Tukey's post hoc test to identify differences between groups. P-values <0.05 were considered statistically significant.

Table 5.1. Antibody information for immunohistochemistry carried out on rat sections

Antibody	Species	Clone and Source	Dilution	Positive Control
Bcl-xL	Polyclonal, rabbit anti human	H-62 sc-7195	1:800	Thymus
Bax	Polyclonal, rabbit anti mouse	P-19 sc-526	1:1000	Thymus
Bak	Polyclonal, goat anti human	G-23 sc-832	1:800	Stomach
Bid	Polyclonal, rabbit anti human	FL-195 sc-11243	1:2500	Spleen
p53	Monoclonal mouse	NCL-p53-240	1:50	Tumour
p21	Polyclonal, rabbit anti human	C-19 sc-397	1:1000	Liver
PCNA	Monoclonal mouse	NCL-L-PCNA PC10	1:500	Tonsil

5.2 Results

5.2.1 Effect of irinotecan treatment on tumour-bearing rats

Irinotecan caused mild diarrhoea in 5 out of 6 rats at 48 h. In the group which received pifithrin-α (PFT), mild diarrhoea was seen in 2 rats. Atropine completely prevented early onset diarrhoea. Rats in other groups showed no signs of diarrhoea at any time point. At 48 h, there was no significant difference in bodyweight for any group, however rats treated with PFT and irinotecan gained weight, whereas irinotecan-only rats continued to lose weight (Figure 5.1). Autopsy inspection found no significant difference in tumour weight between groups at 6 h or at 48 h. Irinotecan caused a significant reduction in small intestinal weight from 6 h to 48 h in rats treated with PFT and irinotecan, however large intestinal weight remained similar across groups at each time point.

5.2.2 Histopathological changes induced by irinotecan

5.2.2.1 Jejunum

Control rats showed no significant histological abnormality. Irinotecan treatment caused widespread apoptosis of enterocytes in basal regions of crypts at 6 h without other significant morphological changes. At 48 h, there was evidence of villous atrophy with clubbing of villi, loose eosinophil infiltration, lymphoplasmacytic infiltration of lamina propria and occasional individual apoptotic enterocytes. There was also regenerative hyperplasia present at this time point. The addition of PFT resulted in increased enterocyte hyperplasia and inflammatory infiltrate (Figure 5.2).

5.2.2.2 Colon

There were no significant histological changes observed in rats that were not treated with irinotecan. Sections that received irinotecan showed widely distributed apoptosis of individual or small groups of crypt enterocytes and scant inflammation at 6 h. At 48 h there was patchy to numerous dilated crypts, lined by attenuated epithelium. Occasional desquamated necrotic enterocytes were visible in lumen and there was scant inflammation. There were no distinguishable differences between rats treated with PFT or not (Figure 5.3).

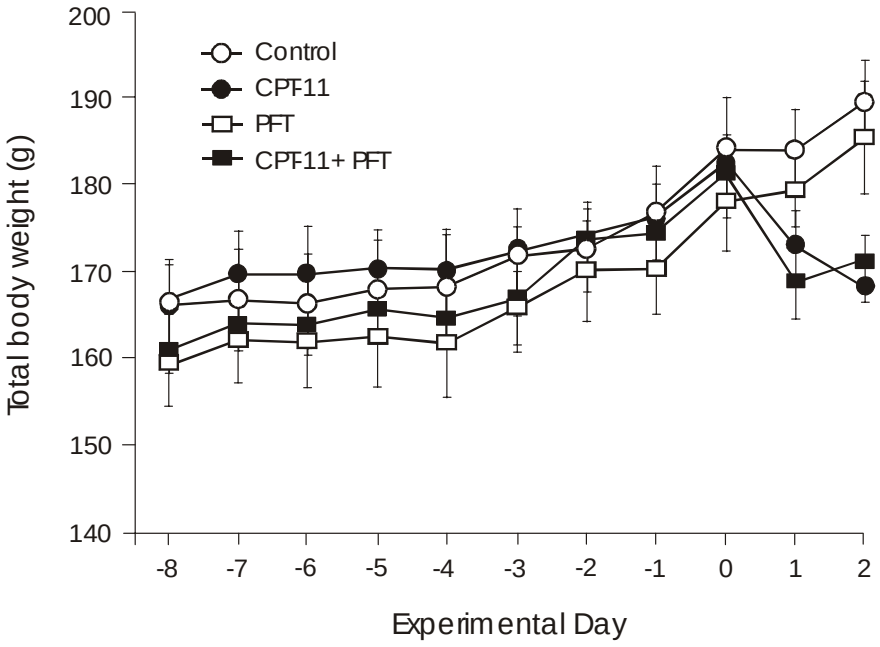

Figure 5.1. Daily body weight measurements. Results are of group means +/- SEM (n = 6)

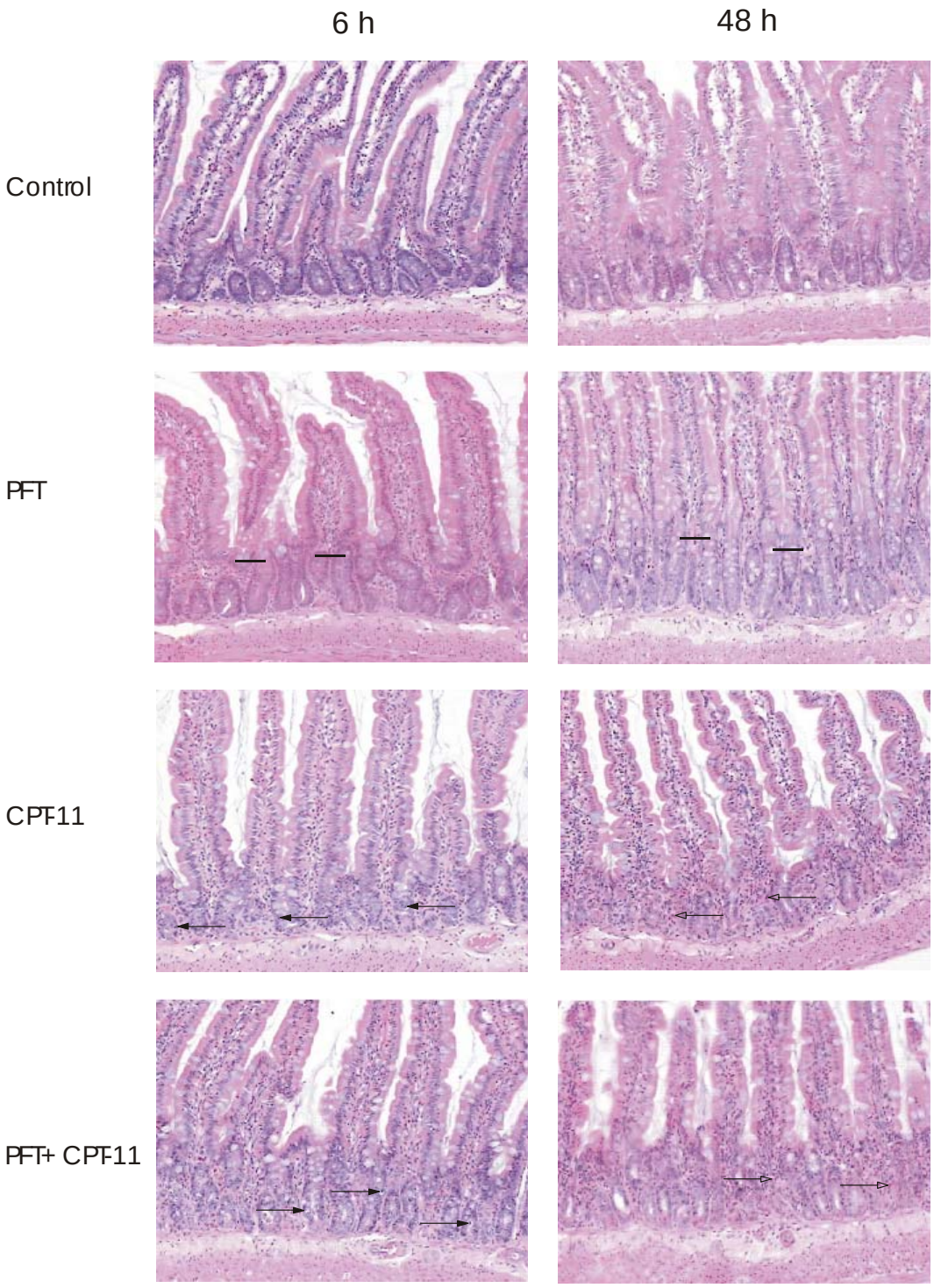

Figure 5.2. Photomicrographs of rat jejunum H&E stained. At 6 h following irinotecan (CPT-11) multiple apoptotic cells were present within crypts, as indicated by arrows with closed heads. By 48 h there was evidence of inflammation with loose eosinophil infiltrate, shown by arrows with open heads. PFT caused crypt hyperplasia, as indicated with bars. Original magnification x 200.

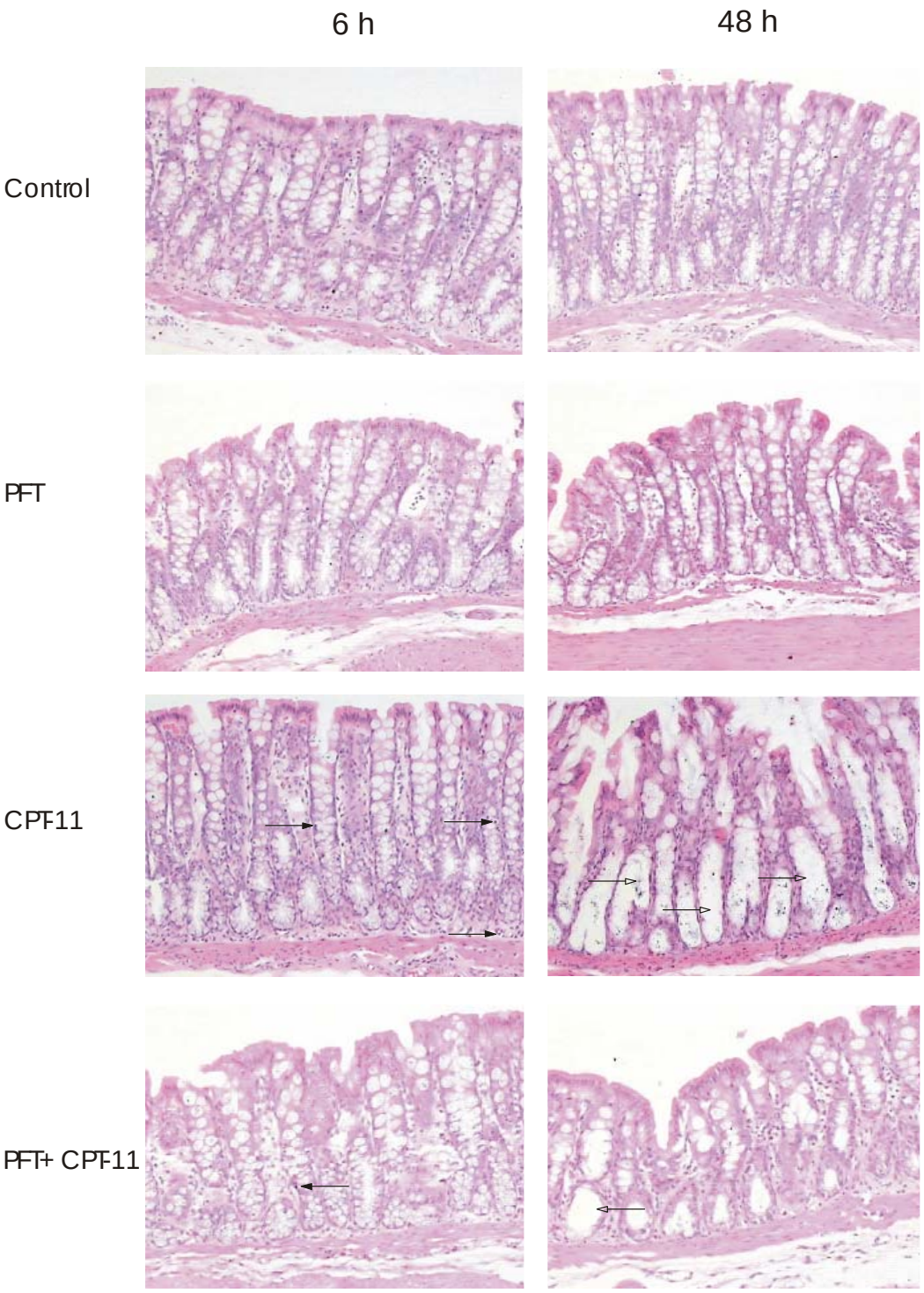

Figure 5.3. Photomicrographs of rat colon H&E stained. At 6 h following irinotecan (CPT-11) multiple apoptotic cells were present within crypts, as indicated by arrows with closed heads. By 48 h there were numerous dilated crypts with attenuated epithelium, shown by arrows with open heads. Original magnification x 200.

5.2.3 Morphological changes induced by irinotecan

5.2.3.1 Jejunal crypt length

Rats treated with irinotecan had a significant reduction in crypt length at 48 h ($P<0.001$) which was not ameliorated by PFT ($P<0.001$). All other groups had similar crypt lengths.

5.2.3.2 Jejunal villous area

Rats treated with irinotecan had a significant reduction in villous area at 48 h ($P<0.05$). PFT did not protect from irinotecan-induced reductions in villous area ($P<0.05$). All other groups were not statistically different (Figure 5.4).

5.2.3.3 Jejunal crypt proliferation

Irinotecan caused a significant reduction in proliferation within jejunal crypts at 6 h ($P<0.001$) and 48 h ($P<0.001$) compared to controls. There was a trend towards improvement in cell cycling by 48 h, however was not considered statistically significant. Combined treatment with PFT resulted in identical results to irinotecan only rats, with a peak decrease in proliferation at 6 h ($P<0.001$), which remained significantly reduced at 48 h ($P<0.001$). Control and PFT only rats had similar levels of proliferation (Figure 5.5a).

5.2.3.4 Colonic crypt length

There were no significant differences in crypt length between any group at either time point.

5.2.3.5 Colonic crypt proliferation

Irinotecan treatment resulted in a significant reduction in proliferation at 6 h only ($P<0.05$). With the addition of PFT, proliferation was maintained in colonic crypts following irinotecan. Rats in PFT only group had modestly increased proliferation at 48 h however was not statistically more than control rats (Figure 5.5b)

5.2.4 Apoptosis in intestinal crypts

5.2.4.1 Jejunum

A peak increase in apoptosis was seen at 6 h following irinotecan ($P<0.001$). Apoptosis was significantly reduced by 48 h ($P<0.001$) but remained modestly higher than control levels ($P<0.05$). Rats treated with irinotecan plus PFT also had a peak increase in apoptosis at 6 h ($P<0.001$), however by 48 h this had returned to control levels ($P<0.001$). Rats in the control and PFT groups had similar low levels of apoptosis (Figure 5.6a).

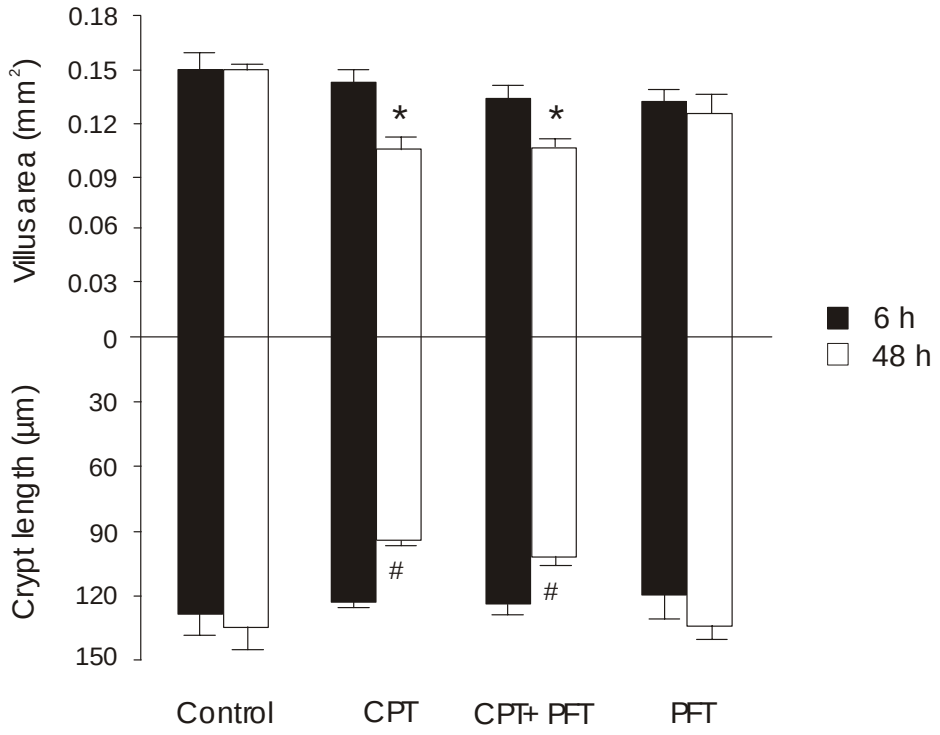

Figure 5.4. Changes in morphometry following irinotecan (CPT) treatment. Results presented are group mean +/- SE (n = 6). * indicates significant decrease in villous area from control value ($P<0.05$). # indicates significant decrease in crypt length from control value ($P<0.001$).

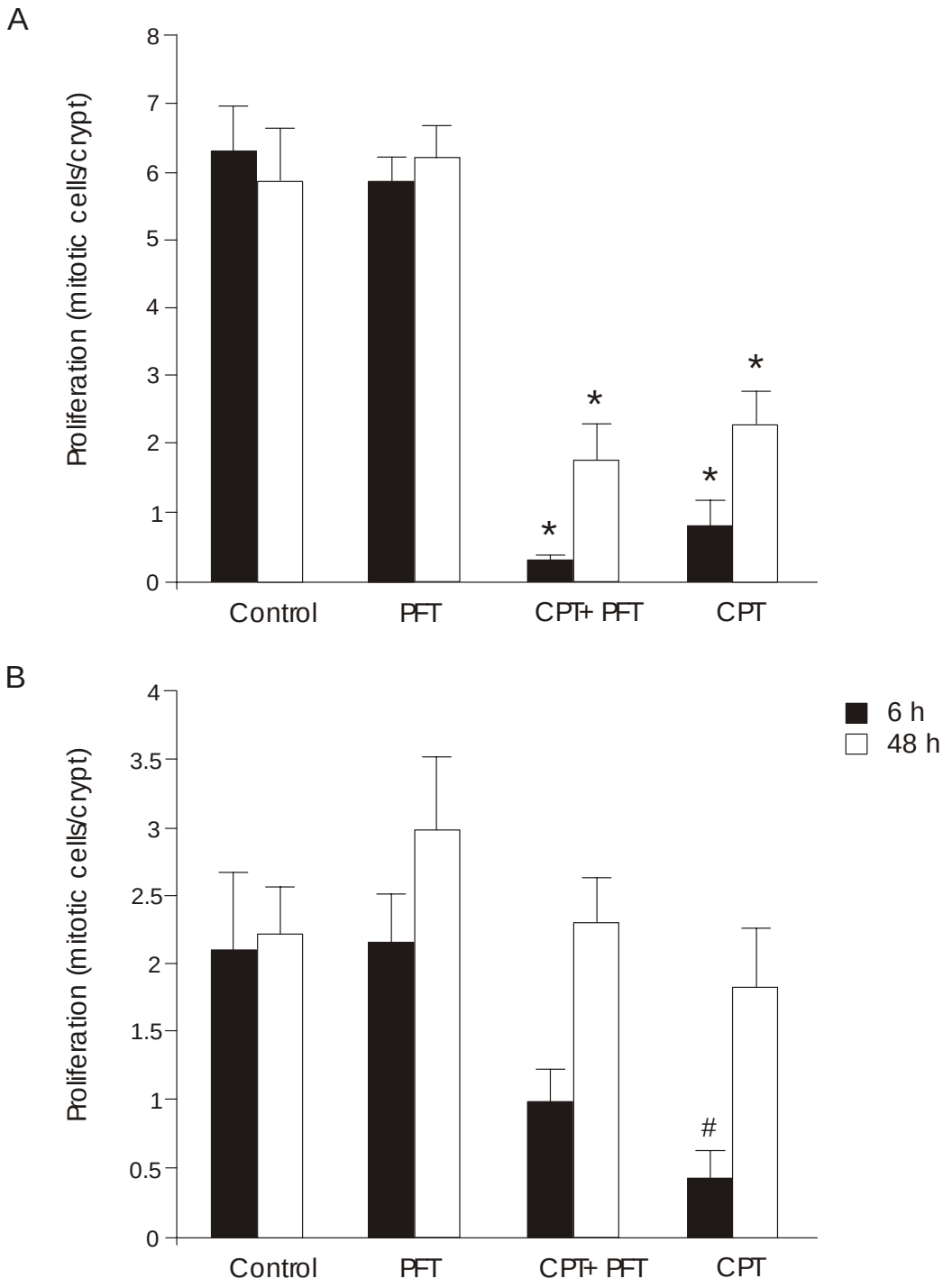

Figure 5.5. Changes in crypt proliferation following irinotecan (CPT) treatment. Results presented are group mean +/- SE (n = 6). A) jejunum; * indicates significant decrease in crypt mitoses from control value ($P<0.001$). B) colon; # indicates significant decrease in crypt mitoses from control value ($P<0.05$).

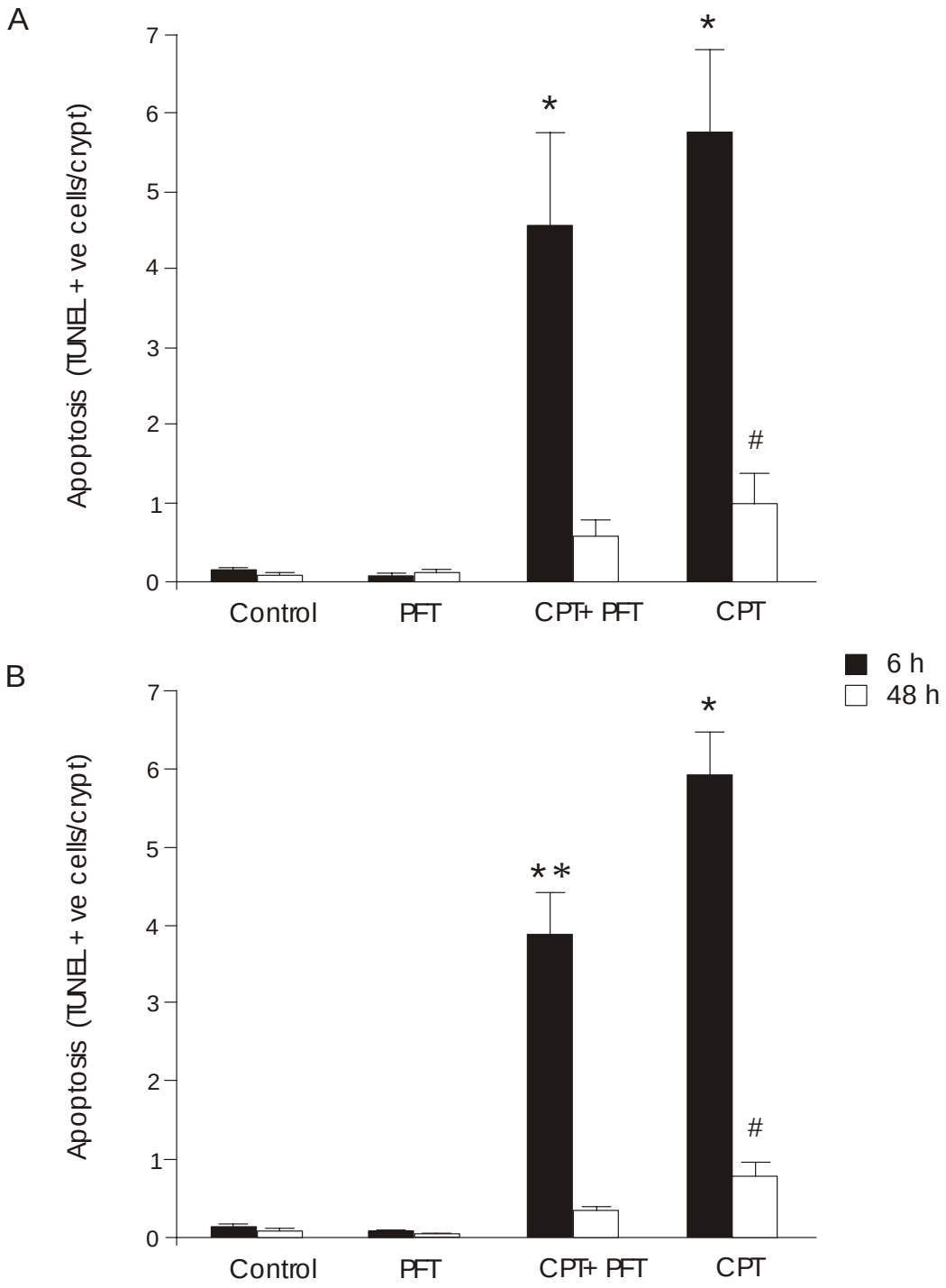

Figure 5.6. Changes in crypt apoptosis levels following irinotecan (CPT) treatment. Results presented are group mean +/- SE (n = 6). A) jejunum; * indicates significant increase in TUNEL staining from control value ($P<0.001$), # indicates significant increase from control ($P<0.05$). B) colon; * indicates significant increase in TUNEL staining from control value ($P<0.001$), * indicates significant decrease in TUNEL staining from CPT-only to CPT+PFT.

5.2.4.2 Colon

Irinotecan caused a significant increase in apoptosis within colonic crypts which peaked at 6 h ($P<0.001$) This reduced significantly by 48 h ($P<0.001$) but remained slightly higher than control levels ($P<0.05$). Treatment with irinotecan plus PFT also resulted in a peak increase in apoptosis at 6 h ($P<0.001$) which was followed by a reduction to control levels at 48 h ($P<0.001$), however, there was significantly more apoptosis in the crypts of rats treated with irinotecan alone ($P<0.01$) (Figure 5.6b).

5.2.5 Crypt protein expression following irinotecan treatment

5.2.5.1 p53

The tumour suppressor p53 protein could not be detected by immunohistochemistry in control or PFT only treated rats at either time point. At 6 h, irinotecan treatment caused a modest increase in p53 expression within the nuclei of jejunal crypt cells which was ameliorated by addition of PFT. At 48 h following irinotecan there was a sustained increase in p53 expression with no obvious differences in rat sections treated with PFT (Figure 5.7). The expression of p53 in colonic crypts was sporadic in control sections and increased modestly following irinotecan treatment. Treatment with irinotecan plus PFT at 6 h resulted in a slight decrease in overall p53 expression, while treatment with irinotecan only resulted in a concentration of cells expressing p53 in the mid crypt region. At 48 h following irinotecan, p53 expression was more evenly distributed through the lower half of crypts with or without PFT. Rats treated with PFT alone had similar expression levels of p53 within colonic crypts as other control rats at each time point.

5.2.5.2 p21

The expression of $p21^{waf/cip-1}$ was not readily detectable in the crypts of the small and large intestine. Sections of jejunum from rats in the control and PFT-only groups had very sporadic p21 staining, with less than one cell per 5 crypts being positive. At 6 h following irinotecan treatment, p21 staining was increased slightly in sections not also treated with PFT. The expression of p21 in sections at 48 h was similar in rats treated with irinotecan with or without PFT. The degree of staining for p21 in the colonic crypts was also identical for each of the groups, in that it remained at an extremely low level.

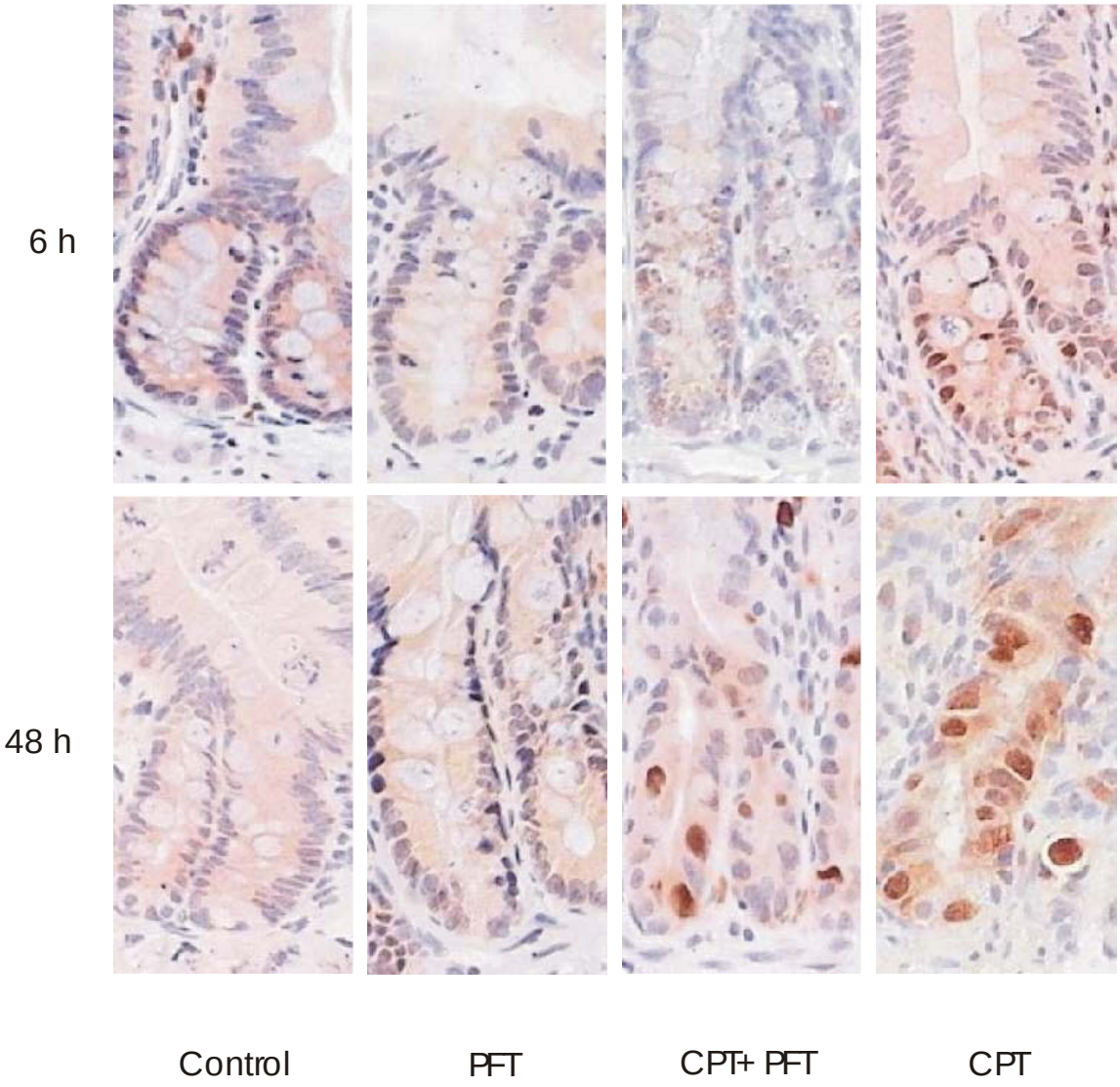

Figure 5.7. Photomicrographs of rat jejunum treated with irinotecan (CPT) and pifithrin-alpha (PFT). Staining for p53 was increased modestly at 6 h and markedly at 48 h. Original magnification x400.

5.2.5.3 PCNA

Investigation of proliferating cell nuclear antigen (PCNA) expression in the rat small intestine found that staining was present in all crypt cells located above position 1. Staining intensity and pattern was similar in control rats and those treated with PFT alone at both 6 and 48 h. Irinotecan treatment caused PCNA expression to contract to the stem cell region in the jejunum at 6 h. Addition of PFT partially maintained PCNA expression, with positive staining of cells present along most of the crypt length. At 48 h following irinotecan, PCNA positively stained cells were present along the entire remaining crypt length, however the intensity of expression was markedly reduced compared to control sections. Within the colon, PCNA was expressed in each cell in the lower 2/3rds of every crypt within control and PFT only sections. At 6 h following irinotecan, staining was reduced and was present in cells in the lower half of the crypt only, which was not prevented by PFT. Apoptotic cells expressed PCNA strongly. The expression of PCNA had increased, although not to control levels, by 48 h following treatment and was substantially stronger in the sections which received irinotecan plus PFT compared to irinotecan alone (Figure 5.8).

5.2.5.4 Bax

Sections from control rats and those treated with PFT alone had weak to moderate Bax staining in the cytoplasm of crypt cells and very weak staining of villous enterocytes. Cells undergoing late stage apoptosis exhibited strong Bax staining. PFT slightly reduced Bax expression within apoptotic enterocytes in jejunal crypts but did not reduce overall expression levels following irinotecan (Figure 5.9). At 48 h following irinotecan, Bax expression was significantly reduced in both treatment groups. Bax staining in the colon was strong in the luminal half of the crypt and weaker in the basal half of the crypt. Treatment with irinotecan did not cause a significant increase in staining.

5.2.5.5 Bak

Within the jejunum, control and PFT only rats had strong cytoplasmic staining of both crypt and villous enterocytes. Furthermore, there was no measurable change in staining intensity for any treatment at either time point. Conversely, Bak expression was significantly increased at 6 h in the crypts of the colon in both irinotecan treated groups. Staining intensity had returned to control levels by 48 h for irinotecan only and irinotecan plus PFT groups. Treatment with PFT only caused no observable change in Bak expression (Figure 5.10).

5.2.5.6 Bid

The full length Bid protein was detected in the nuclei and cytoplasm of control rat enterocytes. Almost all cells within jejunal crypts were moderately stained which was then reduced following irinotecan treatment. This was especially evident at 48 h, where remaining staining localised to nucleoli. Expression of Bid was weaker in the colon compared to the jejunum. A gradient of expression from weak to moderate from the base of the crypt to the apical region was noticeable in control sections. This gradient was not evident in treated sections. There was no measurable difference in colonic crypt staining between groups.

5.2.5.7 Bcl-xL

Jejunal crypt cells had weak cytoplasmic staining which was decreased to extremely weak levels at 6 h by irinotecan treatment. Bcl-xL expression was not maintained by addition of PFT. Control and PFT only treated rats had similar expression profiles at both time points. Within the colon, staining was weak along the length of the crypt until the table region were staining was absent. For this tissue region, no difference in expression was noted at either time point for any group.

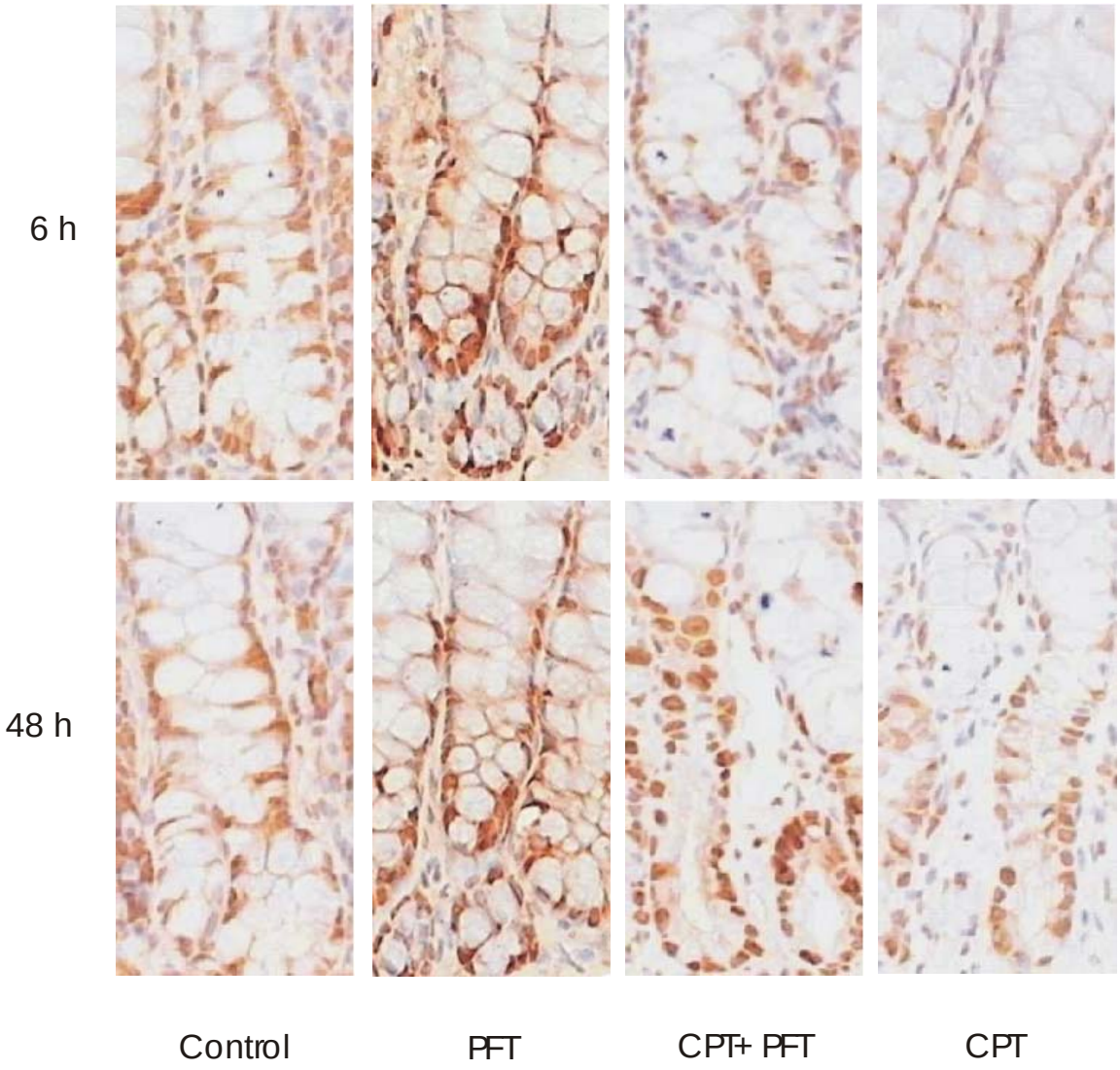

Figure 5.8. Photomicrographs of rat colon treated with irinotecan (CPT) and pifithrin-alpha (PFT). Staining for PCNA was decreased markedly at 6 h and returned to untreated levels by 48 h in rats treated with PFT. Original magnification x400.

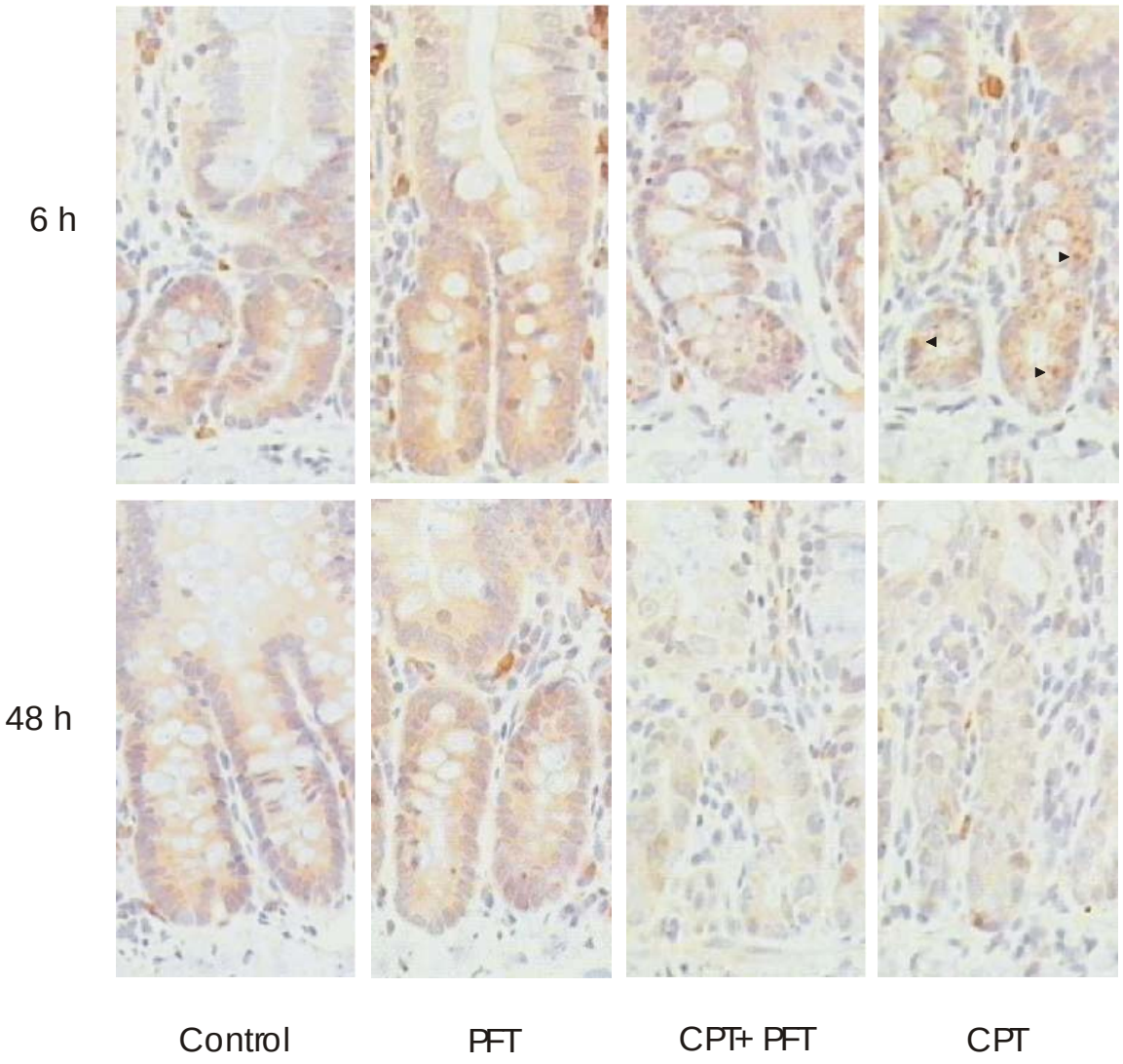

Figure 5.9. Photomicrographs of rat jejunum treated with irinotecan (CPT) and pifithrin-alpha (PFT). Staining for Bax was strong in apoptotic cells as indicated with arrow heads. Bax staining was decreased at 48 h in rats treated with irinotecan. Original magnification x400.

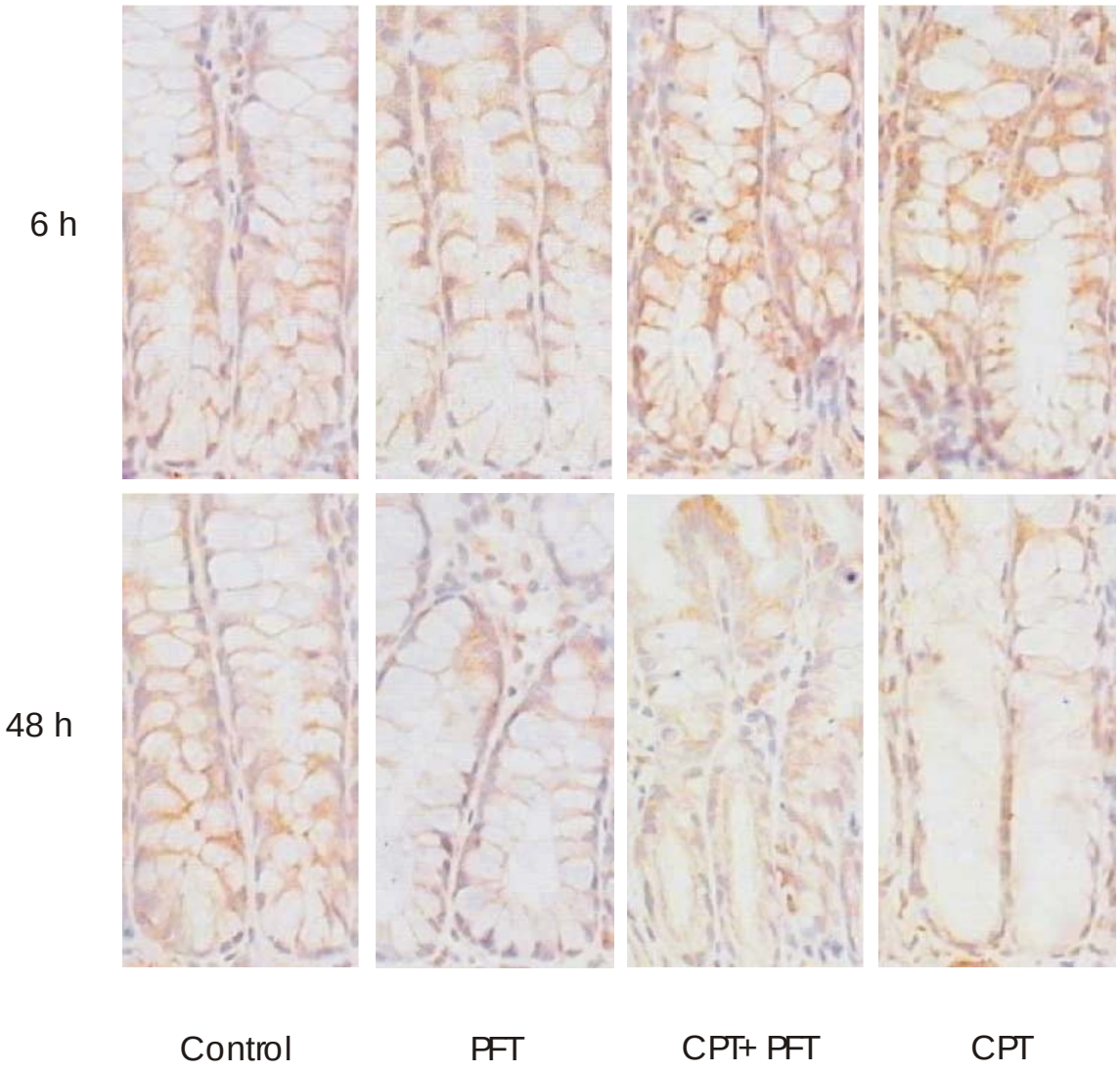

Figure 5.10. Photomicrographs of rat colon treated with irinotecan (CPT) and pifithrin-alpha (PFT). Staining for Bak was increased at 6 h following treatment and returned to untreated levels by 48 h. Original magnification x400.

5.3 Discussion

This study examined the effect of a single dose of irinotecan on the intestine of the rat with breast cancer by concentrating on mechanisms of p53-induced crypt damage. The approach was unique in that it investigated a combination of apoptotic, histological and morphological changes along with alterations in protein expression. Irinotecan caused deleterious effects in both the small and large bowel which was partially ameliorated by temporary blockade of p53.

The DA rat breast carcinoma model was established to investigate gastrointestinal mucositis (Gibson et al., 2005a; Gibson et al., 2003; Gibson et al., 2005b; Gibson et al., 2002a; Gibson et al., 2002b). This study differed however from the traditional mucositis-inducing dosing protocol of two i.p injections to that of a single dose of 200 mg/kg irinotecan. The dual dose administration of chemotherapy has previously been necessary a single dose of methotrexate caused an unreliable level of gastrointestinal mucositis (GIM), that was difficult to reproduce between experiments (Taminiau et al., 1980). However administering multiple doses of chemotherapy on already damaged cells and tissues made it difficult to assess changes in gene and protein expression, which are hypothesised to be critical in the development of GIM (Keefe, 2004; Sonis, 2004a; Sonis et al., 2002). In this trial, irinotecan treatment resulted in damage to both the small and large bowel which was characterised by increased apoptosis within crypts and reductions in crypt cell cycling at 6 h. At 48 h, morphological alterations, especially villous clubbing and attenuation of crypt lining with or without regeneration, and minimal inflammation were observed. Overall weight loss and early onset diarrhoea was minimal within 48 h post irinotecan treatment. These results correspond well with findings from previous multiple dose studies (Gibson et al., 2003; Gibson et al., 2005b) and confirm 200 mg/kg irinotecan given i.p. once is sufficient to cause GI changes that indicate early mucositis.

A plethora of genes have been implicated in control of the apoptotic pathway (Markova, 1998; Norbury and Zhivotovsky, 2004; Oren, 1992; Saini and Walker, 1998). Of particular interest is the p53 transcription factor, which is known as a tumour suppressor (Gottlieb and Oren, 1998; Smith et al., 2003). Changes in the p53 gene are the most frequent mutation seen in human cancers (Lowe et al., 1993; Weller, 1998) and due to this fact it has been studied extensively over recent years. Understanding of its role in the activation of irinotecan induced apoptosis continues to evolve. A primary aim of this study was to examine the effect of temporary inhibition of the transcriptional ability of p53 on

the cytotoxicity of irinotecan. Pifithrin alpha (PFT), was used to prevent movement of p53 into the nucleus of cells following insult which resulted in a marginal improvement in the response to irinotecan. Firstly, rats given PFT lost weight for less time that those treated with irinotecan alone, and the incidence of diarrhoea was reduced. It did not maintain morphology in the small or large intestine but limited the duration of apoptosis in the jejunum and colon and also reduced the amount of apoptosis in colonic crypts. These results indicate that activation of the transcriptional function of p53 is not required for cell death in the intestine, but instead acts synergistically with other irinotecan induced genes. A possible explanation is that there is a direct interaction of cytoplasmic p53 with other inducers of cell death. Such a role for p53-induced activation of the caspase cascade without transcription has been reviewed previously (Moll and Zaika, 2001).

To further characterise the role of p53 in irinotecan-induced damage in the intestine, a number of genes implicated as downstream effecters of p53-dependent apoptosis were examined (Kannan et al., 2001). This study found differential regulation of the pro-apoptotic Bcl-2 family proteins, Bax and Bak, in the jejunum and colon. The crypts of the jejunum upregulated Bax at 6 h following irinotecan with strong expression in apoptotic cells. While conversely, Bak was upregulated in colonic crypts treated with irinotecan at 6 h. This is the first investigation to report a diversity in response of apoptotic proteins between the two intestinal regions following chemotherapy. It appears that Bax is the primary apoptosis regulator in the small intestine and Bak for the large intestine in response to irinotecan. It is worth noting also that the induction of Bax is not always strictly dependent on p53 (Bouvard et al., 2000) in so much that it does not require p53 transcriptional upregulation, which is blocked by PFT.

Immunohistochemistry confirmed the accumulation and change in subcellular location of the p53 protein following irinotecan. However, this remained somewhat mild until 48 h, indicating that p53 was not responsible for the peak increase in apoptosis seen at 6 h. The p53-independent pathways to apoptosis that were activated could include reactive oxygen species (ROS), ceramide and MAP kinase, all of which have been discussed extensively. (Kantrow et al., 2000; Lamkanfi et al., 2004; Okuno et al., 1998; Reed and Zhang, 1997). This finding compliments the new biological explanation of alimentary mucositis proposed in recent reviews (Keefe, 2004; Sonis, 2004b). The concept of simultaneous damage occurring in multiple tissue layers, with activation of numerous cellular pathways has implicated each of the aforementioned as well as others. It therefore seems likely that

irinotecan induces apoptosis and intestinal damage not only by a p53-driven epithelial consequence but instead through a complex series of events involving several of the cell types in the GIT.

This has been the first study to measure apoptosis and protein expression in intestinal crypts following a single dose of irinotecan. It has shown that irinotecan-induced changes in the epithelium are partially ameliorated through manipulation of p53 activation, however it does not result in maintenance of morphology. Blockade of p53 modestly improves diarrhoea and weight loss in tumour bearing rats but overall was not considered an effective anti-mucositis approach. Instead, this study provided further evidence for the common pathway of cancer-induced tissue damage, which implicates epithelial and subepithelial processes and is a consequence of activation of multiple cellular pathways.

Effect of irinotecan treatment on gene expression profiles in the small intestine of the rat with breast cancer.

6.0 Introduction

Irinotecan hydrochloride (CPT-11) is a relatively new chemotherapy drug used primarily to treat advanced colon cancer. It belongs to the topoisomerase I interactive class of anti-cancer drugs, targeting the DNA-topoisomerase I complex and arresting replication leading to cell death (Yu et al., 2005). Irinotecan is highly toxic to both the small and large intestine, causing extensive crypt damage with accompanying changes in mucin distribution (Gibson et al., 2003; Ikuno et al., 1995). The use of irinotecan in the clinic often results in adverse side effects of the drug with dose limiting toxicities including severe diarrhoea and leucopoenia (Alimonti et al., 2004).

There are two types of diarrhoea caused by irinotecan. Firstly, an early onset secretory diarrhoea which is cholinergic in nature which can be ameliorated by the co-administration of atropine during treatment, and secondly, a delayed onset diarrhoea which is prolonged and can be life-threatening. The exact nature of this diarrhoea has yet to be fully elucidated although possible explanations include alterations in normal intestinal microflora and subsequent β-Glucoronidase activity; changes in mucin composition and also enterocolitis with accompanying altered water and electrolyte secretion (Cao et al., 1998; Gibson et al., 2003; Takasuna et al., 1996).

Although the exact cause of downstream side effects of irinotecan, such as diarrhoea, is still unknown, strong evidence exists for the role of apoptosis as an early damage indicator in the small intestine. Previous studies have documented an increase in apoptosis within crypts which peaks by 24 h following administration of the drug. This is followed by a period of crypt hypoplasia which precedes loss of epithelial morphology (Boushey et al., 2001; Gibson et al., 2003; Gibson et al., 2005).

Caspases play the central role in the regulation and execution of apoptotic cell death and so are likely to be important for irinotecan-induced intestinal damage. Further to this, specific caspases are activated in response to varying death inducing signals. The initiator caspases -8 and -10 are recruited following ligation of cell membrane death receptors, while caspase -9 responds to cytochrome c release from the mitochondria, and caspase -12 is activated in response to endoplasmic reticulum stress (Lavrik et al., 2005; Philchenkov, 2004). Also worth noting is that caspase -1 and -5 are activated when complexed with the recruiter

protein NALP1 or adaptor protein Ipaf as part of the inflammasome (Martinon and Tschopp, 2004). By understanding the caspase cascade and observing the members recruited during apoptosis one gets an indication of which pathways are being activated by a given stimulus, such as irinotecan.

Apoptosis of epithelial cells however is not the only toxic effect leading to mucosal injury. The pathobiology of mucositis is now considered substantially more complex, with the involvement and interaction of all the cell and tissue types, tissue factors, cytokines and elements of the intestinal environment. Supporting this is results from a recent study where the transcription factor NFκB, and angiogenesis associated enzyme Cox-2, were both found to be upregulated in patients' colorectal endothelium and lamina propria following radiation treatment (Yeoh et al., 2005). While the elucidation of mechanisms behind oral mucositis pathobiology is making progress, many more studies are required to investigate this theory fully and to describe the diverse changes that occur in the intestine following chemotherapy treatment.

Genome-wide analysis through microarray technology can provide a powerful tool to investigate changes occurring in multiple tissue layers simultaneously and go some way to fill gaps in our knowledge. Thus the primary aim of this study was to identify the genes that are up and downregulated by irinotecan treatment in the rat small intestine. Secondary aims were 1) to determine how these gene changes contribute to apoptosis and 2) to identify any potential candidates as important for mucositis development. An understanding of the genetic pathways utilised by irinotecan to induce intestinal damage would allow for improved intervention therapies to be designed.

6.1 Methods and Materials

6.1.1 Laboratory animals

This study was approved by the Animal Ethics Committees of the Institute of Medical and Veterinary Sciences, Adelaide and of the University of Adelaide and complied with National Health and Research Council (Australia) Code of Practice for Animal Care in Research and Training (1997). Female Dark Agouti (DA) rats, aged 6-8 weeks and weighing approximately 160 g were purchased from the Institute of Medical and Veterinary Sciences MedVet division, group housed and kept under a 12 h light/dark cycle with free access to food and water until the study commenced (approximately 2 weeks).

6.1.2 Preparation of tumour inoculum

All animals used in this study carried a subcutaneous tumour. The mammary adenocarcinoma for this study arose as a spontaneous tumour in the 1970's. It has been propagated since by passage through female DA rats. The tumour was donated by Dr. A. Rofe (Institute of Medical and Veterinary Sciences, Adelaide, South Australia) in 1996 to develop a model to assess small intestinal and tumour effects of chemoprevention (Keefe, 1998). This tumour has since been used extensively in our laboratory. One female donor rat was injected s.c. on both flanks with 0.2 ml (2.0×10^7 cells/ml) tumour inoculum 11 days prior to the study beginning. Over the subsequent days these cells formed a tumour under the skin on both flanks. To harvest the tumour cells the rat was culled by CO_2 asphyxiation and cervical dislocation. Subcutaneous tumours were dissected and placed into ice cold sterile PBS. The tumours were diced, homogenised and filtered through sterile gauze. The resultant cell suspension was spun at 250 g for 3 minutes. The supernate was removed and the cell pellet resuspended in fresh sterile PBS. This was repeated a further 3 times. A viable cell count was carried out using 0.4% w/v trypan blue.

6.1.3 Experimental design

Eight female DA rats (weighing approximately 180 g) were implanted with 0.2 ml tumour inoculum s.c. into each flank and then divided into 2 even groups. Tumours were allowed to grow for 9 days after which time group 1 rats were given irinotecan (150 mg/kg i.p.) on two consecutive days to induce mucositis. Irinotecan was administered in a sorbitol/lactic acid buffer (45 mg/ml sorbitol/0.9 mg/ml lactic acid) that is required for activation of the drug. Group 2 rats received buffer only and were designated controls. All rats also received 0.01 mg/kg s.c. atropine immediately prior to irinotecan to reduce any cholinergic

reaction to the treatment. Animals were culled by CO_2 asphyxiation and cervical dislocation 6 h after the second injection. The gastrointestinal tract from the pyloric sphincter to the rectum was removed and flushed with sterile 0.9% w/v saline. Two cm samples of small intestine (jejunum) at 25% of the length of the small intestine from the pylorus were collected, snap frozen in liquid nitrogen and stored at –70 degrees.

6.1.4 RNA extraction

Total RNA was isolated from 30 mg of homogenised whole jejunal tissue using TRIzol® Reagent (Invitrogen Life Technologies, Mulgrave, VIC). Avoiding contamination with RNases, frozen samples were disrupted by mortar and pestle, placed into 1.5 ml centrifuge tubes containing 500 µl TRIzol® and vortexed thoroughly. Samples were allowed to sit at room temperature for 5 mins before adding 100 µl chloroform. Tubes were hand shaken for 15 sec and left at RT for 3 mins. Samples were then centrifuged at 12,000g for 15 mins at 4°C to separate aqueous and solvent phases. The upper, aqueous phase was collected and placed into a new tube. An equal amount of 70% ethanol was added to change binding conditions of the RNA so as to be purified through a silica gel membrane (Machery Nagel, Berlin, Germany) which results in enriched mRNA. Following multiple washes with ethanol, highly pure RNA was eluted in 60 µl RNase-free sterile water. Finally, RNA was treated with DNAse 1 (Ambion, Austin, TX, USA) to remove genomic DNA. In a new sterile tube, 3 µl of (10x) DNAse 1 buffer (0.1 volume) and 1 µl of DNAse 1 (2 units) was added to 30 µl of RNA. This was mixed gently and incubated for 20 mins at 37°C. The reaction was halted by addition of 5 µl of the DNAse inactivation reagent slurry. After 2 mins incubation at RT, the tubes were centrifuged at 10,000g for 1 min to pellet the slurry. RNA supernate was removed to a new tube and re-frozen until use.

6.1.5 RNA precipitation

To the RNA sample, a 0.1 volume of sodium acetate was added, followed by a 10x volume of cold isopropanol. The sample was then vortexed and frozen at -70°C for 30 mins. RNA was pelleted by centrifugation at 4°C for 30 mins, and the supernate was removed. RNA was then washed through a series of ethanol elutions with subsequent centrifugation. The RNA was allowed to dry at RT before being eluted with 20 µl sterile DEPC H_2O.

6.1.6 Nucleic acid quantification

RNA concentration was quantified by diluting 1:20 with diethyl pyrocarbonate (DEPC) (Sigma)-treated H_2O and measuring the absorption at 260 nm and 280 nm on a spectrophotometer. Concentration of RNA was determined by the formula:

$$A_{260} \times 40 \times 20 = \text{RNA ng}/\mu\text{l}$$

(assuming that an optical density reading of 1.0 represents 40 μg/ml of RNA). Quality of RNA was checked by A_{260}/A_{280} ratio of samples and by visualising 28S and 18S bands on formamide gel.

6.1.7 cDNA synthesis

To 20 μg of RNA the following was added; 3 μg of polyA and 3 μg of hexamers. This was incubated for 10 mins at 70°C to denature RNA. The denaturation was halted by placing samples on ice for 1 min. Reverse transcription was carried out by adding 6 μl of M-MLV buffer, 0.6 μl dNTP's (500 μM), 2 μl M-MLV reverse transcriptase (200 U/μl, Invitrogen) and incubating samples for 150 mins at 42°C. Any remaining RNA was degraded by adding 10 μl sodium hydroxide (0.25M) and 10 μl EDTA (0.5M) and incubating sample for 15 mins at 65°C. Reaction was then neutralised by adding 15 μl acetic acid (0.2M).

6.1.8 cDNA purification and dye coupling

The QIAquick PCR purification kit (QIAGEN) was used to purify cDNA. After adding PE buffer to samples, cDNA was placed into column tubes. After a series of centrifugation and wash steps, cDNA was eluted in 90 μl of sterile Milli Q water into a new tube. cDNA was spun twice for 1 min at 6500g at RT before being spun and dried under reduced pressure in a speedvac for 45 mins at 50°C. The resultant cDNA pellet was then dissolved in 9 μl of freshly made sodium hydroxide bicarbonate (0.1M , pH 9.0). cDNA was then added to Cy dye tubes (Amersham, shown in table 6.1) and incubated in the dark for 60 mins at RT. Samples were then re-purified through QIAGEN columns, however this time cDNA from 1 control and its equivalent experimental rat (which were coupled with different dyes) were each placed on one column together. The now mixed samples were then eluted with 90 μl of sterile Milli Q water. The cDNA was then pelleted and dried in a speedvac for 30 mins at 50°C. A blocking step was then carried out by adding 0.64 μl of yeast tRNA, 4 μl PolyA (2 mg/ml, Sigma) and 20 μl of Cot-1 DNA (1 mg/ml, Invitrogen) to the cDNA. It was then re-dried in a speedvac for 20 mins and the resultant pellet was

dissolved in 16 µl of fomamide and 16 µl of 6.25 x SSC (1M sodium citrate, 1M sodium chloride). The samples were then heated for 4 mins at 100°C before being placed on ice for 1 min to halt reaction. Finally, samples were spun quickly and 0.2 µl of 10% SDS was added.

Table 6.1. Slide dye combinations

Sample	Dye	Sample	Dye
Cont 1	Cy3	Exp 1	Cy5
Cont 2	Cy3	Exp 2	Cy5
Cont 3	Cy5	Exp 3	Cy3
Cont 4	Cy5	Exp 4	Cy3

6.1.9 Hybridisation and slide analysis

Rat 5K MWG oligo array glass slides were purchased from the Clive and Vera Rammaciotti Centre for gene function analysis, University of NSW. To prepare slides they were baked for 30 mins at 60°C before being washed in 0.1% SDS for 1 min at 95°C. They were then rinsed in 5% Ethanol for 1 min, which was followed by 0.2 x SSC for 1 min. Slides were then dried by centrifuging at 750 rpm for 5 mins. Hybridisation chambers were cleaned by wiping with lint-free clean wipe tissues. Chamber reservoirs were then filled with 1 x SSC to keep slides humid. A 30 µl drop of cDNA was placed onto the centre of a 22 x 40 mm glass cover slip. The microarray slide was then placed onto the drop of cDNA and pressed gently to spread the sample over the entire array area. Slides were then placed into chambers and incubated overnight at 42°C. Following this, slides were removed from chambers and immersed in 0.5 x SSC, 0.01% SDS to remove cover slip. Slides were subsequently washed in 0.5 x SSC, followed by 0.2 x SSC for 5 mins each and then dried by centrifuging at 750 rpm for 5 mins. The microarray slides were scanned using a GenePix 4000B Scanner driven by GenePix Pro 4.0 (Axon Instruments, Foster City, CA, USA). All analyses were performed using the freely-available statistical programming and graphics environment R (http://cran.r-project.org) (Yang et al., 2001). The "SPOT" software package (http://experimental.act.cmis.csiro.au/Spot/index.php) was used to identify spots by

adaptive segmentation method and subtract backgrounds utilising morphological opening approach. The extracted information was analysed using limma package (http://bioinf.wehi.edu.au/limma). All data was normalised to remove from the expression measures any systematic trends which arise from the microarray technology rather than from differences between the probes or between the target RNA samples hybridised to the arrays. This was done by Loess print tip method which corrects for dye-bias and intensity within each group of adjacent spots printed by one pin (print tip). Differentially expressed genes were ranked on Bayesian posterior log odds calculated with limma (Lonnstedt and Britton, 2005). The empirical Bayes method was used to shrink the gene-wise sample variances towards common values and, in so doing, augmenting the degrees of freedom for the individual variances. This approach combines expression ratios and their variability between replicates to rank the genes (Lönnstedt and Speed, 2002).

6.1.10 Real time PCR

Quantification of changes in expression of genes of interest was carried out by real time PCR and performed by a DNA Engine OPTICON 2 Continuous Fluorescence Detector (MJ Research). PCR primers for rat 18S ribosomal RNA (Genbank # X01117) were designed according to published information (Altmann et al., 2004), while primers for rat caspase-1 (Genbank # U14647) were designed by Primer Premier version 5 (PREMIER Biosoft International, Polo Alto, CA).

18S forward 5' – GGGAGGTAGTGACGAAAAATAACAA

18S reverse 5' – TTGCCCTCCAATGGATCCT

Caspase-1 forward 5' – CACTAAAAAAGGACCCC

Caspase-1 reverse 5' – ATGGACCTGACTGAAGC

Primers pairs were specific for a 101 and 98 base pair product respectively. 18S and caspase-1 oligonucleotide standards were synthesised by Geneworks (Adelaide, SA) and corresponded to their respective primer pair product. In each experiment, duplicates of 18S and caspase-1 oligonucleotide standards were added in a dilution series along with unknown samples. These were amplified in a 20 µl reaction containing 2x DyNAmo™ SYBR® Green qPCR master mix (Finnzymes, Keilaranda, Espoo, Finland) and 1 µl of cDNA template. The real time thermal PCR profile consisted of 1 cycle of 95°C for 7 mins, 40 cycles of 95°C for 15 secs and 60°C for 1 min and one cycle of 72°C for 10 mins. Fluorescence measurements were recorded at 60°C each cycle. The cycle threshold value

(CT) was used to assess the quantity of 18S and caspase-1 gene expression. The CT was fixed manually in each experiment at the exponential phase of the PCR. The relative copy number of each transcript was determined by interpolating the CT values of the unknown sample to each standard curve and the obtained values were normalised to the 18S copy number. The lack of primer dimer, non-specific product accumulation or DNA contamination was assessed by melt curve analysis. Dissociation curves showed a single peak corresponding to a melting temperature of 76.2 ± 0.2 for 18S and 77.8 ± 0.3 for caspase-1. Samples of rat jejunum taken at 0, 6, 24 and 48 h post irinotecan were included for analysis. This tissue was collected as part of a previous study and is described in chapter 2.

6.1.11 Statistics

Comparison of group means was carried out by Kruskal-Wallis Test (nonparametric ANOVA), where a P value of <0.05 was considered significant.

6.2 Results

6.2.1 Microarray

The investigation into gene expression profiles in control and irinotecan-treated rats by microarray analysis revealed differences between the two groups. An example of an array following hybridisation with dye-coupled cDNA is shown in Figure 6.1. Preliminary statistical analysis of array data by Ashley Connelly (Adelaide Microarray Consortium, The University of Adelaide) gave 232 altered genes following irinotecan which were ranked according to Bayesian plots (Table 6.2). The raw data was then further scrutinised by Anna Tyskin to create a shorter list of genes according to reproducibility and log ratio data. For this study a differential expression ratio of 1.8 or greater between control and treated rats was required for genes to be included in further investigations. This resulted in 16 genes found to be upregulated and 37 downregulated, as shown in Table 6.3 and 6.4 respectively. Genes with similar cellular roles were grouped into according categories using the ontology resource EGAD (The Expressed Gene Anatomy Database, www.tigr.org/tdb/egad) and are shown in Table 6.5. The most highly represented genes were involved in chromosome structure, cell cycle regulation, protein turnover, apoptosis and immunological responses. A literature search was then carried out through web-based resource, PubMed (Entrez, National Centre for Biotechnology Research) to identify from this study, upregulated genes implicated in development of intestinal mucositis. This search identified caspases and dihydropyrimidine dehydrogenase as genes closely associated with intestinal damage in response to chemotherapy treatment. The well defined role of caspases in the apoptotic pathway led to the choice of caspase-1 for further investigations by real time PCR.

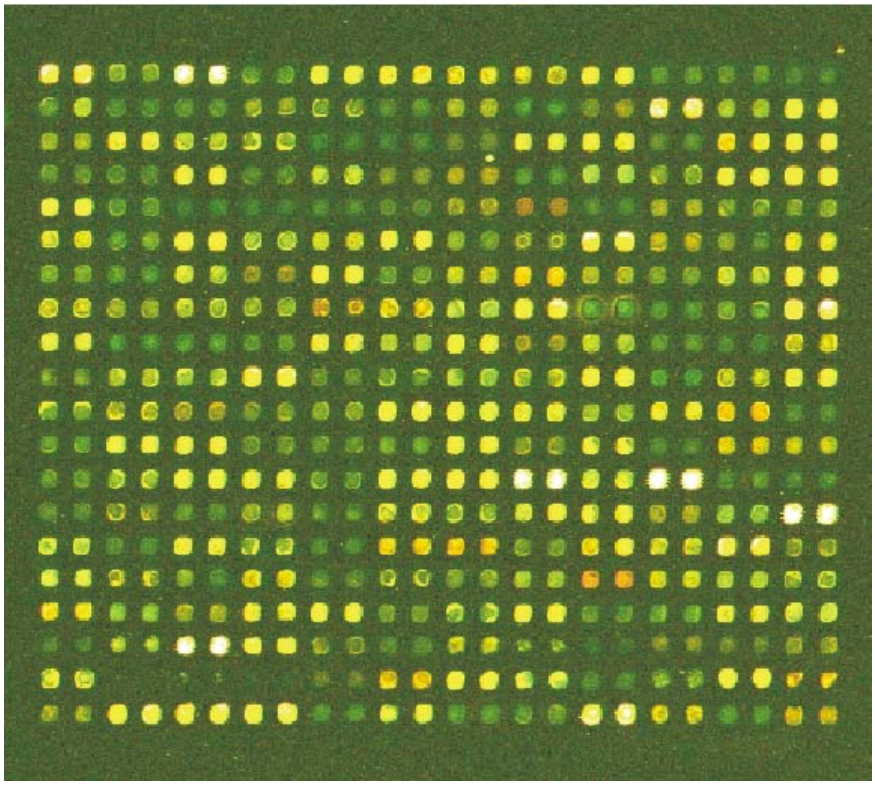

Figure 6.1. Presentation image of microarray, slide 2. Control rat cDNA was coupled with Cy3 and experimental rat cDNA with Cy5. Green spot on array represents downregulated gene, red represents upregulated gene, yellow represents no change and white represents out of range/saturation of spot.

Table 6.2. Initial ranked list of genes with changed expression following irinotecan treatment in the DA rat.

Rank	LogOdds	ID	Name	Change
1	5.67837	J03026	matrix Gla protein.	-
2	4.52268	AF157026	type IIb sodium-phosphate transporter	-
3	4.462493	L29512	metalloproteinase inhibitor (TIMP-1) partial cds.	-
4	4.152706	AF164039	interferon-inducible protein variant 10	-
5	3.629502	X61381	R. rattus interferon induced.	-
6	3.287943	U16022	tissue inhibitor of metalloproteinase I partial cds.	-
7	2.997216	M65253	transformation-associated protein (34A)	-
8	2.946236	X12554	heart cytochrome c oxidase subunit Via.	-
9	2.867966	K01934	hepatic product spot 14, gene and flanks.	+
10	2.771988	X59961	genes for H2A and H2B histones.	+
11	2.635485	U95113	histone H2a gene.	+
12	2.462348	M11794	metallothionein-2 and metallothionein-1 genes.	-
13	2.460548	U35775	gamma-adducin; originally referred to as 35H.	+
14	2.45177	M28259	fibronectin gene, exons 2b and 3a.	-
15	2.253495	D88666	PS-PLA1	-
16	2.174667	AF159104	ad1-antigen partial cds.	-
17	2.078687	X15741	polymeric immunoglobulin receptor.	+
18	2.058201	D85035	dihydropyrimidine dehydrogenase	+
19	2.016023	X61654	ad1-antigen.	-
20	1.7989	AF164040	interferon-inducible protein 16	-
21	1.712049	L35317	cytosolic NADP-dependent isocitrate dehydrogenase	+
22	1.688424	D38629	APC protein	-
23	1.645934	M58040	transferrin receptor 3' end.	+
24	1.628062	U14647	interleukin-1 beta converting enzyme (IL1BCE); caspase-1	+
25	1.557889	M30692	Ly6-A antigen gene, exon 2; putative.	-
26	1.437009	AF132045	foocen-m2 alternate splice product	-
27	1.429459	AF032898	histone H2A and histone H2B genes.	+
28	1.428191	X61667	ant1 adenine nucleotide translocator.	-
29	1.34283	J02954	vitamin dependent calcium-binding protein.	+
30	1.342205	AF257237	oxytocin receptor partial cds.	-
31	1.296005	U17035	(mob-1)	-
32	1.262986	X70871	cyclin G.	-
33	1.253888	M31229	histone H1d gene.	+
34	1.252123	U27767	RGP4	-
35	1.235524	U57042	adenosine kinase	+
36	0.969345	U31598	MHC class II-like alpha chain (RT1.DMa) partial cds	-
37	0.902786	AF087037	BTG3	-
38	0.866272	AF220102	interleukin enhancer binding factor 3	-
39	0.824147	S85184	Cyclic Protein-2 (CP-2) partial cds.	-
40	0.821911	AB012960	FTZ-F1 beta1	+
41	0.749582	X13554	H4 somatic histone H4.	+
42	0.740483	U86635	glutathione s-transferase M5.	-
43	0.6647	AF223677	steroid sensitive gene-1 protein (SSG-1)	-
44	0.661681	L18948	intracellular calcium-binding protein (MRP14)	-
45	0.60434	D84418	chromosomal protein HMG2	+
46	0.598345	U49062	heat stable antigen CD24.	+

47	0.57907	M28409	testis-specific histone H1t and histone H4t;	+
48	0.558835	AF149250	intermediate conductance CA^{++}-activated K^{+} channel	+
49	0.522734	AJ132717	calcyclin.	-
50	0.510949	X13252	muscle nicotinic acetylcholine receptor epsilon subunit.	-
51	0.495962	AF196201	clone LRTVD2c9 T cell receptor V delta 2 partial cds.	-
52	0.364772	M62781	insulin-like growth factor binding protein 5 (IGFBP-5)	-
53	0.1785	X56747	fetal intestinal lactase-phlorizin hydrolase precursor.	-
54	0.168604	J03588	guanidinoacetate methyltransferase.	+
55	0.151012	D16308	cyclin D2	-
56	0.095515	S76513	bcl-x=apoptosis inhibitor {protooncogene}.	-
57	0.090628	M12335	nuc-encoded mitochondrial carbamyl phosphate synthetase.	+
58	0.067499	U42627	dual-specificity protein tyrosine phosphatase (rVH6)	-
59	0.06566	X71127	complement protein C1q beta chain.	-
60	0.061986	AF177683	P-cadherin partial cds.	-
61	0.005263	S87522	leukotriene A4 hydrolase	+
62	-0.03698	AF131912	ephrin A-2 precursor, partial cds.	-
63	-0.04425	AF136583	protein kinase SNK (Snk)	-
64	-0.16707	U48255	CD59 protein precursor,	-
65	-0.18071	AF070475	NBC-like protein 2 (NBC2).	-
66	-0.18396	M30689	Ly6-B antigen.	-
67	-0.18935	AF223678	CBL20 (CBL20); estrogen-regulated 20.4 kDa protein.	-
68	-0.19167	Y10019	DRM protein.	-
69	-0.21273	D88250	serine protease	-
70	-0.2346	M14972	cytochrome P-450-LA-omega	-
71	-0.2673	AF144756	adipocyte lipid-binding protein (ALBP).	-
72	-0.28811	AF076783	plasma membrane Ca2+ ATPase isoform 1kb.	-
73	-0.29799	AF023302	reggie1-1	-
74	-0.31028	AF241259	RGS5	-
75	-0.32086	X99901	ott gene, containing repeat region.	+
76	-0.32611	U73174	glutathione reductase	+
77	-0.36555	D10607	cystatin beta	-
78	-0.39368	X07286	protein kinase C alpha.	+
79	-0.41213	AF159097	SVS-protein F partial cds.	-
80	-0.41685	U07797	(T1-alpha)	-
81	-0.4243	Y08769	microvascular endothelial differentiation gene 2.	+
82	-0.44025	AJ000496	cyclic nucleotide-gated cation channel beta subunit.	-
83	-0.45405	U34685	cysteine protease P32 partial cds; caspase-3	+
84	-0.47396	AF165887	cytosolic branch chain aminotransferase BCATc partial cds.	-
85	-0.48185	AF170918	NAD+-dependent dehydrogenase.	+
86	-0.48747	U72741	36 Kd beta-galactoside binding lectin	+
87	-0.50271	S68245	carbonic anhydrase IV [lung, 1205 nt];	+
88	-0.51917	J03753	plasma membrane Ca2+ ATPase-isoform 1.	-
89	-0.55918	D00753	contrapsin-like protease inhibitor related protein (CPi-26).	-
90	-0.57002	X56917	inositol 1,4,5-triphosphate 3-kinase.	+
91	-0.57997	D42156	Ad4BP, exon 7 and complete cds.	+
92	-0.58818	L19706	H3 histone gene.	+
93	-0.60902	M21210	glutathione peroxidase (GSH-PO.	-
94	-0.6106	U25055	purine specific Na+ nucleoside cotransporter (SPNT)	-
95	-0.63397	M99567	phospholipase C beta-3 partial cds.	+
96	-0.65198	AB043636	ATP-sensitive K+ channel subunit Kir6.1.	-
97	-0.67359	D10757	proteasome subunit R-RING12	+

98	-0.6806	K03249	peroxisomal enoyl-CoA.	+
99	-0.68105	S61804	O6-methylguanine-DNA methyltransferase	-
100	-0.68506	AF091565	isolate QFG-TN1 olfactory receptor partial cds.	+
101	-0.69621	L04739	plasma membrane calcium ATPase isoform 1 gene.	-
102	-0.70076	AJ409332	tissue inhibitor of metalloproteinase type 2 (timp-2 gene).	-
103	-0.74441	D10729	proteasome subunit RC1.	+
104	-0.74545	D38067	DNA for UDP glucuronosyltransferase, exon 1.	+
105	-0.75676	M29853	cytochrome P-450 isozyme 5 (P450 IVB2).	-
106	-0.75676	AB010441	GlcAT-S UDP-glucuronyltransferase-S	+
107	-0.77418	Y07783	ER transmembrane protein.	-
108	-0.77941	AF001897	aldehyde dehydrogenase (ALDH).	-
109	-0.79407	AF136230	bcl-x short	-
110	-0.81481	AF111160	glutathione S-transferase A3 subunit (GSTA3)	-
111	-0.82488	M23697	tissue-type plasminogen activator (t-PA).	-
112	-0.83186	AB032766	legumain	-
113	-0.84497	J05107	corticosteroid 11-beta-dehydrogenase (DHII).	-
114	-0.85489	U02096	fatty acid binding protein	+
115	-0.90587	X62952	vimentin.	-
116	-0.94246	AF118890	s-tomosyn isoform	+
117	-0.95466	K02246	cytochrome P-450c.	-
118	-0.95808	S39779	preproendothelin-3 [734 nt]	-
119	-0.96074	U78134	zinc finger protein 6 (DZF6) partial cds.	+
120	-0.98473	D13121	ATP synthase subunit e	+
121	-0.99778	AF245040	substrate binding subunit of type II 5'-deiodinase D2p29	-
122	-1.02208	AF205713	brain GDNF splice variant 1 partial cds.	-
123	-1.06725	D89070	DNA for non-inducible carbony reductase	+
124	-1.07531	AF153193	winged helix/forkhead transcription factor HFH1	-
125	-1.11315	U76551	mucin Muc3 partial cds.	-
126	-1.12351	M86389	heat shock protein (Hsp27)	-
127	-1.13185	L23077	zinc finger protein	+
128	-1.14375	U18314	lamina associated polypeptide 2 (LAP2)	+
129	-1.14428	AF069511	putative sodium bicarbonate cotransporter (NBC)	-
130	-1.14451	Z22812	interleukin-1 receptor type 2.	-
131	-1.15705	U66322	dithiolethione-inducible gene-1 (DIG-1).	+
132	-1.1693	D78359	drs (a gene down-regulated by v-src).	-
133	-1.17952	U68562	chaperonin 60 (Hsp60) and chaperonin 10 (Hsp10) genes.	+
134	-1.18891	AF201901	interferon-gamma receptor.	-
135	-1.18956	L09216	glycosylated membrane-associated lipase.	-
136	-1.19475	S57478	lipocortin I	-
137	-1.19875	J04979	stathmin	+
138	-1.20395	D50608	cholecystokinin type-A receptor (CCKAR)	-
139	-1.23199	X59859	DCN decorin.	-
140	-1.25327	D28875	osteonectin	-
141	-1.25707	AB045279	beta3GnT5 beta1,3-N-acetylglucosaminyltransferase 5	+
142	-1.2907	S65355	nonselective-type endothelin receptor	-
143	-1.31496	AF324255	global ischemia-inducible protein 11; GIIG11.	-
144	-1.33284	D10693	histamine N-methyltransferase	+
145	-1.33577	L19927	(clone gamma-3) ATP synthase gamma-subunit (ATP5c)	+
146	-1.34642	M22631	alpha-propionyl-CoA carboxylase.	+
147	-1.36216	AF168362	protein associating with small stress protein PASS1 (Pass1)	-
148	-1.37284	M36410	sepiapterin reductase partial cds.	+

149	-1.3762	L07316	dipeptidase (dpep1)	-
150	-1.38409	U05014	Sprague/Dawley PHAS-I	-
151	-1.39179	AB010119	Tctex-1	-
152	-1.39499	D83538	230kDa phosphatidylinositol 4-kinase	-
153	-1.3994	L08446	Fc gamma receptor RIIIH isoform.	-
154	-1.40731	Y08138	dHand protein.	-
155	-1.42018	AF315374	ATP synthase lipid-binding protein P3 precursor (Atp5g3).	+
156	-1.42295	AF167308	secreted frizzled-related protein sFRP-1 partial cds.	-
157	-1.42948	M19036	lung beta-galactoside-binding lectin.	-
158	-1.43354	X91810	Stat3 protein.	-
159	-1.46103	M83678	(clone LRB10) RAB13 3'end.	-
160	-1.47053	U50194	tripeptidylpeptidase II	+
161	-1.47275	M84719	flavin-containing monooxygenase 1 (FMO-1)	-
162	-1.4855	U06752	Fisher 344 pre-sialomucin complex (pSMC)	-
163	-1.49204	M63837	alpha-platelet-derived growth factor receptor	-
164	-1.49361	U53855	prostacyclin synthase (ratpgis); p450-like synthase.	-
165	-1.49481	J05495	Gal/GalNAc-specific lectin.	-
166	-1.49867	M15254	platelet factor 4 (PF4) gene.	-
167	-1.50428	AF226993	selective LIM binding factor	-
168	-1.52454	AF286722	peripheral cannabinoid receptor gene	-
169	-1.52518	X95882	ATP ligand gated ion channel.	+
170	-1.52809	AF159096	ADAMTS protein partial cds.	-
171	-1.52981	AB052882	CSE cystathionine gamma-lyase	+
172	-1.53017	X62660	glutathione transferase subunit 8; subunit 8.	+
173	-1.53946	M81785	syndecan	-
174	-1.54608	M73714	microsomal aldehyde dehydrogenase	+
175	-1.54828	AF317669	BMAL1g' (Bmal1g') partial cds.	+
176	-1.5486	M63101	interleukin 1 receptor antagonist gene	-
177	-1.55543	J04791	ornithine decarboxylase (ODC)	-
178	-1.58737	D83796	UGT1 UDP-glucuronosyltransferase	+
179	-1.59395	L29191	fibronectin.	-
180	-1.59671	AF010323	F1-ATPase epsilon subunit.	+
181	-1.60141	AF087945	nitzin partial cds; similar to band 4.1 family members.	+
182	-1.60179	M69139	SR13 myelin protein	-
183	-1.62455	D87515	aminopeptidase-B	+
184	-1.62792	U65656	gelatinase A	-
185	-1.65874	U57501	protein tyrosine phosphatase gamma partial cds.	+
186	-1.66527	L07127	pancreatitis-associated protein (PAP) gene	-
187	-1.68067	AB029559	BAT1	-
188	-1.68211	AF353305	dopamine responsive protein	+
189	-1.6829	J04791	replica, ornithine decarboxylase (ODC)	-
190	-1.68591	D86041	N-G,N-G-dimethylarginine dimethylaminohydrolase.	-
191	-1.68616	U27201	tissue inhibitor of metalloproteinase 3 (TIMP-3).	-
192	-1.69866	D89983	antizyme inhibitor	+
193	-1.70216	AF177477	clone C42 CDK5 activator-binding protein	-
194	-1.70264	AF255305	superoxide dismutase copper chaperone; rCCS.	-
195	-1.71095	Z19552	DNA topoisomerase II.	+
196	-1.71729	AF074952	epiregulin precursor.	-
197	-1.72501	M24852	neuron-specific protein PEP-19.	-
198	-1.72574	X62528	ribonuclease inhibitor.	-
199	-1.73003	M15793	neuropeptide Y gene, exons 3 and 4.	-

200	-1.73246	X75774	CaM kinase II gene subtype delta 2.	+
201	-1.73356	U75391	B-cell receptor associated protein 37 (BAP-37).	+
202	-1.74205	AF061443	G protein-coupled receptor LGR4 (LGR4).	+
203	-1.74943	U95177	DOC-2 p82 isoform; phoshoprotein.	-
204	-1.76183	AF326741	sclerostin	-
205	-1.7669	AF184983	osteoactivin; membrane associated glycoprotein.	-
206	-1.78243	AF272661	alpha 4 type V collagen.	-
207	-1.79072	J02582	apolipoprotein E gene; ORF1.	-
208	-1.79086	U72353	lamin B1.	+
209	-1.80124	U12402	rARL1.	+
210	-1.80614	AF021350	natural killer cell protein group 2-A (NKG2A.	+
211	-1.82031	X68199	replica, MYR1 myosin I heavy chain.	-
212	-1.84054	AF182101	basic trancription element binding protein 2 (Bteb2).	+
213	-1.84148	L23874	iron-responsive element-binding protein	+
214	-1.85176	L22761	DNA binding protein (GATA-GT2)	+
215	-1.85854	AF239045	kinase D interacting substrate, 220 kDa.	-
216	-1.86327	M17300	cholesterol-regulated 39kd protein.	+
217	-1.89402	M84645	RHS2 class III POU protein (RHS2) complete cds.	+
218	-1.90067	AF154245	chemotactic protein-3 gene	-
219	-1.91399	X57999	type I thyroxine deiodinase; selenocysteine.	+
220	-1.91978	J04473	mitochondrial fumarase.	+
221	-1.92552	AF120100	thiopurine S-methyltransferase (tpmt)	+
222	-1.92845	X03369	beta-tubulin T beta15.	-
223	-1.93547	D00512	mitochondrial acetoacetyl-CoA thiolase precursor	+
224	-1.94927	M27466	liver cytochrome oxidase subunit VIc (COX-VIc)	+
225	-1.95267	AF136230	Bcl2 like 1	-
226	-1.95823	AF041105	organic anion transporter protein 3; oatp3.	-
227	-1.96118	S72637	tumor-suppressive gene.	-
228	-1.97445	X89963	mRNA TSP-4 protein.	-
229	-1.98175	AF271156	CaM-kinase II inhibitor alpha.	+
230	-1.99031	AF179370	insulin-like growth factor binding protein 5 protease.	-
231	-1.99476	M62372	alpha-2-adrenergic receptor protein (RG20) gene	+
232	-1.99829	D86839	DNA for small heterodimer partner homologue; SHP.	+

Table 6.3. List of genes upregulated by irinotecan treatment in the rat jejunum.

Name	ID	Ratio
H2A and H2B histones	X59961	2.266
Polymeric immunoglobulin receptor	X15741	3.231
Interleukin-1 beta converting enzyme (caspase-1)	U14647	2.735
H2a histone	U95113	2.330
Gamma adducin	U35775	1.829
Hepatic product spot 14	K01934	2.360
H2A and H2B (partial cds)	AF032898	2.189
Cytosolic NADP-dependent isocitrate dehydrogenase	L35317	1.914
Transferrin receptor	M58040	2.056
Intermediate conductance calcium-activated potassium channel	AF149250	2.470
H1t and H4t histone	M28409	1.873
Nucleus-encoded mitochondrial carbamyl phosphate synthetase	M12335	2.009
Vitamin D dependent calcium-binding protein	J02954	1.861
Dihydropyrimidine dehydrogenase	D85035	1.919
H3 histone	L19706	1.851
Cysteine protease P32 (caspase-3)	U34685	1.827

Figure 6.4. List of genes downregulated by irinotecan treatment in the rat jejunum.

Name	ID	Ratio
Matrix Gla protein	J03026	7.201
Metalloproteinase inhibitor (TIMP-1)	L29512	7.271
Interferon induced gene	X61381	4.441
Type IIb sodium-phosphate transporter	AF157026	2.651
Tissue inhibitor of metalloproteinase 1	U16022	5.348
Metallothionein	M11794	6.201
Interferon-inducible protein variant 10	AF164039	2.883
Transformation-associated protein	M65253	2.903
Interferon inducible protein 16	AF164040	2.633
Cytochrome c oxidase subunit	X12554	2.199
Ad1-antigen partial cds	AF159104	2.220
Ly6-A antigen	M30692	2.991
Mob-1	U17035	2.487
Oxytocin receptor	AF257237	5.085
Fibronectin	M28259	1.833
Foocen-m2	AF132045	1.860
PS-PLA1	D88666	1.879
Ad1 antigen	X61654	1.881
Cyclic protein 2	S85184	2.230
Cyclin G	X70871	2.727
Glutathione tranferase	U86635	1.827
CD59	U48255	2.787
Adenine nucleotide translocator	X61667	1.921
DRM protein	Y10019	2.285
MHC class II-like alpha chain	U311912	1.818
Contraspin-like protease inhibitor	D00753	3.140
Insulin-like growth factor binding protein 5	M62781	1.918
Purine specific Na^+ nucleoside cotransporter	U25055	1.996
Bcl-xL	S76513	1.845
Cytochrome P-450c	K02246	5.404
Fatty acid binding protein	AF144756	1.831
ATP-sensitive K^+ channel	AB043636	2.256
Cytochrome P-450 isozyme 5	M29853	1.948
Heat shock protein 27	M86389	1.899
Ly6-B antigen	M30689	2.454
Beta-galactoside-binding lectin	M19036	1.996
WDNM1	X13309	6.818

Table 6.5. List of differentially regulated genes grouped according to cellular role.

Cellular role	Gene	Regulation
Cell signaling/communication		
Cell adhesion	*Fibronectin*	Down
Channels/transport proteins	*Ca^{++}-activated K^{+} channel*	Up
Effectors/modulators	*Vitamin D-dependent Ca^{++} binding protein*	Up
Growth factors	*Insulin-like growth factor binding protein 5*	Down
Receptors	*Oxytocin receptor*	Down
Cell defence		
Immunology	*Transferrin receptor*	Up
	Polymeric Ig receptor	Up
	CD59	Down
	Mob-1	Down
	Ly6-antigen	Down
	Ad1 antigen	Down
	Interferon inducible protein 10 & 16	Down
	MHC class II-like alpha chain	Down
Apoptosis	*Caspase-1*	Up
	Caspase-3	Up
	Bcl-xL	Down
Stress response	*Heat shock protein 27*	Down
Homeostasis	*Metallothionein*	Down
Cell division		
Cell cycle	*Foocen-m2*	Down
	DRM protein	Down
	Cyclin G	Down
Chromsome structure	*H2A and H2B histon*	Up
	H3 histone	Up
	H1t and H4t protein	Up
Metabolism		
Amino acid	*Carbamyl phosphate synthetase*	Up
	Glutathione s-transferase	Down
Lipid	*Fatty acid binding protein*	Down
Energy	*Isocitrate dehydrogenase*	Up
	Cytochrome c oxidase	Down
Sugar	*Beta-galactoside-binding lectin*	Down
Drug	*Dihydropyrimidine dehydrogenase*	Up
	Cytochrome P450 isozyme	Down
Gene/protein expression		
Protein turnover	*Cyclic protein-2*	Down
	TIMP-1	Down
	Cpi-26	Down
	Transformation-associated protein	Down
	WDNM1	Down
Cell structure		
Extracellular matrix	*Gamma adducin*	Up
	Matrix Gla protein	Down
Unclassified	*Hepatic product spot 14*	Up

6.2.2 Real time PCR

Candidate upregulated gene, caspase-1, was selected for further analysis by real time PCR. Expression of caspase-1 mRNA in the rat jejunum was investigated in untreated controls and at 6, 24 and 48 h following irinotecan treatment. There was a significant increase in caspase-1 expression from control levels at 6 h. Expression returned to pre-treatment levels at 24 h and then modestly increased again at 48 h. All samples were run with internal control rat rRNA 18S to allow for quantification. The expression of 18S did not change at any time point, as should be expected of an internal house keeping gene. Results of typical PCR shown in Figures 6.2, 6.3, 6.4 and 6.5.

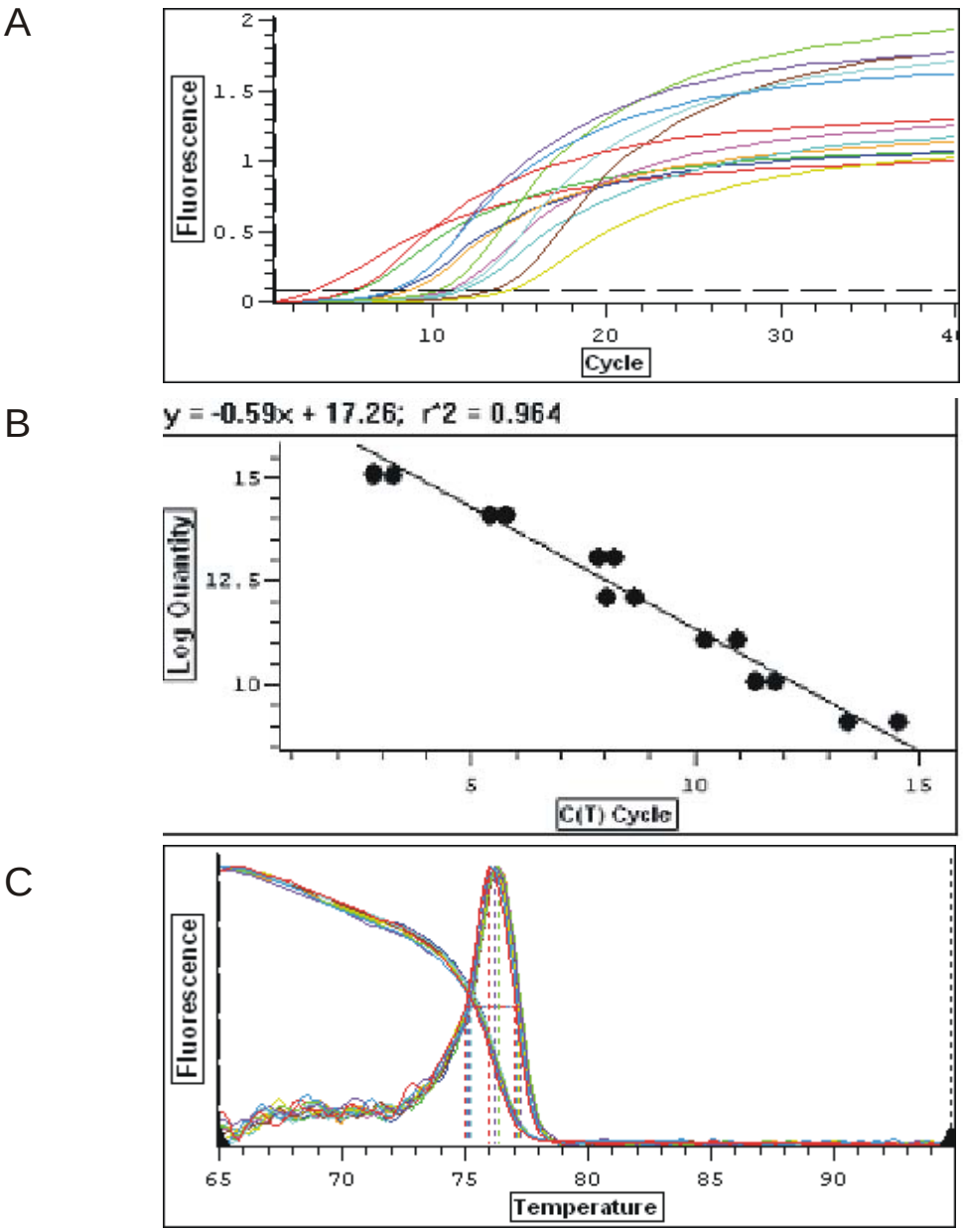

Figure 6.2. Results of RT-PCR for 18S oligo standards. A) data graph, B) standards graph, C) melt curve analysis graph

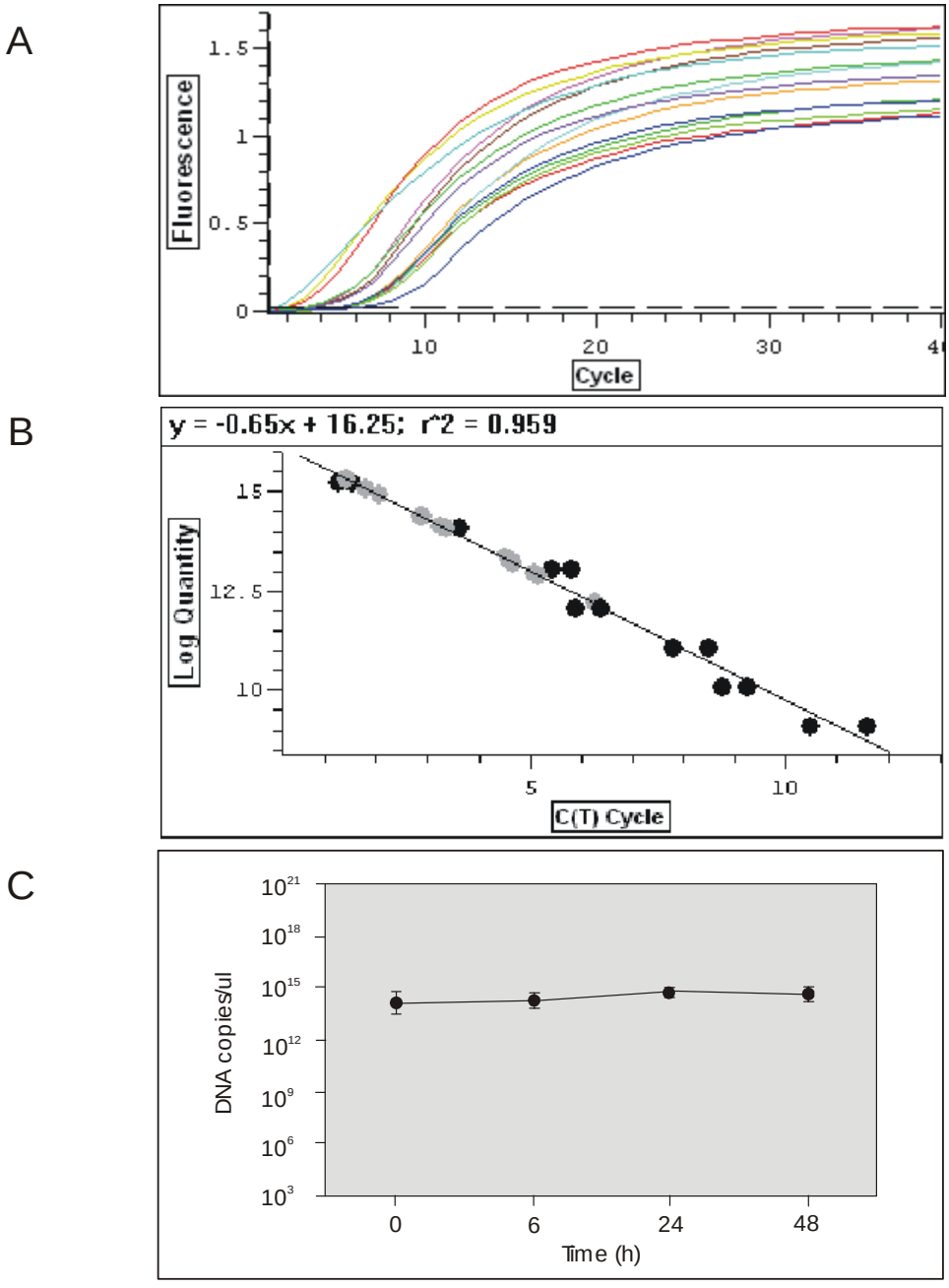

Figure 6.3. Results of irinotecan-induced 18S changes in rat jejunum. A) data graph, B) standards graph and C) graph of gene expression over time, where data shown is group mean +/- SE (n = 4).

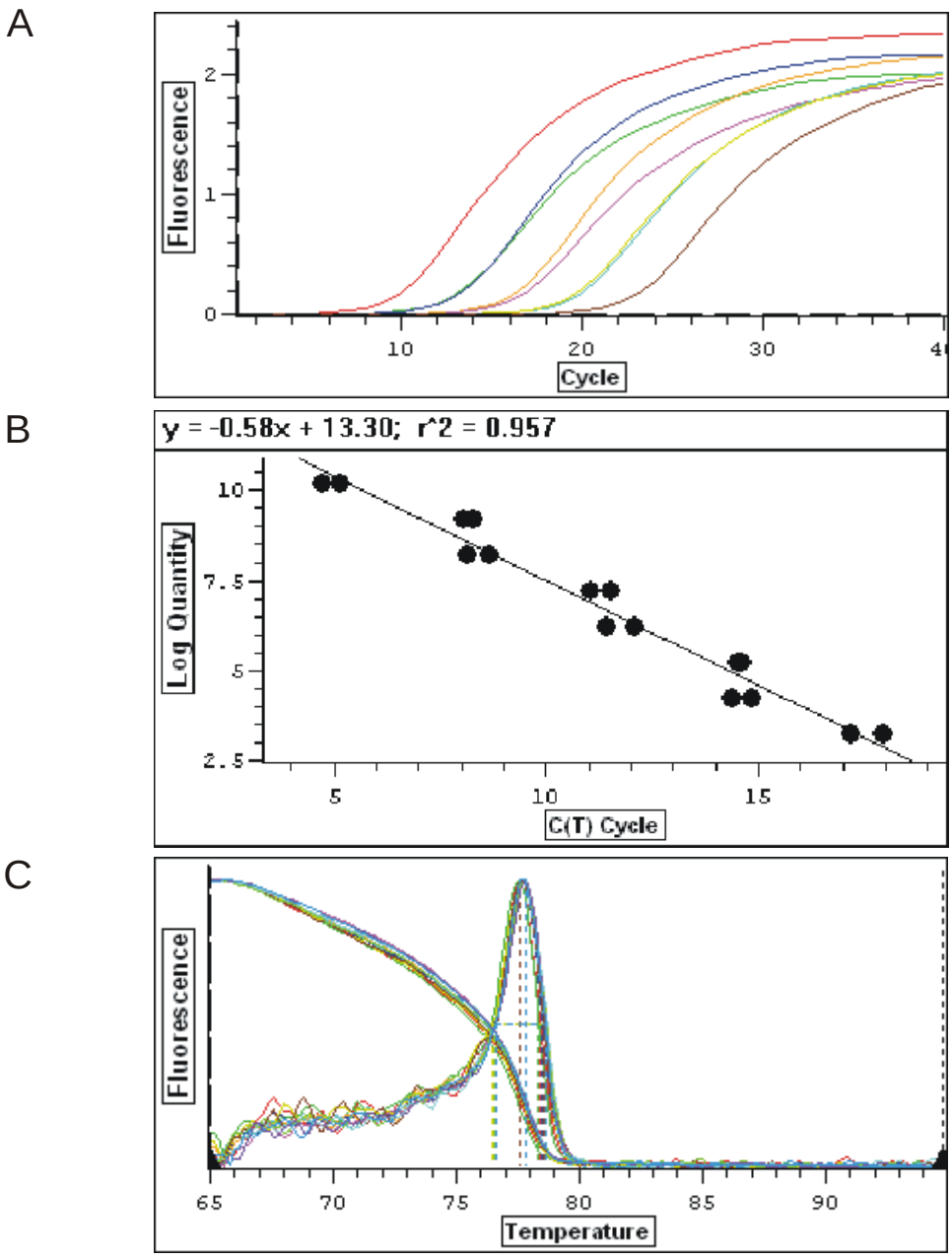

Figure 6.4. Results of RT-PCR for caspase-1 oligo standards. A) data graph, B) standards graph, C) melt curve analysis graph

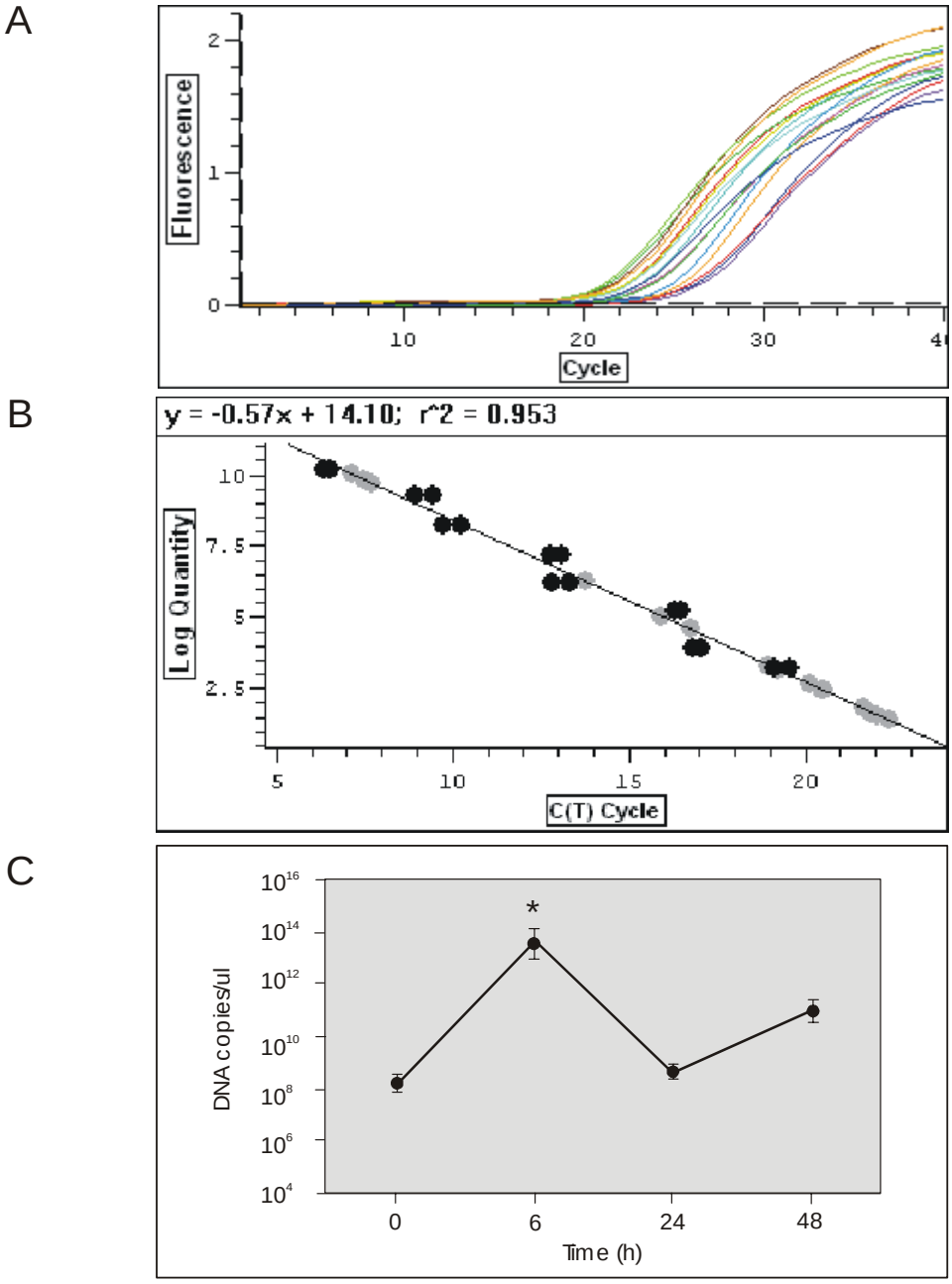

Figure 6.5. Results of irinotecan-induced caspase-1 changes in rat jejunum. A) data graph, B) standards graph and C) graph of gene expression over time, where data shown is group mean +/- SE (n = 4). * indicates significant increase in caspase 1 from control ($P<0.05$).

6.3 Discussion

This study has investigated gene changes that occur in the rat small intestine following irinotecan treatment through simultaneous genome-wide analysis, and characterised the profile of expression of the apoptosis regulator caspase-1.

Irinotecan (CPT-11) is a relatively new drug in the clinic and so its full range of physiological actions and their implications are yet to be fully understood, especially on normal tissue. As such, it would prove useful to have a list of all genes affected by this chemotherapy agent and how they interact to cause downstream effects and toxicities in the intestine. To investigate any connections with specific gene changes and the induction of cancer treatment-induced damage, a literature search was conducted through Entrez PubMed for each of the listed genes grouped with the word mucositis or intestine. This resulted in only a few published articles being retrieved, indicating the major gaps in knowledge of the pathobiology of mucositis which still exist. In the upregulated genes list, two caspases were identified, caspase-1 and caspase-3. The involvement of caspase-3 in apoptosis has been described in detail (Grutter, 2000; Marshman et al., 2001; Philchenkov, 2004) and has been shown to be upregulated at both the protein and mRNA level following various cytotoxic treatments in intestinal cells. The transcriptional control of caspase-1 in the intestine is less well defined. In a previous study, CPT-11 was shown to increase caspase-1 mRNA expression in myeloid leukemia cells (Shibata et al., 1996) and it was suggested to enhance apoptotic cell death. The chemotherapy agent cisplatin has also been shown to increase caspase-1 mRNA expression in malignant glioma cells (Kondo et al., 1995). Apoptosis induced by cisplatin and also by forced caspase-1 overexpression can be suppressed by the caspase-1 inhibitor Ac-YVAD-CMK, suggesting its requirement for apoptotic cell death in this model. Further to this, caspase-1 mRNA expression is downregulated in colon cancer (Jarry et al., 1999), an environment of decreased apoptosis, indicating a disruption to the normal apoptotic pathway.

In addition to its role in apoptosis, caspase-1 is responsible for the proteolysis and maturation of pro-inflammatory cytokines, namely interleukin-1β (IL-1β) and IL-18 (Creagh et al., 2003; Launay et al., 2005). Activation of the TNF receptor through increases in circulating TNF induces caspase-1 activation as part of the MAPK signalling pathway, an important stress kinase pathway (Lamkanfi et al., 2004). Therefore the upregulation of caspase-1 in the rat jejunum by irinotecan suggests that the treatment may induce an inflammatory response as a component of intestinal damage. Histopathological

examination of intestinal sections conducted as part of the trial not included in this report revealed that irinotecan treatment caused lamina propria oedema and the presence of degenerate polymorphonucleocytes within crypts, without increasing the normal mixed inflammatory cell population within the lamina (Gibson et al., 2005). Thus without overt inflammation being present at any time point investigated, we assume that irinotecan-induced caspase-1 upregulation in the intestine is primarily contributing to apoptosis. But there is also bone marrow suppression induced by chemotherapy, resulting in a reduced ability to mount an effective inflammatory response which should be considered.

A range of other genes were changed by irinotecan treatment and their regulation provides information about the actions of the drug on normal intestinal cells. For example, dihydropyrimidine dehydrogenase (DPD) is known to be closely associated with the toxicity of the chemotherapy agent 5-FU. DPD is the first and rate-limiting enzyme in the catabolism of 5-FU (Katona et al., 1998). DPD deficiency leads to impaired break down of 5-FU and therefore increases cytotoxicity, with patients with low levels of DPD at an increased risk of high grade mucositis development (Chu et al., 2004; Johnson et al., 1999). Upregulation of this enzyme in response to irinotecan treatment most likely represents an attempt by the rat intestine to breakdown toxic CPT-11 or SN-38, the active metabolite of irinotecan. Another enzyme, already characterised for its role in irinotecan-induced toxicity, is uridine diphosphate (UDP)-glucuronyl-transferase (UGT1A1) (Ando and Hasegawa, 2005) and it was upregulated in this study. UGT1A1 is involved in the glucuronidation of SN-38 and is important for detoxification of SN-38. UGT1A1 glucuronidates and transforms SN-38 into the inactive form SN38 glucuronide (SN 38G), which is then excreted in the bile by the small intestine. In cases of low UGT1A1 activity the accumulation of high levels of SN-38 can cause severe diarrhoea and leucopoenia (Russo et al., 2005).

Of interest, A number of genes involved in cellular calcium regulation were upregulated by irinotecan treatment. Firstly, protein kinase C (PKC) has been shown to increase intracellular Ca^{++} levels in intestinal epithelial cells which affects cell integrity and the epithelial barrier (Tepperman et al., 2005). The pro-inflammatory cytokine TNF is known to mediate its apoptotic affects via activation of PKC (Chang and Tepperman, 2003). PKC is an important molecule in the MAP kinase pathway. Further to this, compounds that are capable of reducing or inhibiting PKC activation are effective at ameliorating apoptosis and may reduce acute cytotoxic treatment sequelae such as mucositis (Chang and

Tepperman, 2003; Hallahan et al., 1994). Next, inositol (1,4,5)-trisphosphate (Ins(1,4,5)*P*3) is a key intracellular messenger in cells, and has been well established as a mediator of Ca^{++} release from intracellular stores. Like all second messengers, Ins(1,4,5)*P*3 has a short half-life within the cell, and is rapidly metabolised. Ins(1,4,5)*P*3 metabolism is partly carried out by Ins(1,4,5)*P*3 3-kinase (IP3-3K) (Pattni and Banting, 2004) which was upregulated in this experiment. Finally, CaM kinase II, is a calcium/calmodulin-dependent protein kinase that is involved in a number of downstream processes. It is a ubiquitous mediator of Ca^{++}-linked signalling that phosphorylates a wide range of substrates to co-ordinate and regulate Ca^{++}-mediated alterations in cellular function. Its activity is increased during times of elevated intracellular calcium (Hudmon and Schulman, 2002). Together, the increase in expression of these kinases indicates an environment where intracellular calcium storage is perturbed and cellular integrity diminished.

Genes involved in the immune response were highly represented both in the up and downregulated list, suggesting that irinotecan does induce an early, if somewhat mild, inflammatory response in the intestine. Of the former, the polymeric immunoglobulin receptor (pIgR), which mediates the transport of IgA across intestinal epithelial cells and provides immune protection at a number of levels has been shown to increase in inflammation. During the acute inflammatory phase there is upregulation of TNF with subsequent activation of NFκB, which has been shown to interact and transcriptionally upregulate the pIgR gene (Bruno and Kaetzel, 2005). The transferrin receptor has also shown to be upregulated in response to inflammation (Barisani et al., 2004; Cairo and Pietrangelo, 1995; Schreiber et al., 1991) and here may also indicate changes in iron homeostasis due to irinotecan treatment. On the downregulated side, we firstly have CD59 which is also known as protectin. CD-59 is expressed on gut epithelium and is the main defence of cells against complement. It has previously been shown to be decreased in regions of inflammation (Scheinin et al., 1999) and it has been postulated that loss of CD59 could be a marker of injured cells waiting for clearance by the complement system (Vakeva et al., 1992). The interleukin-1 type 2 receptor (IL-1RII) is a natural antagonist of proinflammatory cytokine IL-1. This is due to its ability to bind the IL-1 ligand but inability to transmit a signal to the cell, which is unlike the type 1 receptor which mediates all the activities of IL-1 (McGee et al., 1996). Again, this receptor has been shown to be downregulated during inflammatory bowel disease (Ludwiczek et al., 2004), thus indicating a shift in the balance towards an inflammatory state within the intestine following irinotecan.

The downregulation of protective genes appears to be a major strategy by irinotecan to induce tissue injury. For example, multiple members of the tissue inhibitor of metalloproteinase (TIMP) family were decreased in the treated group. The requirement for a balance in expression between cell destructive matrix metalloproteinase's (MMP) and their inhibitors, TIMPs in tissue homeostasis has been shown clearly by a previous experiment where during 5-FU-induced oral mucositis there was an increase in MMP-2 and MMP-9 with concurrent decreases in TIMP-1 and TIMP-2 in damaged hamster cheek pouches (Morvan et al., 2004). Further to this, stabilisation of TIMP expression by the anti-inflammatory agent RG1503 prevented mucositis in that model. Secondly, metallothionein acts in the cell to bind zinc, which has numerous protective and healing roles in the intestine (Tran et al., 2003). Metallothionein has also been shown to sequester free radicals during inflammatory states and thus contribute to cellular protection (Mulder et al., 1994). As such, decreases in the gene will be detrimental to overall intestinal integrity after irinotecan. The anti-apoptotic members of the Bcl-2 family, Bcl-xL and Bcl-2L1 were also decreased by irinotecan. This indicates that the balance between pro-survival and pro-apoptotic proteins within the intestine is altered to allow cell death. Finally, the reduction in cytochrome c oxidase, a component of the mitochondrial respiratory chain, indicates an inability of the cell to maintain activity, and hence initiate repair. The use of low energy lasers, which interact with cytochrome c oxidase, promote cellular proliferation and cytoprotection and have recently been shown to protect against development of oral lesions and speed healing of oral mucositis following bone marrow transplant (Cowen et al., 1997; Eells et al., 2004).

An effect of irinotecan treatment of particular interest was the activation of multiple genes implicated in the MAPK signalling pathway. Differentially regulated genes included the interleukin 1 receptor, caspases, protein kinase C, dual specificity phosphatase 6 and heat shock protein 27, which all been identified at act at different sites along the pathway. This finding implicates MAP kinase signalling intimately with irinotecan induced intestinal damage and hence should receive more attention to distinguish potential therapeutic targets.

This study has shown that irinotecan has wide ranging effects on gene expression in the rat intestine and that a combination of apoptotic and inflammatory changes along with changes in cell cycling through cyclin G and D2 all contribute to the damage seen following treatment. This work has also highlighted the common pathway of caspase-

dependent cell death due to irinotecan which may prove to be a useful intervention target to prevent intestinal apoptosis following chemotherapy with this agent.

General discussion

7.0 Introduction

Mucositis is currently one of the most frequent dose-limiting toxicities associated with cancer treatment. It occurs along the entire gastrointestinal tract and damage is pan-mucosal (Keefe, 2004). Apoptosis in epithelial crypts is currently the best defined early marker of intestinal damage following chemotherapy (Keefe et al., 2000). However, the apoptotic pathway has many regulators and it has yet to be defined which of these apoptotic genes are involved in intestinal cell death in response to different cytotoxic agents. The studies contained in this thesis investigated three important gene families involved in the control of apoptosis; p53, Bcl-2 and caspases. This work has detailed the effect of a range of chemotherapy agents on expression of these genes in the intestine and has utilised *in vitro*, established rat *in vivo* and human models of mucosal damage. Furthermore, the final research chapter described the findings from a genome-wide analysis of the effects of irinotecan on the rat jejunum, identifying new pathways not dependent on classical apoptosis regulators.

7.1 Chemotherapy-induced intestinal damage

Studies investigating the effects of chemotherapy on the intestine have been carried out for a number of decades. Interest was first generated by a series of reports on the effect of methotrexate on the small intestine in the 1960s by Trier et al (Trier, 1962a; Trier, 1962b). An acute awareness of the damaging side effects of chemotherapy agents on the intestine has since existed. This thesis continued to investigate this by examining the effect of the chemotherapy agent, irinotecan, on the small and large intestine in the rat with breast cancer. A single dose of irinotecan caused severe damage in both regions which was characterised by apoptosis, decreases in morphometry and a mild inflammatory response. These findings are consistent with that of previous investigations using a variety of chemotherapy drugs (Boushey et al., 2001; Gibson et al., 2005; Gibson et al., 2003; Gibson et al., 2002b; Morelli et al., 1996). The similarities seen following treatment with chemotherapy agents has been proposed to be a factor of intestinal cells having a limited repertoire for response to a damaging stimulus. Most often the acute outcome being crypt cell death, which can occur as a consequence of a multitude of inducers including activation of pro-inflammatory cytokines, direct genomic damage, generation of reactive oxygen species and induction of the ceramide pathway (Hockenbery et al., 1993; Norbury

and Zhivotovsky, 2004; Plevova, 2002; Reed and Zhang, 1997). All of which are known to occur in response to cytotoxic drug therapy. The use of intestinal epithelial cell lines within the thesis has also contributed to the body of evidence for induction of cell death and cytostasis by varying chemotherapy agents. The *in vitro* experiments detailed in Chapter 4 investigated the effect of irinotecan and doxorubicin on intestinal cells. The results followed a similar pattern as observed in the *in vivo* models of intestinal damage where by cytotoxic treatment caused an increase in epithelial cell death which peaked by 24 h when administered at clinically relevant doses. Thus crypt apoptosis is an epithelial process not requiring sub-epithelial interactions to occur. Although, this does not exclude the possible synergistic effects on epithelial apoptosis by other mucosal mediators of tissue injury.

7.2 Apoptosis

Apoptosis has been shown to be involved in the development of mucositis in all areas of the GIT (Gibson, 2004). The work done by Gibson et al and others has shown apoptosis occurs rapidly within epithelial layers along the entire length from the oral cavity to the rectum after chemotherapy treatment (Gibson et al., 2005; Pritchard et al., 1998; Suzuki et al., 2004). The study described in Chapter 5 showed over a 30-fold increase in apoptosis at 6 h following irinotecan administration, which is in line with previous results (Gibson et al., 2003; Gibson et al., 2002a). This highlights the importance of cell death in the sequela of intestinal damage after chemotherapy. Apoptosis is an active event requiring coordinated cellular processes involving a large number of molecules to be carried out (Adams, 2003). The apoptotic pathway often utilises the transcription factor, p53, as an immediate signalling message of damage to the cell which is followed by the regulation of a number of proteins belonging to the Bcl-2 family capable of enhancing or inhibiting the signal. When the pro-apoptotic signal prevails, members of the cystine protease family, caspases, are recruited and effectively complete the apoptotic process by dismantling the cell (Cory et al., 2003; Creagh et al., 2003; Slee et al., 2004). This thesis is the first to investigate each of these components of the apoptotic pathway together within the mucositis setting. Through a series of studies which have concentrated on each it has been shown that changes in p53, Bcl-2 and caspase expression are associated with intestinal damage and will be described individually in turn.

7.3 p53

The tumour suppressor protein, p53, is known to be activated in response to a wide variety of stimuli, including DNA damage, hypoxia, oncogene overexpression and nucleotide depletion (Yu and Zhang, 2005). Many chemotherapy agents act on proliferating cells to interrupt replication and cause DNA damage (Hickman et al., 1994). Investigations carried out during this thesis found that p53 increases in accordance with apoptosis levels in the rat jejunum following methotrexate treatment for breast cancer. Methotrexate is a folate-inhibitor known to induce cell death in a p53-dependent manner (Palacios et al., 2000). The method of apoptosis induction in the intestine by the topoisomerase I inhibitor, irinotecan, is yet to be fully defined. Both *in vitro* and *in vivo* investigations in this thesis found only mild and late induction of p53 following irinotecan. Furthermore, blockade of p53 did not significantly interrupt apoptosis. As such it appears irinotecan causes cell death in the intestine through other p53-independent pathways. Alternatively, the chemotherapy agent doxorubicin was found to activate p53 in intestinal epithelial cells. Blockade of the transcriptional ability of p53 reduced apoptosis, indicating that this drug causes apoptosis in a p53-dependent manner in the intestine. The use of p53-inhibitors as a possible way to ameliorate the intestinal side effects of cancer therapy was explored in detail by Komovera et al (Komarov, 1999; Komarova and Gudkov, 2000; Komarova et al., 2003). They identified the function of p53 in early wave apoptosis (8 to 24 h) within intestinal crypts following irradiation (IR), which could be prevented by pifithrin-alpha (PFT) (Komarova et al., 2004). They also described the importance of the temporary nature of PFT-induced p53 blockade, since a second wave of p53-independent cell death, classed as mitotic catastrophe, occurs in the intestine in p53 gene knockout mice which actually worsens gastrointestinal toxicity. As such, the diverse and complex role of p53 in chemotherapy induced intestinal cell death is 1) variable between *in vitro* and *in vivo* models, 2) changes in response to different cytotoxic agents and 3) is disposable for apoptosis in response to irinotecan in intestinal cells, leaving p53 inhibition an non-viable approach to prevent intestinal mucositis.

7.4 Bcl-2 family

The Bcl-2 family consists of over 20 evolutionary conserved members that can both positively and negatively control the apoptosis pathway (Schinzel et al., 2004). They primarily act at the mitochondrial membrane to control the release of apoptogenic factors into the cytoplasm which induce cell destruction, often through activation of caspases

(Gross et al., 1999). Eight members of the Bcl-2 family were investigated in this thesis, anti-apoptotic Bcl-2, Bcl-xL, Bcl-w and Mcl-1 and pro-apoptotic, Bax, Bak, Bim and Bid. The studies carried out in Chapters 2 and 3 showed, firstly, that the normal expression levels of pro-apoptotic Bcl-2 family proteins are significantly higher in the crypts of the rat jejunum compared to the colon, and secondly, that following chemotherapy treatment Bax and Bak proteins are increased and these both correlate to increased apoptosis. Similar increases in Bax and Bax protein levels were also shown in patient samples undergoing chemotherapy treatment from cancer. Thus, changes in Bcl-2 family expression within small intestinal crypts occurs in response to treatment with a variety of cytotoxic agents and is similar in both rats and humans. Importantly, increases in Bax and Bak protein expression was also noted following cytotoxic treatment of intestinal cell lines, indicating the conserved pathway of Bcl-2 family regulation which exists in each model of intestinal injury. The obvious importance of Bcl-2 family regulation in intestinal cell death could provide a new approach to ameliorate cancer treatment-induced damage, possibly through manipulation of local Bax and Bak expression. This is a plausible option since studies have shown prevention of apoptosis when both Bax and Bak expression has been genetically deleted (Wei, 2001). The forced overexpression of anti-apoptotic members such as Bcl-2 and Bcl-xL has also proven effective in prevention of cell death in a number of settings (Lu et al., 2004; Shinoura et al., 2000; Takahashi et al., 1999).

7.5 Caspases

Caspase-3 has long been associated with the execution phase of apoptosis and toted as the gatekeeper in the caspase cascade (Grutter, 2000). Its processing from a pro-caspase zymogen to the active cleaved form represents a point of no return for the cell and is often quantified as a marker of apoptosis (Marshman et al., 2001). Through investigations carried out for this thesis, it was found that caspase-3 protein expression increases in the small intestine of the rat treated with methotrexate for breast cancer while caspase-3 messenger RNA is increased in response to irinotecan treatment. Both of these are associated with intestinal crypt apoptosis, which is in accordance with previous reports (Marshman et al., 2001; Papaconstantinou et al., 2001; Yuan et al., 2002). The role of the pro-inflammatory caspase member, caspase-1, in anticancer therapy–induced cell death in the intestine had not been previously reported. Irinotecan was found to rapidly increase caspase-1 expression in the jejunum during peak levels of apoptosis. This expression subsequently returned to control levels during the time of peak intestinal damage and was

increased again as the healing phase was initiated. Caspase-1 is well known for its role in processing of the cytokine, interleukin 1β (IL-1), and activation of inflammatory signalling (Lamkanfi et al., 2004; Martinon and Tschopp, 2004). It seems likely then that caspase-1 has a dual role in apoptosis and inflammation in the intestine treated with chemotherapy. Broad spectrum and specific caspase inhibitors have been shown to reduce apoptosis in cells in response to a number of stimuli (Lavrik et al., 2005; Philchenkov, 2004). The role of caspases in intestinal mucositis is that of downstream executioners of cell death, and inhibition of this process could represent a potential therapeutic target for anti-mucotoxics.

7.6 Future directions

Intestinal mucositis occurs as a consequence of a complex biological cascade involving transcription factor activation, mitochondrial protein regulation and proteasomic degradation. These have generally been investigated independently in previous studies. Future studies should examine each component together in relation to stress pathways and induction stimuli to create a map of key players in the pathogenesis of mucositis. Thus creating a reference for targeting multiple points along the map to effectively design anti-mucotoxics. Multifactorial agents, acting on a number of side effects simultaneously will prove to be the only way to significantly ameliorate intestinal damage in response to chemotherapy treatment. The technology to initiate this does exist. Microarray experiments are emerging as a powerful tool in the identification of genetic profiles important in the development of mucosal injury, through investigating genome-wide changes in gene expression following chemotherapy treatment (Arcellana-Panlilio and Robbins, 2002; Kannan et al., 2001; Sonis et al., 2002). The experiment described in Chapter 6 contains results generated from a small microarray experiment, the first examining the effect of irinotecan on gene expression in the small intestine of the rat. Genes involved in a number of pathways including calcium regulation and the phosphatidylinositol signalling system, JNK and MAP kinase pathways and multiple metabolism pathways were differentially expressed following treatment. The role of cellular calcium regulation especially is known to be critically important for intestinal cell viability (Pattni and Banting, 2004; Tepperman et al., 2005), while the MAPK pathway is activated in times of inflammatory damage in the intestine (Chang and Tepperman, 2003; Lamkanfi et al., 2004). This indicates the wide ranging biological effects of irinotecan on intestinal cells and the multiple routes to apoptosis activated by this agent.

7.7 Conclusions

To target anti-mucotoxics effectively, we must first have a thorough understanding of the mechanisms controlling mucositis development. The studies carried out for this thesis aimed to increase our knowledge of the role that apoptosis regulators play in the induction of intestinal damage following chemotherapy treatment. This thesis has provided evidence that although chemotherapy agents all induce cell death in the intestine to some degree, the pathway to which apoptosis is initiated varies. The activation of p53 is not required in every case to induce apoptosis, nor is the effect on every Bcl-2 family member identical following treatment with different agents. However, these components of the apoptosis pathway do play a major role in intestinal cell death and should continue to be investigated to further define their role in mucositis. In conclusion, the role of apoptosis regulators in chemotherapy-induced intestinal mucositis is complex and we have yet to discover a universal initiator of the pathway which is required for cell death in all settings.